Surface Core Level Shift Studies of Adsorbate Covered Tungsten Single Crystal Surfaces:

Thesis submitted in accordance with the requirements of the University of Liverpool for the degree of Doctor in Philosophy by

Glyn Peter Derby,

September 1989.

"Zeurr are many ways of 'aving fish zat are not fishcakes"
J.J., January 1986, when confronted with a Big Breakfast.

"If you tie two birds together, although they have four wings they cannot fly"
Old Chinese proverb.

This thesis is dedicated to
My Parents,

Christine, Paul, David

and our Michael.

Declaration.

The work presented in this thesis was carried out jointly between the department of Inorganic, Physical and Industrial Chemistry at The University of Liverpool and SERC Daresbury Laboratory between 1st October 1985 and 1st October 1988. Funding was provided by the SERC.

I am the sole author of all the work presented in this thesis, none of which has previously been submitted for a degree at this or any other university.

Glyn Peter Derby.

Acknowledgements.

I would like to acknowledge firstly my academic supervisor Professor David A. King for providing direction and encouragement throughout the period of my post-graduate career. Also I thank Dr. David Norman for on-site moral support at Daresbury and useful discussions (including some really hairyendous jokes) during the many runs.

I would also like to thank Doc. Kevin Purcell for teaching me the 'ins and outs' of coping with the beamline, and of course for compiling a relatively user-friendly fitting package out of bits and bobs from here and there.

You cant leave your fellow SS post-grads out can you, so here they are: Danny (Hank B. Movie the 23rd), Dave (The Boy), Simon (Dangerhusband), Gaz-A (Smart! look you boyo), Chris ('Look at the size of my portfolio.'), Mark (walks-far, 'Alright my Lov'..?.. Good game. Good game.'), Tim ('went for a few beers', 'fancy a curry actually boys') and Mr. G35 himself Damien ('tsappnen beoyz?', 'see you guyyyzz'). I would also like to mention the less permanent members of the group who have passed through during their undergraduate honours years, I enjoyed passing on whatever experimental tips I may have thought I'd picked up in a previous life. It was a good laugh most of the time.

On a purely social note I have to thank 'The Square' for making the good times better, and providing a healthy piss-taking environment to relax in between leak testing sessions. The trouble with 'The Square' is that the membership changes too often to name everybody involved. The original hard core know who they are (Diane, Stuart, Suzanne, Anne-Marie) most of them are leaving themselves this year ... but murky buckets to all the generations of the square.

On the whole I've thoroughly enjoyed my time in the surface science group at 'The IPI' as was (those bits of it that I actually spent *in* Liverpool). And it has been due in no small part to the generally light and breezy atmosphere upheld by the permanent members of the technical and clerical staff.

So thanks to firstly our very own John 'pretty boy' Leadward who has, in his time, rebuilt most of the machines in the group at least twice. John 'dad' Kitson, Bert 'the glass' Chappells, Steve and Tony (the Morcambe and Wise of lab two), Jean and Rachel (the Little and Large of lab two), and not forgetting The One and Only, The Original ... Dan 'The Man' Dare, plus John 'Crystals' Stevens (the 'mans' with the vans).

Then there's Judi, Anne F., and Ann B., the list is endless to cut short the Richard Attenborough impression darlings I'll just say '...and everybody else'. Oh, I nearly forgot Malcolm the 'cheerful' mountie (if you need a cupboard he's your man).

Could I forget Roger, Daniel, Frances and Arthur on-site at 'THE BIG-D'? No way, thanks for the backup. And 'fellow users lend me your cauliflower cheese' if it hadn't have been for you lot tea-time would have been such a ... ...civilised affair? The Birmingham Buglers Featuring Hawaii Five-0's very own Steve Barratt, Tony 'if you want to get to florida get a hat' Begley, Mike 'Brendan Foster' Hoyland and Robin 'Alligator' Jordan, Britains answer to Crocodile Dundee. The Manchester Hardy Annuals including the old guard Ranal and Winkers, and the new guard Chris

'chuckles the bunny' Peter 'fingers Tibet' And 'cuddly' Douglas (or so we hear). The original Cambridge Bucaneer (Cavalier?) Julian 'jas' Scarfe. And finally, but by no means last, The Warwick Wigglers, featuring in his entirity Nicholas Quincy Prince the world famous Swedish dancing bear who is never let out without his favourite pair of fluorescent pink cycling shorts Mark 'the organ grinder' Ashwin.

Ta' Very Much Folks.

Abstract.

Photoemission from the W $4f_{7/2}$ core level has been stimulated using photons in the energy range 60 to 80 eV. Several adsorption systems have been investigated employing the {110} surface as a substrate. Overlayer structures of oxygen and hydrogen produce several adsorbate induced features the behaviour of which have been discussed in terms of identification of adsorption sites. The fit to the hydrogen spectra differs from that a previous study in that one of the adsorbate induced features has been included in the bulk peak, but the intensity behaviour of each of the components is consistent with the double site (2x1) model of Holmes and King in agreement with the previous study. The pure oxygen system yielded similar results to those obtained by Spanjaard et al following re-analysis of their data. Defining the energy positions of the adsorbate induced features for this adsorption system has laid the basis for the analysis of the high temperature phase of the CO/W{110} adsorption system where only dissociated CO exists. However, it has not been possible to complete the analysis of data from this adsorption system before the final submission date of this thesis, and so the results will not be presented here but will form the core of a forthcoming publication. The same is true for a study of thermally induced clean surface roughening transitions using W{610} and W{320} single crystal surfaces. The sticking coefficient of nitrogen on the W{110} surface is of the order of 10^{-3} at room temperature. However, it is possible to adsorb up to 0.25 monolayers by cycling the sample between 300 and 700 K in $2x10^{-6}$ of nitrogen for several minutes. The structure previously observed at this coverage is (2x2) where the nitrogen adatoms sit in the threefold hollows of the underlayer. On the basis of this model the flat topped spectrum produced by this structure has been tentatively fitted with seven component peaks.

Contents.

Chapter 1

Introduction

The work presented here represents the natural progression of earlier work carried out in this group which is documented in several journal publications, and collectively in the thesis of K.G. Purcell. I was also involved with some of that earlier work. By way of an introduction I would like to highlight the main features of that work which have been applied directly to the analyses undertaken here.

Tungsten was the subject of these initial investigations for several reasons, not least of which is the fact that the {100} surface undergoes a rather well studied phase transition. In addition to this the W $4f_{7/2}$ core level is relatively narrow and therefore well suited to such studies, and is readily accessible with photons of less than 100 eV having a reasonable cross-section in this range. Here the photoelectron kinetic energies lie in the minimum of the escape depth curve thus maintaining optimum surface sensitivity.

The most striking result that emerged from the previous study was the dependence of the magnitude of the surface core level shift on effective coordination of clean surface atoms. When the third coordination shell is included there is almost a linear relation between the two; on clean tungsten surfaces as the effective coordination is reduced the magnitude of the shift is increased. This result served to end the controversy concerning spectra taken from the W{111} surface. Citrin et al maintained that

the only way the spectra could be accounted for was to allow the bulk component a greater FWHM than those of the surface, of which there were two; surface and first underlayer. However with the emergence of this coordination number relationship it seemed clear that the W $4f_7/2$ core level spectrum taken from a clean W{111} [1] surface should be divided into four components; surface, first underlayer, second underlayer, and bulk of equal linewidth and asymmetry. The proposal had been made in several theoretical works on the subject. This result was demonstrated and shown to be possible only if the linewidths of bulk and surface components were made equal. The bulk line width of course can be measured experimentally as will be described in the introductory section of the results chapter.

This coordination dependence curve was constructed by careful fitting (the same as has been applied here) of experimental data taken from several stepped surfaces [2, 1]. Each atom type within the surface i.e. terrace, top-of-step, base-of-step, and underlayer gives rise to a different shift dependent on the surface. It is the clear analysis of the stepped {320} and {610} surfaces which we have applied here to spectra collected at a surface temperature of 80 K in the thermal roughening section of the results chapter. The experimental determination of the effects of phonon broadening [3] has also played its part in the deconvolution of the high temperature spectra taken from these surfaces. Due to the slightly better statistics provided by the High Brightness Lattice combined with the inclusion of a post-focussing mirror, which was absent for the previous study, we feel we have been able to more accurately determine the positions of these component peaks.

One other aspect of the previous work which we have applied here is the induced shift due to adsorption of nitrogen. Initially measured for W{100} where it forces a reconstruction [4, 5] it has served to provide us with an initial estimate in the

deconvolution of complicated spectra collected from a nitrogen underlayer on W{110}. We were then able to combine the two in the analysis of data collected from nitrogen adsorption on W{320}, although the complexities of this system make a complete analysis of the data extremely difficult.

Postscript.

The analyses presented in this thesis have been based on the premise that the core level lineshape due to photoemission from atoms in the surface is the same as that due to atoms in the bulk. This is a procedure which has not been without precedent, many other groups in the past have applied similar reasoning to their deconvolution [7, 8, 9]. However, following the submission of this thesis for examination Riffe, Wertheim and Citrin [6] have published new high resolution experimental evidence that this is in fact not the case. Their data shows that the FWHM of the surface band for a W{110} single crystal surface is quite in excess of previously calculated and experimentally derived values for the bulk. We have applied here, as in the past, a doniach-sunjic lineshape of fixed width (FWHM = 50 meV) and asymmetry ($\alpha = 0.05$). Riffe et al maintain that the bulk peak has FWHM = 60 ± 3 meV and the surface has FWHM = 84 ± 3 meV. In addition to this they also propose that the asymmetry parameter differs for the two, quoting values of 0.063 for the surface and 0.035 for the bulk. Their estimates of phonon broadening show that there is no difference within experimental error here between surface and bulk peaks at 210 K, although the absolute values that they quote seem to be smaller than previously accepted values by around 20 meV. Should these results prove to be substantiated by further independent investigations into core level lineshapes, it is not clear how this will affect or alter the analyses presented here in later sections.

Bibliography

[1] K.G. Purcell, J. Jupille, G.P. Derby, D.A. King Phys. Rev. B36 (1987) 1288.

[2] K.G. Purcell, J. Jupille, D.A. King Surf. Sci. 208(3) (1989) 245.

[3] K.G. Purcell, G.P. Derby, D.A. King J. Phys. Condensed Matter 1 (1989) 1373.

[4] J. Jupille, K.G. Purcell, D.A. King Solid State Comm. 58 (1986) 529.

[5] J. Jupille, K.G. Purcell, G.P. Derby, J. Wendelkin, D.A. King The Structure of Surfaces II. Vol.II of Springer Series in Surface Sciences, Eds, J.F. van der Veen and M.A. van Hove (Springer, Berlin, 1987) 285.

[6] D.M. Riffe, G.K. Wertheim, P.H. Citrin Phys. Rev. Lett. 63 (1989) 1976.

[7] D. Spanjaard, C. Guillot, M-C. Desjonqueres, G. Treglia J. Lecante Surface Science Reports 5 (1985) 1.

[8] P. Soukiassien, R. Riwan, J. Cousty, J. Lecante, C. Guillot Surface Science 152/153 (1985) 290.

[9] Tran min Duc, C. Guillot, Y. Lasailly, J. Lecante, Y. Jugnet and J.C Vedrine Phys. Rev. Letts 43 (1979) 789.

Chapter 2

The Theoretical Origins of Surface Core Level Shifts

There are two main approaches to surface core level shifts;

1. The Microscopic Model.
2. The Thermodynamic Model.

2.1 The Microscopic Model

There exists a shift in the core level binding energies of an atom as it is moved from the free-state to the solid environment. Williams and Lang [1] proposed that in order to evaluate this fairly elusive quantity it is necessary to break down the process into a series of stages for which values could be readily calculated using the computational procedures available at the time. They divided the shift into three main components

1. Configurational change is that due to the redistribution of electrons between the s, p, and d states in the free atom to that which it will adopt in the solid environment.
2. Chemical shift is the degree to which the change in the chemical environment (before removal of an electron) displaces the core level.

3. **Relaxation shift** contains the final state effects of the core hole on the observed core level binding energy i.e. the effects of screening the resultant core-hole positive charge.

Or, to put it mathematically,

$$\Delta = \Delta_{config} + \Delta_{chem} + \Delta_{relax}. \tag{2.1}$$

While evaluation of the first two of these components is relatively straight forward, the third required the use of *the excited atom model* in which the core-excited atom in the solid is approximated by a free atom whose core charge has been excited to a valence orbital. Local charge neutrality is effected by the presence of metallic screening, which can be approximated by the addition of an extra valence electron.

This approach was taken up by Spanjaard/Desjonqueres et al [2, 3] who extended it to surface core level shifts in transition metals, i.e. where Williams and Lang refer to free-atom and solid environments the French group refer to *surface* and *bulk*. However they do not include any final-state relaxation contribution, since they propose that the screening behaviour is not modified when moving from the bulk to the surface. Screening may be either intra-atomic or extra-atomic, and intra-atomic effects may be neglected when moving from bulk to surface. The extra-atomic relaxation, being mainly due to the d-electrons which are fairly localised, should not be affected by the presence of the surface. Therefore this view is one of purely initial-state causes of surface core level shifts in transition metals, i.e.

$$\Delta^{SB} = \Delta^{SB}_{conf-chem} = (\varepsilon_c^B - \varepsilon_c^S) \tag{2.2}$$

The qualitative description of the underlying causes of surface core level shifts with regard to the 5d transition series is as follows. A more detailed discussion of the

effect is presented by both the French group, and Citrin and Wertheim [3, 4].

The reduced number of bonds at the surface (compared to bulk) causes a narrowing of the surface density of states. The effect of this, in the case where there is a more than half filled d-band, is to bring unoccupied surface bands below the Fermi level which is pinned by the bulk (see Figure 2.1). There is then a certain degree of charge transfer from the occupied bulk states to these unoccupied surface bands. The amount of charge transfer involved is small enough to maintain layerwise charge neutrality [5, 6]. However the resultant coulomb potential raises the energy of the surface d-bands i.e. causes a shift in the centre of gravity (C o G) of the surface density of states and at the same time raises the energy of the surface core levels by a comparable amount. Thus the surface atom core levels exhibit lower binding energies with respect to the Fermi level than do the bulk atoms.

In cases where there is a less than half-filled d-band the narrowing of the surface density of states results in occupied surface bands being raised above the Fermi level in which case there is charge transfer in the opposite direction and an accompanying displacement of the centre of gravity of the surface d-band , hence core levels, in the opposite sense to that described above.

We see here that there is a change of sign involved in moving across the transition series from $n_d<5$ to $n_d>5$ electrons. There should be zero shift for the case where the d-band is exactly half-filled. In fact due to the often complex asymmetrical nature of the surface d-band structure the change of sign occurs between Ta and W where the respective configurations are equivalent to $5d^{3.4}$ and $5d^{4.6}$. This has been confirmed experimentally [3].

Within this model the core levels rigidly follow the displacement of the valence d-band caused by the presence of the surface, so the above equation may be written;

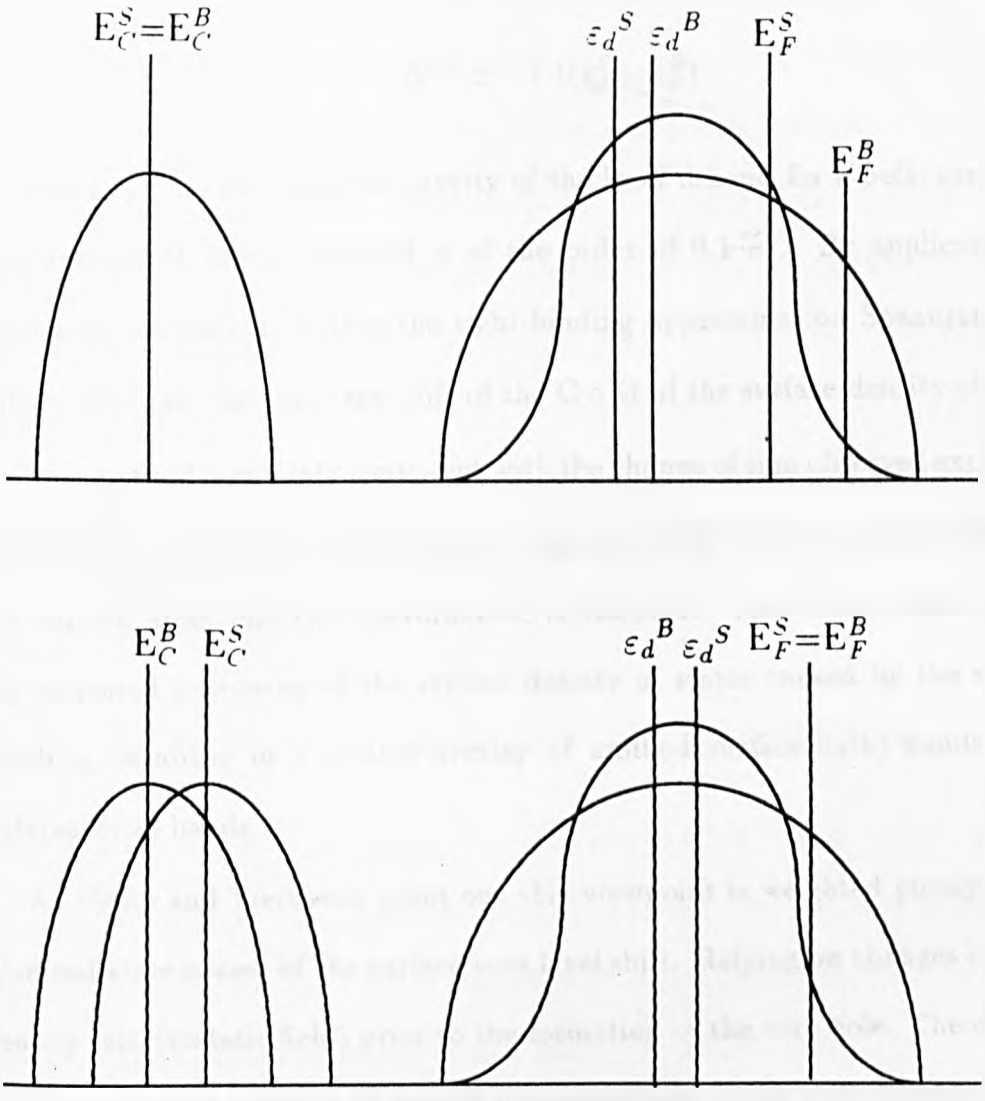

Figure 2.1

Surface d-band narrowing caused by reduced effective coordination results in unoccupied surface bands (for $n_d > 5$) falling below the Fermi level. Charge transfer from bulk to surface bands alters the electrostatic field thus causing a shift in core level binding energies.

$$\Delta^{SB} \simeq -1.1(\varepsilon_d^S - \varepsilon_d^B) \tag{2.3}$$

where $\varepsilon_d^{B(S)}$ is the centre of gravity of the local d-band for a bulk(surface) atom. The amount of charge involved is of the order of 0.1 e^-. By application of self-consistent calculations within the tight-binding approximation Spaanjard et al are able to calculate the resultant shift of the C o G of the surface density of states.

This method is not only consistent with the change of sign observed experimentally between Ta and W , but also produces a greater shift for more open surfaces where the surface atom effective coordination is reduced. This latter effect stems from the increased narrowing of the surface density of states caused by the reduction in bonding, resulting in a greater overlap of unfilled surface(bulk) bands with filled bulk(surface) bands.

As Citrin and Wertheim point out this viewpoint is weighted purely on the side of initial-state causes of the surface core level shift. Relying on changes in the charge density (electrostatic field) prior to the formation of the core hole. The effects of the final-state in this model is to modify the magnitude of the shift observed.

For completeness it may be useful to describe the mechanism responsible for shifts in non-transition metals. The noble metals also exhibit surface core level shifts despite having a completely filled d-band. How does this fit in with the above model? In developing their explanation of the underlying causes of this shift within the transition series, Citrin and Wertheim begin by accounting for the surface shift observed in the noble metals. The need to do so was brought about by their own observation of a surface shift in gold [7, 8]. In such metals there is considerable s-d hybridisation. At the surface this hybridisation is reduced and as a result the surface atom electronic configuration contains a greater fraction of d-states which are of non-bonding and

antibonding character. Hence these states are less strongly bound and therefore have core level binding energies intermediate between those of the bulk solid and free atom values. To put it into the same descriptive terms as above, the surface density of states is narrowed due to the reduced coordination. The effect of this narrowing where no charge transfer has been allowed between the surface and bulk environments, is to produce a misalignment of bulk and surface Fermi levels. Now, in the case of noble metals the only way in which a single (real-case) Fermi level can be achieved is to allow charge-transfer from the bulk into the surface bands. This causes a shift in the C o G of the surface density of states and associated core level binding energies to lower binding energies.

2.2 The Thermodynamic Approach.

The thermodynamic approach has its roots in the work of Rosengren and Johansson [9], and Martensson and Johansson [10, 11], although the fundamental aspects of this method have been taken up and simplified by other groups in order to explain such phenomena as surface and interfacial segregation [12, 13, 14].

Here [9] the shift on moving from the free to the metallic state is defined in the following manner

$$\Delta\, E_c = E_c^A - E_{c,F}^M \tag{2.4}$$

where E_c^A is the atomic binding energy in the free state, and $E_{c,F}^M$ is the binding energy in the metallic state relative to the Fermi level. The main axis of this approach then lies in a Born-Haber cycle which again breaks down the complex single-step determination of E_c^M into a series of readily accesible parameters. Figure 2.2 shows the BH cycle presented by Johansson and Martensson.

- E_{coh}^Z, is the cohesive energy i.e. that energy required to remove a single atom

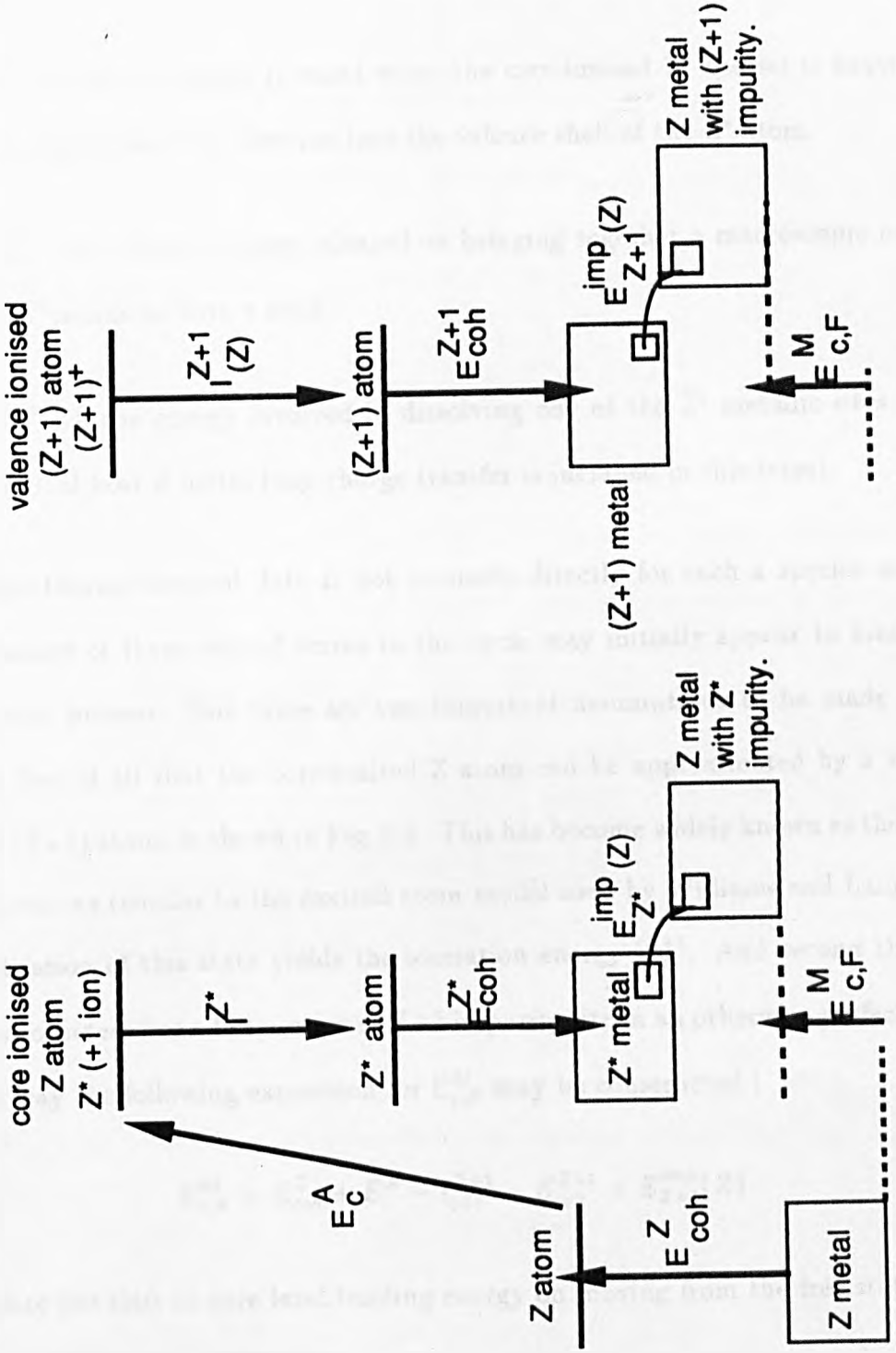

Figure 2.2

Born-Haber cycle produced by Johansson and Martensson to determine free-atom to solid core level shifts from empirical quantities via calculation of $E_{c,F}^{M}$.

from the metal Z and arrive at the free atom.

- E_c^A, the energy required to core ionise the free atom.
- I^{Z^*}, ionisation energy released when the core-ionised Z^* species is neutralised by acquisition of an electron into the valence shell of the Z^* atom.
- $E_{coh}^{Z^*}$, the cohesive energy released on bringing together a macroscopic number of Z^* atoms to form a solid.
- $E_{Z^*}^{imp}(Z)$, the energy involved in dissolving one of the Z^* metallic sites in the original host Z metal (any charge transfer is included in this term).

However, thermochemical data is not available directly for such a species as Z^* so the presence of these related terms in the cycle may initially appear to hinder the calculation process. But there are two important assumptions to be made in this model, first of all that the core-ionised Z atom can be approximated by a valence-ionised (Z+1) atom, as shown in Fig. 2.2. This has become widely known as the *(Z+1) approximation* (similar to the excited atom model used by Williams and Lang). The neutralisation of this state yields the ionisation energy $I_{(Z)}^{Z+1}$. And second the final-state is considered as a fully screened Z+1 impurity site in an otherwise perfect metal. In this way the following expression for $E_{c,F}^M$ may be constructed ;

$$E_{c,F}^M = E_{coh}^Z + E_c^A - I_{(Z)}^{Z+1} - E_{coh}^{Z+1} + E_{Z+1}^{imp}(Z) \tag{2.5}$$

Therefore the shift in core level binding energy on moving from the free state to the metal environment is given by ;

$$\Delta\, E_c = I_{(Z)}^{Z+1} + E_{coh}^{Z+1} - E_{coh}^Z - E_{Z+1}^{imp}(Z). \tag{2.6}$$

With modification this cycle can be applied to the observation of surface core level shifts [9]. Figure 2.3 shows a simplified Born-Haber cycle with two possible paths for the initial free-state atom to take

1. into the bulk of a metallic environment,
2. into the surafce of a metallic environment.

The energy difference between the two paths is given by

$$\Delta_c(Z) = \Delta_c^S - \Delta_c^B = E_{c,F}^S - E_{c,F}^B \tag{2.7}$$

where the superscripts S and B denote surface and bulk respectively. Taking the implantation energy to be small in comparison to the other terms involved , which stems from the small heats of solution between neighbouring elements, this gives us

$$E_{c,F}^{S(B)} = E_{coh}^{S(B)}(Z) + E_c^A - I_{(Z)}^{Z+1} - E_{coh}^{S(B)}(Z+1) \tag{2.8}$$

and so,

$$\Delta_c(Z) = E_S(Z+1) - E_S(Z) \tag{2.9}$$

where E_S is the surface energy defined as

$$E_S = E_{coh}^B - E_{coh}^S \tag{2.10}$$

In their initial calculations JM have employed the empirical relationship

$$E_{coh}^S = 0.8 E_{coh}^B \tag{2.11}$$

So the expression for the surface core level shift of a Z metal further simplifies to become

$$\Delta_c = 0.2(E_{coh}^{Z+1} - E_{coh}^Z) \tag{2.12}$$

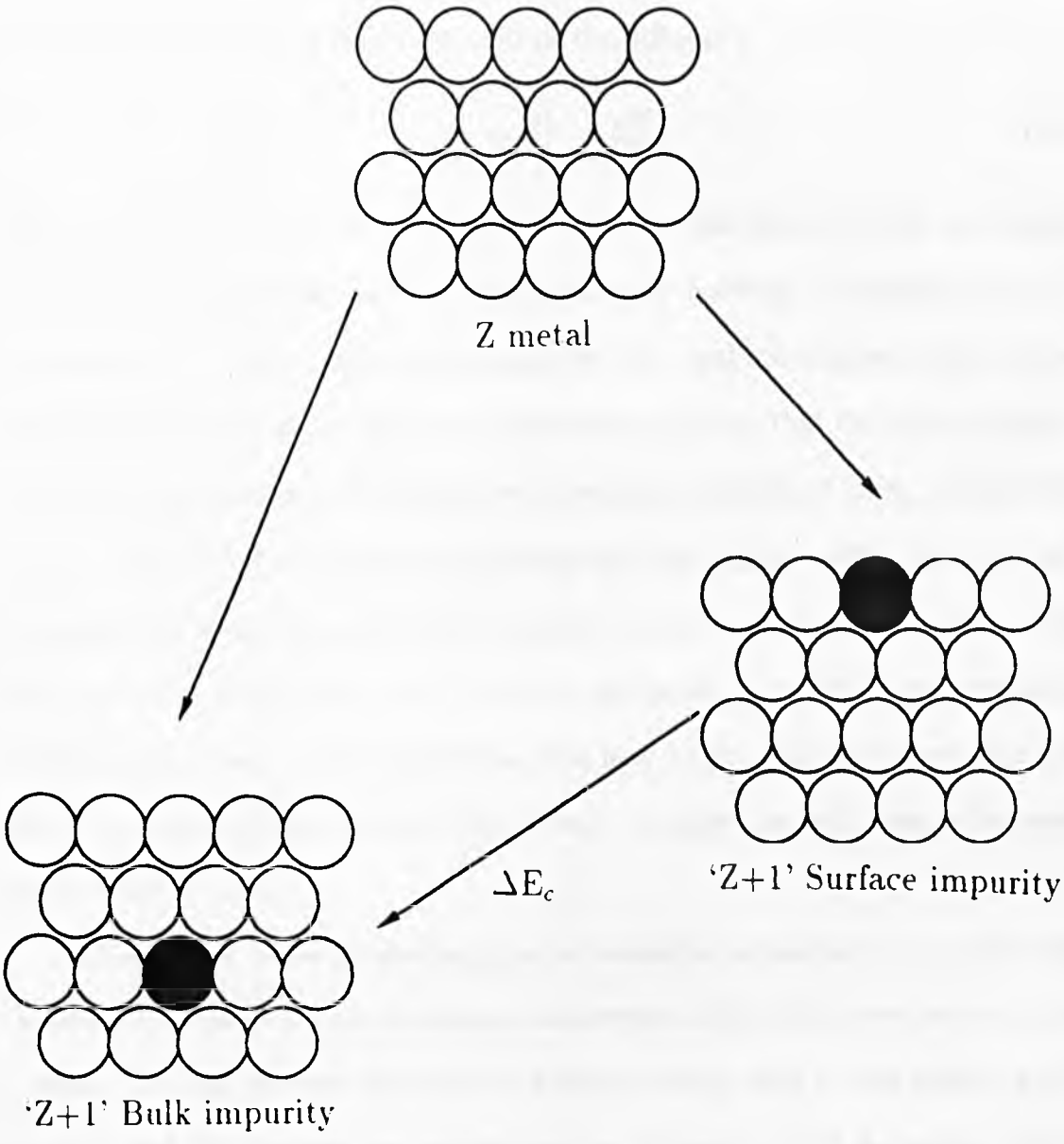

Figure 2.3

Relationship of initial to final states within the equivalent core approximation showing two final states one resulting from photoemission in the surface layer and the other coming from photoemission events within the bulk layers.

Rosengren and Johansson [9] arrive at the same expression as is given in equation 2.12 but this time defining the shift as the difference

$$\Delta_c = E^S_{Z^\bullet} - E^B_{Z^\bullet} \tag{2.13}$$

Where $E^{S(B)}_{Z^\bullet}$ is the total energy difference between the metal Z with an impurity atom at the surface(bulk) and the pure metal. The bonding is described within the framework of the tight-binding approximation. The final calculations of the shift are modified from those of Johansson and Martensson (JM) in that the surface energy is deduced by application of the surface tension variation with band filling, calculated by Desjonqueres et al [15, 16], in conjuction with calculated band widths. Having applied the method to several planes for both *fcc* and *bcc* metals it has been demonstrated that the magnitude of the surface shift is heavily dependent on the effective coordination of the surface atoms. JM proposed that this may be the case and it has since been shown experimentally for tungsten that there is an approximately linear relationship between the two [17].

Surface energy varies parabolically across transition series and so it is clear from the above that there will occur a change in direction of the shift as we proceed across a series. For the heavier elements the binding energy shift at the surface will be negative, and the opposite true for elements in the early part of the series. This has been experimentally established.

The success of this method is largely due to the fact that the use of such empirical quantities automatically takes into account several competing effects, for example the final-state relaxation excluded in the previous model and the initial-state band narrowing effects. However Johansson and Martensson have interpretted the trends arising from this scheme in terms of variations in the final-state. They attribute the change in sign of the shift to the bonding and anti-bonding nature of the screening

charge.

Perhaps it may be easiest to envisage the effect within the total energy framework. For elements occuring in the earlier part of a transition series the screening electrons of the (Z+1) final state are of bonding character. The core level shift is the difference in total energy of the two final states shown in figure 2.3. By virtue of the increased coordination of the bulk these atoms will experience to a greater effect any changes brought about by bonding state variations. So for elements in the early part of the transition series the total energy decrease caused by the addition of an extra electron of bonding character, as occurs in the Z+1 approximation, will be greater for an atom in the bulk than for one at the surface. Thus the surface core level shift observed is positive i.e. on moving an atom from the bulk to the surface its core level binding energies will be increased. In the case of the heavier metals the gain of an extra valence electron means an increase in antibonding character which again is felt more by the bulk than the surface. The relative total energy gains involved therefore predict that there will be a negative surface core level shift.

This notion that the change in sign is due to final-state variations is vigorously disputed by Citrin and Wertheim [4], who maintain that the difference between final-states for surface and bulk atoms is small in comparison to the initial-state variations. They base this argument on measured surface and bulk photoemission lineshapes, combined with surface and bulk density of states C o G determinations.

2.3 Effects of Adsorption on Substrate Core Level Shifts.

Over and above the clean surface core level shifts discussed earlier there is an additional effect induced as a result of adsorption. This is the area of surface core

level shift spectroscopy on which most of the results presented in the later sections of the current work are based. There have in the past been many such studies mainly involving the adsorption of simple diatomics [13, 39, 40, 41, 42, 43].

We have seen how the initial-state characteristics affect the magnitude and direction of the surface shift. Whereas previously for the clean surface the initial-state is altered as a result of charge transfer between the surface and the bulk during adsorption charge transfer occurs between the adsorbate and the substrate. The direction of transfer is dependent on the relative electro-negativities of the two. For example when caesium is adsorbed onto tungsten there is electron donation to the substrate, as demonstrated by Soukiassien [38], and the surface core level binding energies are shifted in the opposite direction to that observed during oxygen adsorption where charge is donated to the adsorbate.

Within the initial-state framework described earlier for the clean surface core level shift involving surface d-band narrowing, there is a change in the direction of the shift as one crosses the transition series from the elements exhibiting less than half filled d-band structure to those displaying a more than half filled d-band. Given that the effect of adsorbing oxygen on tungsten is to increase the surface core level binding energies we might expect within this model that the presence of the oxygen causes a broadening of the surface d-band. This would produce an overlap of filled surface bands with empty bulk bands (or alternatively, in the hypothetical case, inducing a misalignment of surface and bulk Fermi levels). In a similar way to that argued for the clean surface shift there must be a small amount of charge transfer from the surface to the bulk (or, re-alignment of bulk and surface Fermi levels). This behaviour is accompanied by a shift in the density of states of the surface layer with respect to the bulk in such a way as to produce the observed effect.

However if we were to apply these arguments to those transition metals with less than half-filled d-bands they would predict a decrease in surface atom core level binding energies. It has already been shown that the shift induced by adsorption of oxygen and hydrogen is in the same direction for both tungsten and tantalum i.e. to higher binding energies [3]. Clearly this simple qualitative band-narrowing/broadening picture meets its limitations when it comes to predicting adsorbate induced shifts.

Initial-state reasoning is not totally inapplicable. Consider oxygen adsorption on tungsten with its associated work function increase. There is charge transfer *from* the tungsten *to* the oxygen. Tungsten, by virtue of its negative clean surface shift, may be considered part of the latter half of the transition series. During adsorption it loses electron density which is antibonding in character hence the surface atoms become more bound and their core level binding energies are driven towards (and past) those of the unaffected bulk atoms. The surface atoms become more 'bulk-like' and exhibit higher binding energies. Now consider the same situation for tantalum lying in the earlier part of the series. Here we see a reduction of bonding character electron density during charge transfer to the oxygen. The surface atoms become even less bound with core level binding energies pushed further away from the bulk values. Since tantalum has a positive clean surface shift, an increase in binding energy is again observed. The opposite would be true for adsorption of electro-positive species.

It becomes clear from this explanation that the greater the interaction i.e. the larger the degree of charge transfer involved, then the greater will be the alteration of surface atom core level binding energy. In practice this implies that a surface atom bound to two or more adsorbate atoms will experience a greater shift than one which is bound to a single adatom.

There is also an accompanying effect on the final-state screening potential. Reduc-

tion(increase) in screening charge density will lead to loss(gain) in effective screening, the result of which being an apparently larger(smaller) core level binding energy shift.

Desjonqueres and Spanjaard have extended their model within the tight-binding approximation to include the adsorbate effects. Previously for clean surfaces they have broken down the shift into two components $\delta^{SB}{}_{conf-chem}$ and $\delta^{SB}{}_{relax}$, the latter of which they assumed to be the same for bulk and surface atoms for reasons explained earlier, which they have linked directly to the shift in the centre of gravity of the surface d-band. Assuming that adsorption is quasi-neutral resulting from a small amount of charge transfer then within the tight-binding formalism the substrate is described by its 5d orbitals (for the third transition series) and the adsorbate by its corresponding outer valence shell orbitals. The adsorbate-substrate interaction then may be described by hopping integrals. For a given proposed structural model involving a particular adsorption site the calculation is carried out and the results compared with experiment to eliminate one or more of the structural possibilities.

Within the thermodynamic framework there are now three possible final-states resulting from the photoemission event. They are (Z+1) impurity in the bulk, on the surface, or on the surface and bound to the adatom. The difference in total energies of the latter two is the adsorbate induced shift. It is possible to derive a value for this by application of a Born-Haber cycle similar to that constructed by JM for the clean surface shift. Spanjaard et al have quite recently constructed such a cycle in which the essential difference is the inclusion of an adsorption energy term in the early stages hence producing a clean surface and adsorbate gas. The underlying principles of the method remain unchanged.

2.4 Lineshapes

The observed lineshape of a photoemission spectrum is dependent on several factors. In the absence of any lifetime effects the spectrum may be described by a series of delta functions. However in real systems the observed lines have both width and asymmetry. There exist many detailed publications on this subject [20-36]: the main processes involved are listed below.

Core-Hole Lifetime :

For an experiment with fixed emission angle and photon frequency the effects of core hole lifetime would be to replace the delta function with a Lorentzian

$$I_s = \frac{\alpha\Sigma}{(E - E_s)^2 + \Sigma^2} \tag{2.14}$$

where the width of the peak is given by

$$\Delta\ E_s = 2\Sigma = \frac{1}{\tau} \tag{2.15}$$

τ is the lifetime in atomic units.

Here we are concerned with the effects of broadening on the 4f core levels of tungsten which have binding energies of less than 100 eV. The dominant mode of decay at these energies is by the non-radiative (fluorescence yield $\approx 7 \times 10^{-6}$) Auger transition $N_7O_{4,5}O_{4,5}$ involving two valence electrons. The process may be either intra-atomic or inter-atomic, the latter is however less probable (details of the likelihood of this event depend on the exact chemical and structural environment). It has recently been argued [52] that the lifetime width of lines resulting from photoemission events at the surface differs from those originating in the bulk. It is argued that the greater natural width at the surface is due to an enhanced rate of auger decay relative to the bulk. This stems from the reduced delocalisation of the narrowed surface 5d band which thereby increases the overlap between the 5d and 4f bands.

Until recently most experimeters in the field have assumed that the effects of core hole lifetime on the core level linewidth i.e. Lorentzian broadening, are the same for both surface and bulk species. For tungsten the accepted FWHM is 50 meV as determined for example by Wertheim et al, and verified by several other groups. A recent publication by Riffe et al claims that the degree of Lorentzian broadening differs greatly for the two environments quoting FWHM as 60 $\pm$ 3 meV for the bulk, which is in line with previous determinations, but 84 $\pm$ 3 meV for the surface. They propose the reason for this to be that the overlap between the 4f and 5d orbitals at the surface is greater than for the bulk. This arises from the reduced delocalisation of the d orbitals in the surface region for the more atomic-like surface d-band. The result of this therefore is to enhance the auger decay rate relative to the bulk thereby reducing the lifetime of the core hole and causing increased lifetime broadening.

Phonons : The ground state lattice oscillations are reflected via the Franck-Condon principle in the width of the core lines. The sudden creation of a core hole at some point in the lattice will cause a response by surrounding nuclei. The system will tend, with a time constant inversely proportional to the induced phonon frequency, to reach a new equilibrium position yielding a relaxation energy E_R. The nuclear and electronic motions may be separated (by the Born-Oppenheimer approximation) and potential energy corves for the initial and final states, V_i and V_f respectively, as a function of nuclear separation (figure 2.4) may be drawn. The ground state equilibrium position of the nuclei is represented by q_0. The redistribution of charge during relaxation will displace the minimum of V_f from that of V_i. The vertical electronic transitions will therefore proceed into the steep part of the final state curve. Small instantaneous deviations from q_0 caused by thermal vibrations in the ground state will thus result in a spread in energy of the electronic transitions proportional to the

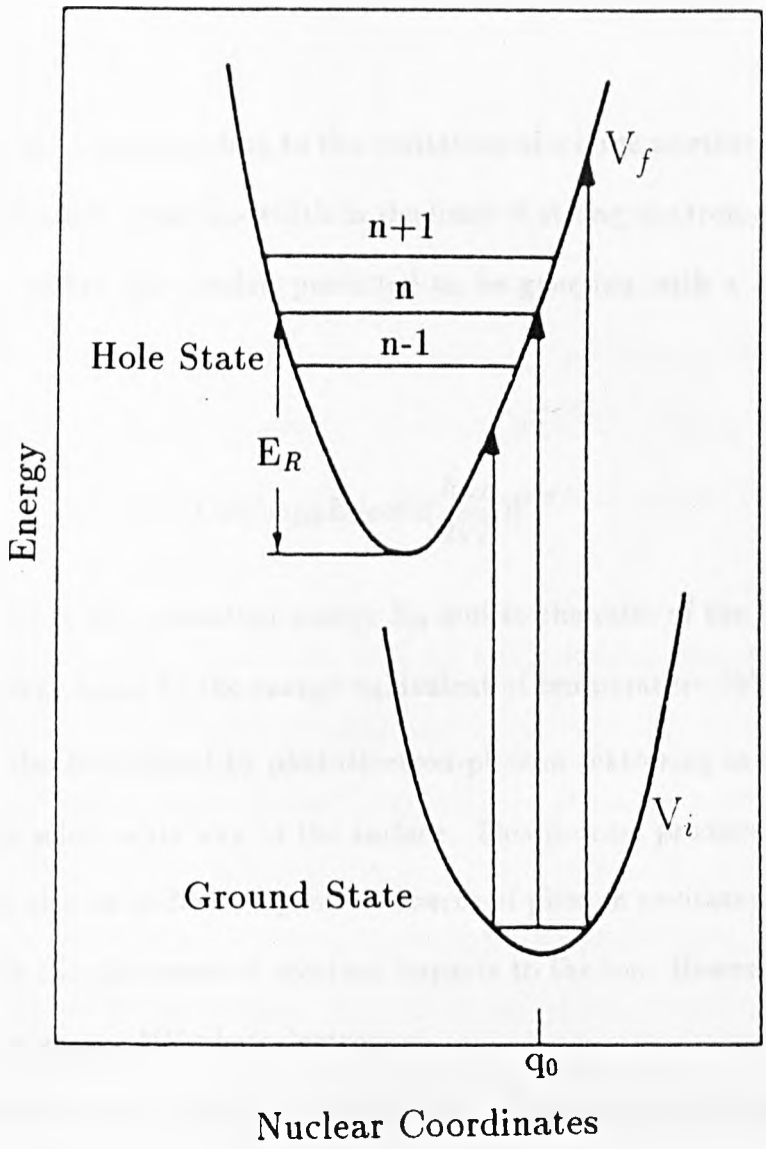
Energy
V_f
n+1
n
n-1
Hole State
E_R
V_i
Ground State
q_0
Nuclear Coordinates

Figure 2.4

curvature of V_f at q_0. Corresponding to the excitation of a large number of phonons. The phonon contribution to the linewidth in the limit of strong electron-phonon coupling is therefore, within this model, predicted to be gaussian with a temperature dependence

$$\Gamma = 2.35[\hbar\omega_{LO} E_R coth(\frac{\hbar\omega_L}{2kT})]^{1/2} \tag{2.16}$$

Γ is proportional to the relaxation energy E_R and to the ratio of the longitudinal optical phonon energy $h\omega_{LO}$ to the energy equivalent of temperature 2kT.

Phonons may also be induced by photoelectron-phonon scattering as the electron passes through the solid on its way to the surface. This process produces secondary electrons. There is also an additional possible source of phonon excitation due to the recoil energy which the photoejected electron imparts to the ion. However, this effet is negligible for low energy UV photoelectrons.

The presence of the surface in real systems leads to the presence of surface phonons with their own dispersion characteristics, and these may cause the phonon broadening of core level lines from bulk and surface environments to differ. However, the theoretical estimates for phonon broadening quoted by Sebilleau et al show that at 77 K on a W{100} surface there is no difference between surface and bulk phonon broadening. At 300 K the difference is only 20 meV, the greater effect being attributed to the surface levels. For the W{110} surface Purcell et al have determined experimentally that within the limits of experimental error the inhomogeneous broadening of this close-packed surface is relatively small. The bulk values in this case agree well with the theoretical expectations of Sebilleau. More recently Riffe et al have presented some high resolution core level data taken from a W{110} surface from which they have determined the excess Gaussian broadening due to phonons for both the bulk

and surface peaks. They quote an increased broadening for the surface peak of only 7 meV at 300 K, which is within their experimental error. It would seem therefore that use of a single gaussian width for both surface and bulk components is a valid assumption based on the previous evidence. However, the Riffe et al report while concurring with the others on the issue of surface to bulk broadening, quotes values which are in the region of 20 meV smaller than those which appear in the work of both Sebilleau et al and Purcell et al.

Plasmons : Formation of a core hole within a metal causes the surrounding conduction electrons to undergo some rearrangement such that they screen the resultant charge. This charge rearrangement may induce excitations such as plasmons or electron-hole pairs. Plasmons created in such a way are referred to as intrinsic plasmons. There may also be excitation of extrinsic plasmons, these would be the result of disturbance of the conduction electrons by the photoelectron as it makes its way through the solid to the surface, given that it has sufficient kinetic energy.

In the former situation where the Fermi-sea reacts to the formation of the hole-photoelectron dipole there is no plasmon creation when the photoelectron binding energy within the atom is close to the threshold, since the hole and electron separate relatively slowly. It is possible to envisage this as the intrinsic and extrinsic plasmons interacting destructively. However if the kinetic energy is high and the two separate 'explosively' then the result is a large number of plasmon excitations, giving rise to satellites on the low kinetic energy side of the core lines. The separation of these satellites is $\hbar\omega_p$ where ω_p is the plasmon frequency. The effect of extrinsic plasmon losses is to add to the intensity of these satellites.

If the core hole is created at the surface of the metal then there is a possibility of forming surface plasmon modes, thereby creating two sets of plasmon frequencies

and two sets of satellites. Bulk and surface plasmon losses occur at different places in the spectrum.

The limit between the two cases i.e. 'explosive' separation of hole and electron where plasmons are created, and slow separation where there are no satellites observed can be defined as being when

$$\omega_p \approx k_{TF}\nu \tag{2.17}$$

where k_{TF} is the Thomas-Fermi wave vector and ν is the photoelectron kinetic energy. In UV photoemission where the kinetic energy of the escaping electron is typically less than 40 eV, we are very close to this threshold.

Electron-Hole Pairs

Many body effects come in two types, those which provide width λ but maintain a symmetrical Lorentzian form,

$$I^L(\epsilon) = \frac{\lambda/\pi}{\epsilon^2 + \lambda^2}. \tag{2.18}$$

And those that provide asymmetry and are directly associated with the edge effect, i.e creation of a large number of weak energy e-h pairs during the photoemission process. Mahan presented a theory which predicts an enhancement in the absorption over and above that of the one-electron theory near the threshold for excitation of a core electron into unoccupied conduction states of the metal.

The positive core hole in the metal leads to excitations which tend to be localised around the core. As a result the probability of filling a core hole from screening electrons relaxed at E_F is enhanced. In addition to this Anderson pointed out that when a screening cloud forms in a metal in response to the creation of a core hole the initial-state wave function of electrons in the conduction band is slightly modified in its final state by the presence of the core hole. The transition matrix element must not only therefore contain the overlap of the initial and final state of the excited

core electron, but also all the other wave functions pertaining to the many-body system. Because the overlap of each of the many-electron states is less than unity the product quickly approaches zero, the effect of which is to severely reduce the transition strength.

These two effects were combined by Nozières and DeDominicis who showed that the absorption coefficient A(ω) near threshold (ω_0) has the frequency dependence

$$A(\omega) \propto \left(\frac{\xi}{\omega - \omega_0}\right)^{\alpha_l} \tag{2.19}$$

where ξ is an energy of the order of the width of the conduction band. The many body effects here are contained in the exponent α_l given by

$$\alpha_l = 2\delta/\pi - \alpha \tag{2.20}$$

The term $2\delta_l$ corresponds to the absorption enhancement described by Mahan, while α represents the suppression introduced by Anderson, alpha being defined in terms of Friedel phase shifts δ_l

$$\alpha = 2\sum_l (2l+1)(\frac{\delta_l}{\pi})^2. \tag{2.21}$$

In the absence of any lifetime broadening the delta function gains a tail on the high binding energy side due to this electron-hole pair phenomenon. The result of combining this tail with the effects of a finite hole-state lifetime i.e. Lorentzian broadening, is the well known Doniach-Sunjic lineshape which has been used frequently by experimenters in the past to fit xps data and takes the form,

$$I(\epsilon) = \frac{\Gamma(1-\alpha)cos[\frac{1}{2}\pi\alpha + (1-\alpha)arctan(\epsilon/\gamma]}{(\epsilon^2+\gamma^2)^{(1-\alpha)/2}} \tag{2.22}$$

where 2γ is the FWHM, and α the singularity index. This description of a photoemission line gives a good fit over an energy range of a few eV. A measure of the 'skewness' is the asymmetry parameter adopted by xray spectroscopists which is defined as being the ratio of | peak energy − half-height energy | on the low frequency

side to that on the high frequency side. The asymmetry parameter and α are related. For the Doniach-Sunjic lineshape the position of the peak ϵ_{max} is give by

$$\epsilon_{max} = \gamma cot\left(\frac{\pi}{2-\alpha}\right) \tag{2.23}$$

Nozieres-De Dominicis and Doniach-Sunjic have shown that the edge effect can be described by a power law in X-ray spectra and XPS. However, although providing expressions for α they do not quote one for the calculation of ξ which would require the use of a more realistic potential. Extension of the theory to the more real case where a surface is present requires reevaluation of the power law exponent, as the phase shifts are not only determined by the core hole alone but also by charges induced at the surface. Therefore the only way to realistically evaluate α and ξ is to include interactions of the electrons with both the core hole and surface.

Bose, Kiehm, and Longe (BKL) have attempted to extend the DS theory to make calculation of α and ξ possible in the presence of a surface. The BKL theory [54] is essentially the lowest order expansion of the ND theory (i.e. the ground state oscillator is calculated between times 0 and s at which times the core hole potential is suddenly introduced and removed respectively). Application of the BKL model to the problem allows the DS lineshape to be approximated by a logarithmic law,

$$I^A(\epsilon) = \delta(\epsilon)\left[1 - \alpha ln\frac{\xi}{e^{\mu} \mid \epsilon \mid} - \alpha\frac{P}{\epsilon}\theta(\epsilon)\right] \tag{2.24}$$

Here they have assumed γ to be zero and μ to be equal to 0.577 and is the Euler constant. The important point about this approximation is that the quantities ξ and α can becalculated using various types of realistic potentials. Longe et al [19] using this approximation have shown that α attains its bulk value within a distance of several $k^{-1}{}_F$ from the surface. The calculated value of α increases with increasing electron density parameter r_s, and is greater at the surface by between 4 and 8 %.

However, experimental evidence recently reported by Riffe et al shows there to be a significant difference in the value of the singularity index α for the surface and bulk regions of a metal, 0.035 ± 0.003 for the bulk and 0.063 ± 0.003 for the surface. The surface value is close to that previously quoted [31] but the bulk value seems grossly to differ.

Both the energy position of the peak height maxiumum and the peak height itself are functions of the asymmetry paramter and hence the singularity index. This stems from the fact that a considerable degree of the peak intensity resides in the tail. As α is increased then the peak of the line moves towards higher binding energy away from where it would lie if α were zero (lorentzian line). Therefore for binding energy determinations of less than 50 meV, such as are required for surface core level shift studies of this kind, α must be accurately determined. Since the integrated intensity under the line is a function of the photoemission cross-section variations in the size of the tail will cause fluctuations in the absolute peak heght. Since the high binding energy tail is an intrinsic feature of the spectrum, any attempts to background subtract before fitting would mean that the singularity index would be in error.

The effects of adsorption on core level lineshapes have in the past been largely ignored, Formation of an adlayer may have the effect of quenching or enhancing a particular phonon mode for example. However, as discusssed earlier, the difference in phonon broadening between surface and bulk environments is only small compared to the total width of the line. In the light of a recent report by Riffe et al [52] the area where adsorption might be expected to have the greatest effect is that of lifetime broadening. The argument put forward by Riffe is that the reduced delocalisation of the surface d-band compared to that of the bulk causes a comparitively greater overlap with the 4f band thereby increasing the rate of auger decay. By this

method therefore the core hole lifetime is reduced and the lorentzian width of the observed photoemission line correspondingly increased (by $\approx$ 25 meV). Therefore one might expect that a reduction in d-band occupancy following charge transfer to an electronegative adsorbate would cause a reduction in the auger decay rate hence increasing the core hgole lifetime and reducing the lorentzian width. The opposite is therefore implied for an electropositive adsorbate.

Bibliography

[1] A.R. Williams and N.D. Lang Phys. Rev. Letts. 40(14) (1978) 954.

[2] M.C. Desjonqueres, D. Spanjaard, Y. Lassailly, c. Guillot Solid State Comm. vol. 34 (1980) 807.

[3] D. Spanjaard, C. Guillot, M-C Desjonqueres, G. Treglia, J. Lecante Surface Science Reports 5 (1985) 1 and references therein.

[4] P.H. Citrin and G.K. Wertheim Phys. Rev. B27(6) (1983) 3176.

[5] D.G. Demsey and L. Keinman Phys. Rev. B16 (1977) 5356.

[6] S.G. Louie Phys. Rev. Lett. 40 (1978) 1525.

[7] P.H. Citrin, G.K. Wertheim, Y. Baer Phys. Rev. Lett. 41 (1978) 1425.

[8] P.H. Citrin, G.K. Wertheim, Y. Baer Phys. Rev. B27 (1983) 3160.

[9] A. Rosengren and B. Johansson Phys. Rev. B22(8) (1980) 3706.

[10] N. Martensson and B. Johansson Solid State Comm. vol. 32 (1979) 791.

[11] B. Johansson and N. Martensson Phys. Rev. B21(10) (1980) 4427.

[12] W.F. Egelhoff, Jr. Phys. Rev. Lett. 50(8) (1983) 587.

[13] W.F. Egelhoff, Jr. Surface Science Reports and references therein.

[14] A. Rosengren and B. Johansson Phys. Rev. B23(8) (1981) 3852.

[15] M.C. Desjonqueres and F. Cyrot-Lackman Surf. Sci. 50 (1975) 257.

[16] M.C. Desjonqueres and F. Cyrot-Lackman J. Phys. F 5 (1975) 1368.

[17] K.G. Purcell, J. Jupille, and D.A. King Surface Science 208 (1989) 245.

[18] B.W. Veal and A.P. Paulikas Phys. Rev. B31(8) (1985) 5399.

[19] P. Longe, P. Kiehm, S.M. Bose Phys. Rev. B27(10) (1983) 6000.

[20] S. Doniach and M. Sunjic J. Phys. C vol. 3 (1970) 285.

[21] C.P. Flynn Phys. Rev. Lett. 37(21) (1976) 1445.

[22] G.K. Wertheim Phys. Rev. B25(3) (1982) 1987.

[23] G.K. Wertheim Phys. Rev. Lett. 35(1) (1975) 53.

[24] M. Cini Solid State Comm. 41(9) (1982) 671.

[25] G.K. Wertheim and P.H. Citrin Topics in Applied Physics vol. 26 'Photoemission in Solids I' ed Cardona and Ley. Springer (1978).

[27] G.K. Wertheim and L.R. Walker J. Phys. F vol. 6(12) (1976) 2297.

[28] C.P. Frank, S.E. Schnatterly, F.J. Zutavern, T. Aton, T. Cafolla and R.D. Carson Phys. Rev. B31(8) (1985) 5366.

[29] P.H. Citrin. and G.K. Wertheim Phys. Rev. B16(10) (1977) 4256.

[30] G. Wendin in Structure and Bonding 45 published by Springer-Verlag

[31] D. Sebilleau, G. Treglia, M.C. Desjonqueres, C. Guillot, D. Chauveau and D. Spanjaard J. Phys. C June 30^{th} (1987) 2647.

[32] L. Hedin and A. Rosengren J. Phys. F vol. 7(7) (1977) 1339.

[33] G.K. Wertheim Emission and Scattering Techniques (1981) ed. P.Day published by D. Riedel 61.

[34] P.W. Anderson Phys. Rev. Lett. 18 (1967) 1049.

[35] B.H. Verbeek Solid State Comm. vol. 44(6) (1982) 951.

[36] J.R. Smith, F.J. Arlinghaus, J.G. Gay Phys. Rev. B26(2) (1982) 1071.

[37] H.J. Brocksch, D. Tomanek, K.H. Bennemann Phys. Rev. B27(12) (1983) 7313.

[38] P. Soukiassien, R. Riwan, J. Cousty, J. Lecante, C. Guillot Surface Science 152/153 (1985) 290.

[39] Tran min Duc, C. Guillot, Y. Lasilly, J Lecante, Y. Jugnet and J.C. Vedrine Phys. Rev. Letts 43 (1979) 789.

[40] J.F. van der Veen, F.J. Himpsel, and D.E. Eastman Phys. Rev. Letts. 44 (1980) 189.

[41] G. Treglia, M-C. Desjonqueres, D. Spanjaard, Y. Lasailly, C. Guillot, Y. Jugnet, Tran min Duc, and J. Lecante J. Phys. C14 (1981) 3463.

[42] P.J.F. Feibelman Phys. Rev B27 (1983) 2531.

[43] W. Egelhoff Jr. J. Vac. Sci. Technol. A1 (1983) 1102.

[44] D.E. Eastman, F.J. Himpsel, and J.F. van der Veen J. Vac. Sci. Technol. 20(3) (1982) 609.

[45] M. Cardona and L. Ley Topics in Applied Physics, 'Photoemission in Solids I' Introduction

[46] D. Tomanek, V. Kumar, S. Holloway, K.H. Bennemann Solid State Comm. vol. 41(4) (1982) 273.

[47] D.A. Shirley Chem. Phys. Lett. 16 (1972) 220.

[48] A. Rosengren Phys. Rev. B24 (1981) 3952.

[49] P.J. Feibelman, J.A. Appelbaum, D.R. Hamann Phys. Rev. B20(4) (1979) 1433.

[50] B. Johansson Phys. Rev. B19(12) (1979) 6615.

[51] G.K. Wertheim and G. Crecelius Phys. Rev. Lett. 40(12) (1978) 813.

[52] D.M. Riffe, G.K. Wertheim, P.H. Citrin Phys. Rev. Lett. 63 (1989) 1976.

[53] G.K. Wertheim, P.H. Citrin and J.F. van der Veen Phys. Rev. B30 (1974) 4343.

[54] S.M. Bose, P. Kiehm and P. Longe Phys. Rev. B23 (1981) 712.

Chapter 3

Experimental

3.1 SCLS Requirements.

The measurement of surface core level shifts is experimentally quite demanding. The relatively small magnitude of some adsorbate induced shifts (150 meV in the case of hydrogen on W{110}) makes a high resolution photon source a necessity. Earlier studies made use of lab X-ray sources which not only lacked sufficient energy resolution but also do not offer much in the way of surface sensitivity. They produce photoelectrons with kinetic energy in excess of several hundred electron volts. What is required is a tunable photon source to allow photoemission of electrons with a kinetic energy occuring at the minimum of the escape depth curve. In recent years the development of synchrotron radiation sources has provided the high intensity tunable photon source with the necessary resolution to observe surface core level shifts of less than 100 meV.

3.2 The Hardware.

All the data presented in this text were collected at the SERC Synchrotron Radiation Facility at Daresbury using a standard V.G. ADES 400 U.H.V. spectrometer attached to a Torroidal Grating Monochromator (TGM) on beamline 6.2. The main

chamber incorporates many of the established analytical techniques available to the modern day surface scientist. The Auger system is a V.G. RFA LEED/Auger combination, which while sometimes being a little temperamental is adequate enough for determining initial cleanliness of the surface. Once this has been determined a spectrum collected from the sample in its clean state may be used as a reference for 'spot checks' during an experimental series. Gas dosing and desorption were monitored using a V.G. SX200 quadrupole mass analyser mounted in a non-line-of-site position on the chamber. In the absence of a fast easy to operate Auger system such as is available on line 6.1, surface coverages were determined from comparisons of LEED patterns and desorption curves with those found in the literature combined with the application of sticking probability curves. The electron analyser itself is hemispherical with an entrance aperture of 1.3 mm giving it an acceptance half angle of 4° and is situated about 0.5 cm from the target.

The chamber is pumped by two turbomolecular pumps, one directly and the second via a preparation chamber, and both are liquid nitrogen cold trapped. Base pressures following bakeout are usually in the area of $1x10^{-10}$ mbar without liq. N_2, there is also a titanium sublimation pump in the base of the chamber.

3.3 Sample Mounting and Preparation.

The mounting of a tungsten sample is restricted by the extremely severe heat treatment required to clean it. When in its 'raw' freshly cut and polished state the main contaminant within the bulk of a tungsten crystal is carbon, and the easiest and quickest way to remove it is to convert it to CO and desorb it.This process requires the sample to be heated to a temperature in excess of 1800 K initially.

Cleaning is carried out *in situ* under a pressure of $1x10^{-6}$ mbar of oxygen. The

bulk contamination must first be brought to the surface, and this is effected by heating the sample to around 2000 K (28 mV), where it combines with the oxygen to form CO and is desorbed. In order to purge the sample completely this heating of the sample must be carried out many times in between which it is allowed to cool to near room temperature adsorbing oxygen as it does so. This cycling procedure is controlled automatically until the pressure of CO in the chamber as monitored on the mass analyser remains constant during a complete flashing-cooling cycle. At this point the sample is free of bulk contamination and has a heavily oxidised surface which is removed by heating the sample in U.H.V. to around 2600 K (32 mV). It is the high temperatures required that dictate the mounting arrangement.

Most of the samples used are roughly circular and about 1 mm thick (the stepped samples used for the thermal roughening observations are the exception to this, being 3 x 5 mm for the {610} and 2.5 x 3 mm for the {320}) and in order to reach the temperatures required to flash off the oxide it is necessary to employ electron bombardment. This requires electrical isolation, but there is also in the case of the more reactive surfaces a need to cool the sample quickly to maintain a low level of contamination from the background before and during a scan. However most 'off-the-shelf' manipulators cool the sample via a copper braid/cooling tank arrangement and the rate of cooling is restricted by the thermal conductivity of the electrical insulators. In order to circumvent this slow cooling problem we have sacrificed azimuthal rotation and effectively electrically isolated the cooling tank allowing the sample to be mounted directly onto a tungsten hairpin which is clamped to the tank. Now the only restriction on the cooling rate is the thermal conductivity (dependent on its cross-sectional area) of the hairpin. 0.250 mm and 0.125 mm diameter tungsten wires were used for the hairpin. The cooling curve for a .250 mm hairpin is shown in

Figure 3.1.

The cooling tank takes the form of a hollow stainless steel manipulator probe, the base of which terminates in a specially machined block of OFHC copper; the two are silver soldered together. This arrangement is mounted on a differentially pumped rotary feedthrough (DPRF) allowing 360° of uninterrupted rotation. The filament is supported on two tantalum tabs bolted onto a stainless steel collar which is simply clamped to the probe about 2 cm above the copper block; two alumina ceramics are used to isolate the filament from the probe (Figure 3.2). The filament itself is a coil of 0.250 mm tungsten wire and should ideally be less than 0.5 mm away from the sample to reduce the requirement for excessive currents and hazardous voltages. Heating of the supply leads (F-Glass) and subsequent release of potential surface contaminants (F, CO, and related hydrogen compounds) can occur if the filament current necessary to heat the sample to flashing temperatures is too great.

During sample heating the filament is earthed externally and usually run at a current in the range 5.0–6.5 Amps. At the same time the sample is held at high positive voltage, typically between 500 V and 700 V although a bad mount can require up to 900 Volts, to accelerate the slow thermal electrons generated at the filament. Emission currents between the filament and sample are typically measured at around 200–250 mA, which should be sufficient to heat the sample to almost 3000 K in less than 15 seconds. The high voltage power supply is of a Daresbury in-house design capable of providing a maximum voltage of 3 kV while drawing 300 mA emission current.

An advantage to using this type of probe is its contribution to the maintanence of the vacuum. It is necessary to flash the sample before and after each gas dose or clean surface spectrum. When doing so the liquid nitrogen filled probe acts in the

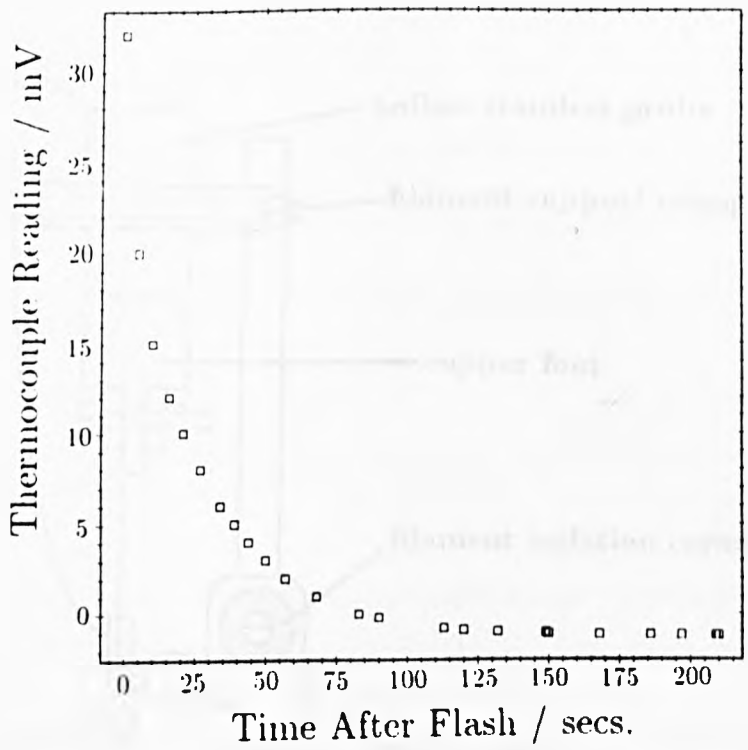

Figure 3.1

Cooling curve for a tungsten sample heated to 2500 K on a liquid nitrogen cooled probe. Sample heating was terminated at t=0 and the 8 mm diameter sample was supported on a .250 mm tungsten hairpin.

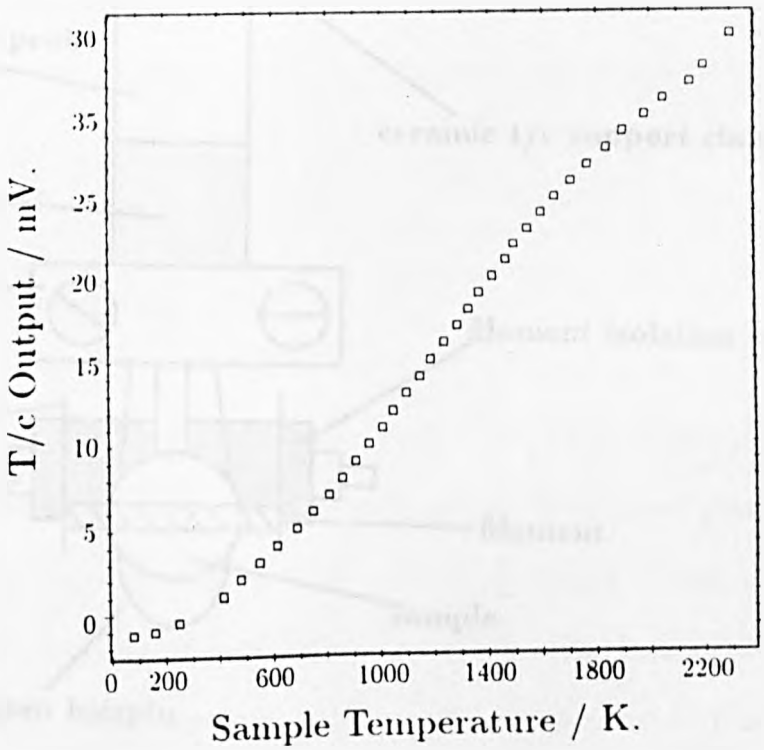

Figure 3.3

Thermocouple calibration curve for the non-standard W-Re(3%)/W-Re(25%) thermocouple which was attached directly to the sample for all of the experiments described.

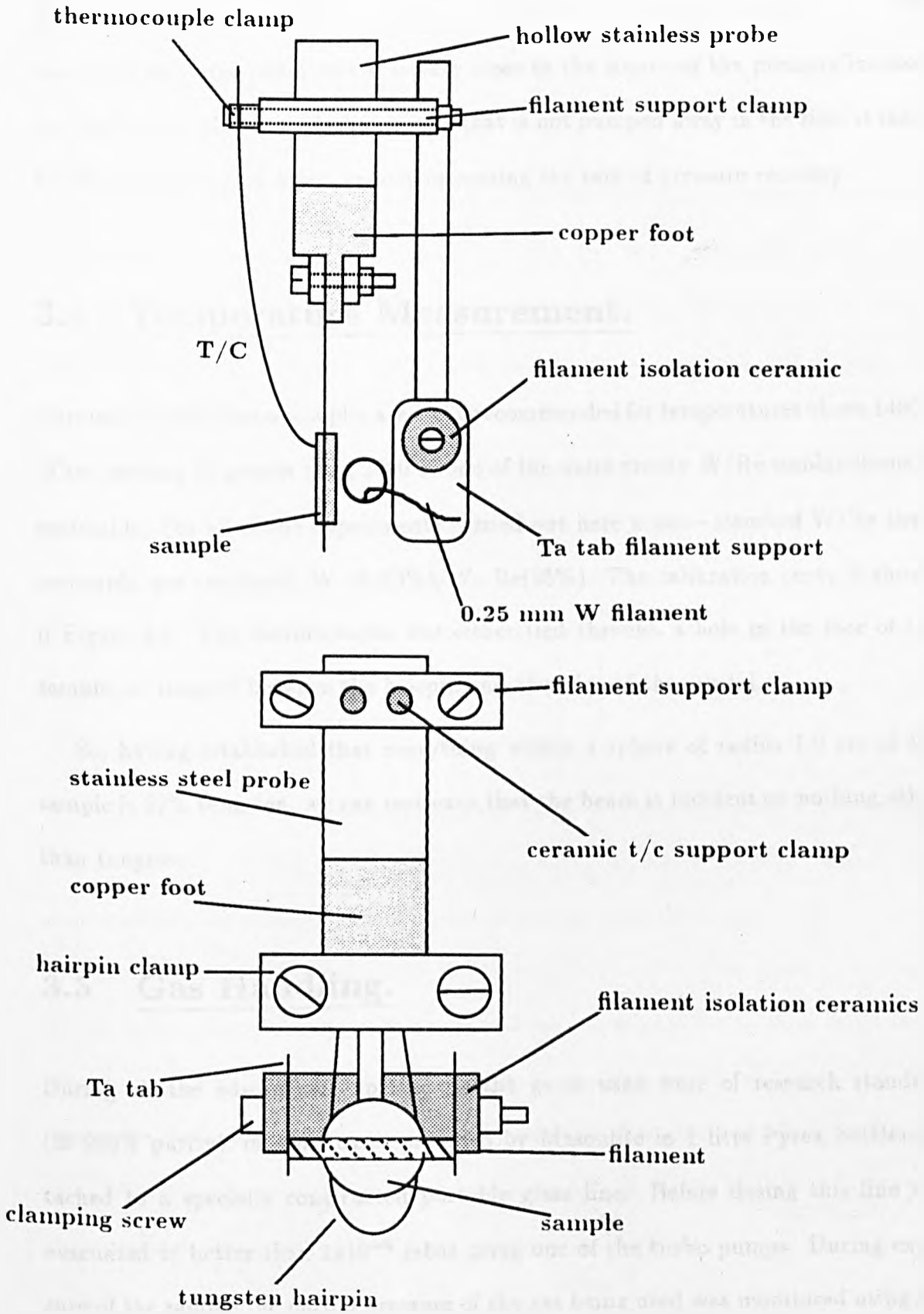

Figure 3.2

Details of the sample mount showing points of electrical isolation, and thermal contact. Note: there is no azimuthal rotation possible.

same way as a cryo-panel, but it is very close to the source of the pressure increase i.e. the hot sample, so it adorbs any gas that is not pumped away in the time it takes for the crystal to cool down, greatly increasing the rate of pressure recovery.

3.4 Temperature Measurement.

Chromel-Alumel thermocouples are NOT recommended for temperatures above 1400 K. When heating to greater than 2000 K one of the more sturdy W/Re combinations is preferable. For all of the experiments carried out here a *non−standard* W/Re thermocouple was employed, W−Re(3%)/W−Re(25%). The calibration curve is shown if Figure 3.3. The thermocouple was either tied through a hole in the face of the sample, or trapped between the hairpin and the edge of the crystal.

So, having established that everything within a sphere of radius 1.0 cm of the sample is 99% tungsten, we can rest easy that the beam is incident on nothing other than tungsten.

3.5 Gas Handling.

During all the adsorption experiments the gases used were of research standard (99.999% purity), in some cases provided by Masonlite in 1 litre Pyrex bottles attached to a specially constructed portable glass line. Before dosing this line was evacuated to better than $1x10^{-6}$ mbar using one of the turbo pumps. During exposure of the sample the partial pressure of the gas being used was monitored using the quadrupole mass spectrometer, and the indicated reading corrected for variation in relative sensitivity. Impurity concentration was always in the range of 0.001−0.010 %.

3.6 The Beamline.

The light passes through several optical stages before becoming incident on the sample in the chamber, as shown schematically in Figure 3.4. After leaving the ring it passes into a mirror box which serves to divide the light into three channels, one for each of the line 6 stations. The high energy constituents of the radiation pass through this chamber undeviated to feed the SEXAFS station. Light for the two V.U.V. stations are deflected off the initial path using platinum coated silicon carbide mirrors. For the T.G.M during the first hour of beam after a refill the temperature of this pre-mirror (horizontally deflecting) is raised to some equilibrium value, and as it does so it distorts slightly and the beam becomes misaligned with the monochromator entrance aperture. This affects the intensity of the light incident on the sample and so it is necessary to re-align the pre-mirror accordingly.

During this period of the lifetime of the beam it is also quite important to check the maximisation of the zero order radiation using the beam monitor , which is the last item to be encountered by the beam before entering the chamber. When dealing in alterations of core level shifts of the order of 100 meV or less small variations in photon energy become crucial if not monitored. It is possible to keep track of the photon energy by periodically scanning across the Fermi level; if this is done after each core level scan then the problem of mono-drift does not arise since the spectra may be related directly to the Fermi level photelectron kinetic energy and converted to a binding energy scale. That is the procedure applied here.

The chamber is situated at a height of about 8 feet above the plane of the storage ring and as a result the beam must be vertically deflected. This is achieved by the inclusion of a second mirror between the pre-mirror and the monochromator.

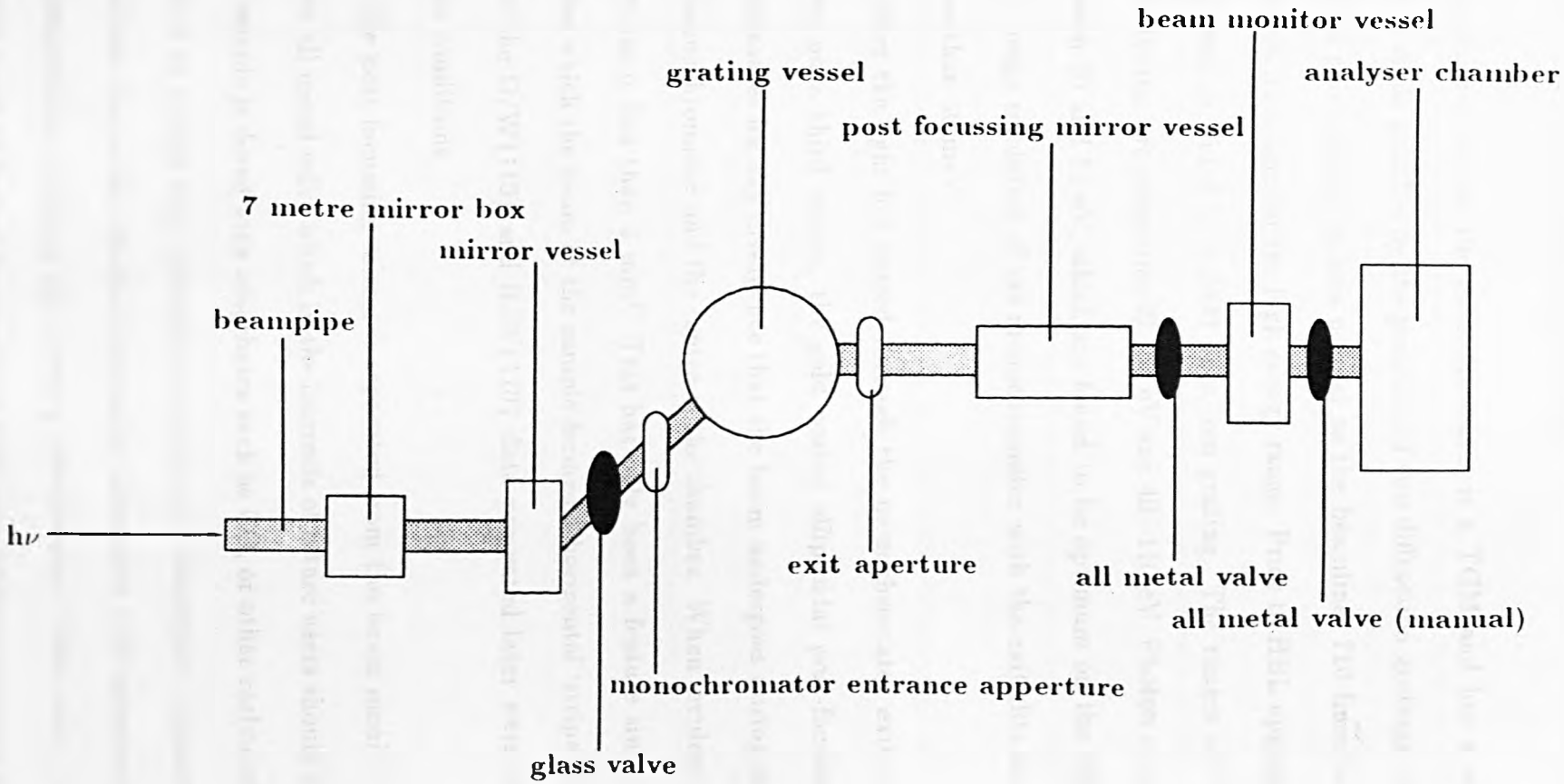

Figure 3.4

Schematic representation of beamline 6.2 at the SRS, Daresbury.

3.6.1 The Monochromator.

As mentioned earlier the monochromator is a TGM and has a split energy range. This is made possible by the presence of two diffraction gratings which rotate in the vertical plane about an axis normal to the beamline, 710 lines/mm for low energy and 1800 lines/mm for the high energy range. Prior to HBL upgrade the high energy range was provided by a 2400 lines/mm grating. The ranges are roughly split into the following two catagories 10−60 eV and 40−110 eV. Photon energies used here are between 60 and 85 eV, which are found to be optimum on the high energy grating. The energy resolution of the monochromator with the exit slits set to the maximum is less than 50 meV.

After the light has passed through the monochromator exit slits it becomes incident on a third mirror, the gold coated ellipsoidal post-focussing mirror, which compensates for any divergence that the beam undergoes during its passage between the monochromator and the centre of the chamber. When incident on the sample the spot size is less than 2 mm^2. This has only been a feature since the HBL upgrade before which the beam at the sample formed a horizontal 'stripe' 1x10 mm in dimension; the O/W{110} and H/W{110} data presented later were collected under the latter conditions.

The post-focussing mirror is separated from the beam monitor vessel by a pneumatic all metal valve which in the interests of future users should be closed whenever the sample is dosed with adsorbates such as CO, or other carbon related compounds. This is to ensure that the optical surface and absorption characteristics do not deteriorate due to the effects of excessive adsorption and subsequent photon induced decomposition, reducing the mirror's effectiveness. When using tungsten where the sample must be heated frequently to high temperatures releasing in some cases up to

$1x10^{-8}$ mbar of CO and related compounds, the mirror must also be isolated during sample flashing.

The beamline has only two user-operable components (apart from the manual grating exchange mechanism), the pre-mirror fine tuning and the monochromator exit slit width which must be set separately for each photon energy chosen. The value is calculated by the station software in the monochromator driving routine. The combined resolution of both monochromator and analyser at 70 eV photon energy is around 160 meV.

All sections of the beamline apart from the beam monitor vessel are protected from pressure bursts in the chamber, and adjacent sections , by pneumatically operated all-metal valves linked to a bank of pressure trips. These trips are initiated by a series of ion gauges monitoring each sectional pressure. In this respect the beamline and ring (which is protected by a fast flap valve) are user−proof ..... almost.

A detailed breakdown of the beamline, and the operational physics involved may be found in the appropriate Daresbury technical support documents.

Chapter 4

Experimental Results

4.1 Introduction.

Brief Overview.

As discussed in previous chapters spectroscopically observed surface core level shifts are the result of the modification of the screening potential and initial state perturbations brought about by the presence of the surface. In addition to this effect a further shift may be induced during adsorption since in most cases of adsorption there is at least a small amount of charge transfer involved, both the direction and magnitude of which are clearly reflected in the core level spectra. A decrease in core level binding energy is indicative of charge transfer from the adsorbate to the substrate, and more weakly bound species produce a smaller alteration in binding energy. These two properties combined make surface core level spectroscopy (SCLS) a useful tool for determining the number of adsorption states and adsorption site of an atom or molecule on a surface [1]

The results presented here involve adsorption of various di-atomics on W{110}. The W $4f_{7/2}$ core level of the {110} surface readily lends itself to studies of this kind for two reasons. Firstly, the width of the band is narrow compared with the magnitudes of the shifts observed, and secondly the clean surface spectra may be unambiguously decomposed into two components [2], see Figure 4.11, with a splitting

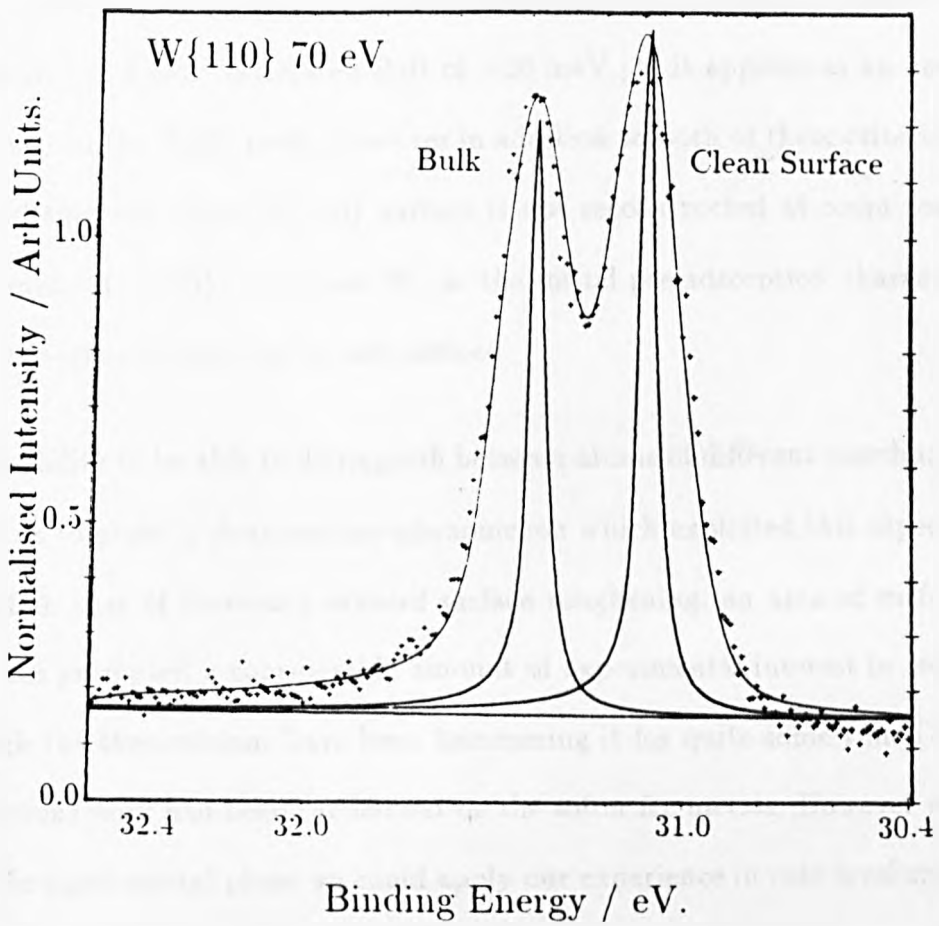

Figure 4.11

Fitted W $4f_{7/2}$ core level spectrum taken from a clean {110} sample at 80 K under Normal emission. Photon energy is 70 eV, and the incidence angle is 70° to normal. The crosses represent the actual raw data points, the solid peak shapes are the Doniach-Sunjic lines without any gaussian instrument or phonon broadening included, and the solid line describing the data points is the sum of the individual peak inclusive of all broadening factors. The narrow spectrum below the main one is a difference spectrum between the data points and the best fit line.

of 298 ± 10 meV, the top layer atoms having lower binding energy. Since the first underlayer differs in coordination number from the bulk by only one next next nearest neighbour, and has an estimated shift of −20 meV [3], it appears as an unresolvable component of the 'bulk' peak. However in addition to both of these criteria it should be noted that the clean W{110} surface is not reconstructed at room temperature [4, 5], unlike its {100} couterpart [6], so the initial pre-adsorption characteristics of the core level spectrum can be well defined.

The ability to be able to distinguish between atoms of different coordination number led us to probe a clean surface phenomenon which exploited this aspect of SCLS to the full, that of *thermally induced* surface roughening, an area of surface science which has prompted a considerable amount of experimental interest in recent years, although the theoreticians have been hammering it for quite some time [7]. Most of the previous work had been carried out on the softer fcc metals. However we felt that given the right crystal plane we could apply our experience in core level spectroscopy of tungsten surfaces to this area. The reason for this being that the magnitude of the shift is dependent on the chemical environment of the photoexcited atom. It has been demonstrated [10] that there is an almost linear relationship between effective coordination number and magnitude of observed shift. The associated straight line plot is shown in Figure 4.12. With this in mind the W{610} with its relatively open terraces of {100} orientaion was chosen and the results contrasted with those for W{320} which has close-packed terraces as mentioned above.

Unfortunately due to software/hardware problems it was not possible to complete analysis of this data in the alloted time. As a result the data will not be discussed in this work, but will form the basis of a forthcoming publication. this also applies to the discussion of CO adsorption on W{110}.

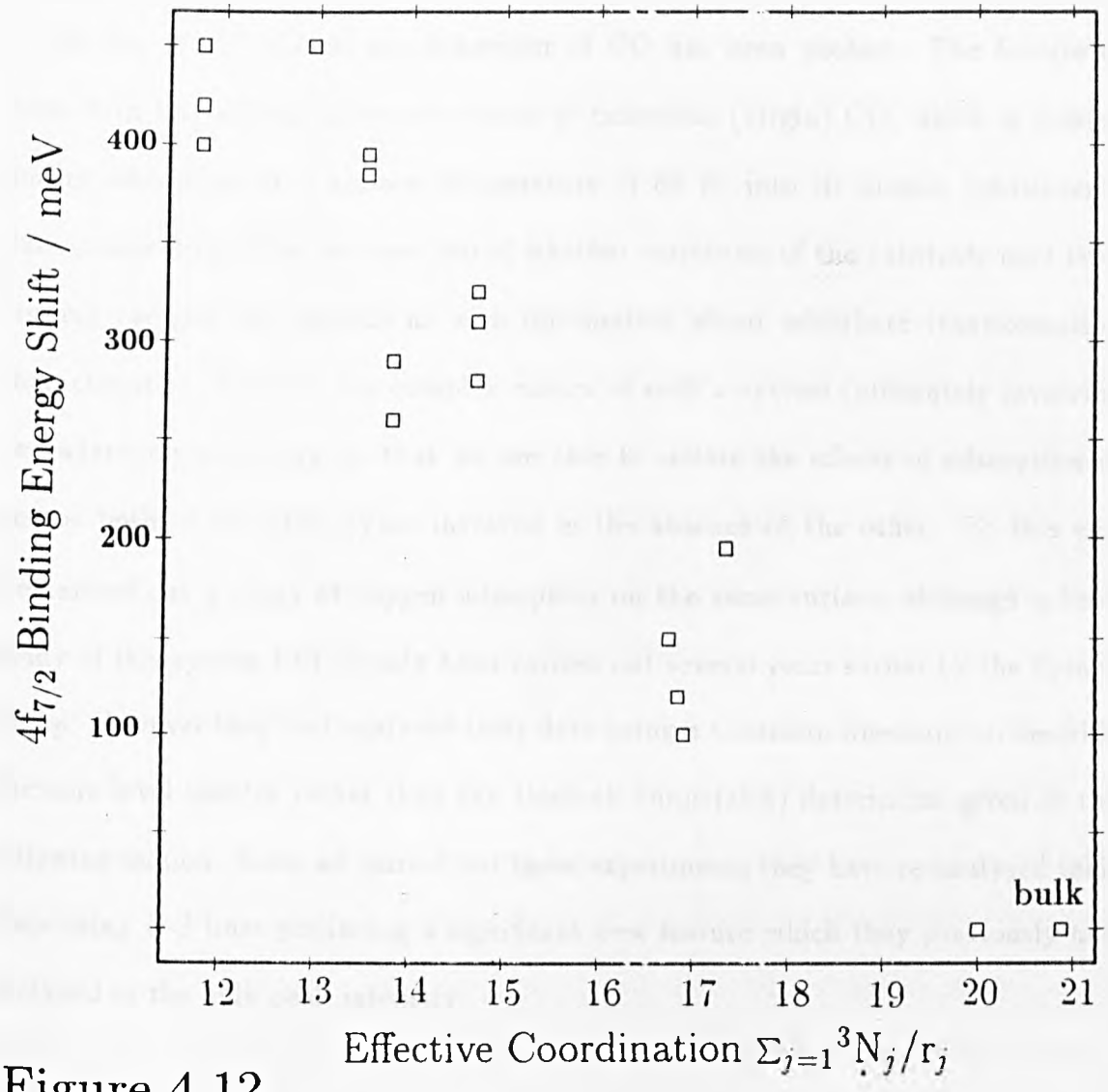

Figure 4.12

Plot of estimated shift of the W $4f_{7/2}$ core level with effective coordination number reproduced from Purcell et al [10].

On the {110} surface, the behaviour of CO has been probed. The feature of interest in this system is the conversion of molecular (virgin) CO, which is formed during adsorption at a surface temperature of 80 K, into its atomic constituents during annealing. Here we have tested whether variations of the substrate core level binding energies can provide us with information about adsorbate transformation characteristics. However the complex nature of such a system (ultimately involving two adatom types) requires that we are able to isolate the effects of adsorption of one or both of the atom types involved in the absence of the other. To this end we carried out a study of oxygen adsorption on the same surface, although a brief study of this system had already been carried out several years earlier by the French group. However they had analysed their data using a Gaussian lineshape to describe the core level spectra rather than the Doniach-Sunjic(D-S) description given in the following section. Since we carried out these experiments they have re-analysed their data using D-S lines producing a significant new feature which they previously had included in the bulk peak intensity.

Hydrogen forms a (2x1) overlayer structure on the {110} surface of tungsten when adsorbed at 80 K, and there has been much controversy as to whether more than one type of adsorption site is occupied. Evidence for and against the co-existence of two adsorption sites comes from a variety of techniques, including an SCLS study carried out again by the French group. However, in addition to this the overlayer undergoes a symmetry reducing transition at 300 K, and there are also several views as to the exact nature of this transition. This includes the proposal that a surface reconstruction is responsible. Since this technique has been applied to the study of surface reconstructions [8] before we saw here the possibility of reconciling this question.

The fact that surface atom core levels can be separated from bulk and underlayer atom core levels provided us with the possibility of studying the underlayer adsorption of nitrogen on the {110} surface of tungsten. It was then thought that having characterised the effects of this system on the W 4f core levels, the basis was laid for a study of the same adsorbate on a stepped tungsten surface of principally {110} character. The driving force behind this line of investigation was the question as to whether surface core level shift spectroscopy could be used to distinguish *site dependent adsorption* at steps and defects. Since nitrogen is thought to populate W{110} via dissociative adsorption at {100} step sites it seemed a logical progression to apply the technique to the N/W{320} system. The {320} surface of tungsten is composed of {110} terraces 3–4 atoms wide, and {100} steps. In this way it was hoped to observe the formation of a β-N species similar to that seen on the {110} surface via initial adsorption at the steps. However the resultant spectra could realistically be decomposed into at least seven well separated components each of which could be due to more than one substrate/adsorbate combination. This therefore made a complete analysis of the processes occuring at the surface impossible under the present restrictions of resolution.

The photon energies used for these experiments vary between 60 and 85 eV which produces photoelectrons from the bulk 4f core levels (binding energy 31.4 eV) in the kinetic energy range of $\approx$ 24-44 eV, exhibiting escape depths between $\approx$ 5 and 9 Å [9]. For tungsten {110} with its interlayer spacing of 2.24 Angstroms, and less than 2% relaxation in the first interlayer spacing [4] this means we are in a highly surface sensitive regime, sampling a maximum of only 3 to 4 layers. This surface sensitivity is clearly demonstrated in the clean surface spectra of the {110} surface (Fig. 4.11) taken at normal emission with a photon incidence angle relative to the surface normal

of 70°.

Fitting Methodology.

Spectra collected from adsorbate structures are usually a lot more complex than the clean surface spectra from which they are derived, and hence it is necessary to reduce the number of variables during the fitting procedure. With this aim in mind other members of this group sought to determine experimentally both the lineshape parameters of the W $4f_{7/2}$ core level, and binding energy positions of the bulk and clean surface contributions to the spectra [10].

The method used to obtain these parameters is quite simple in concept but highly effective. When oxygen is adsorbed at a tungsten metal surface the result is a net charge transfer towards the oxygen causing an increase in the 4f core level binding energy for the surface atoms as will be demonstrated in detail later on in this chapter. If the tungsten-oxygen interaction is sufficient it is possible to induce a chemical shift in excess of 1 eV, and this is the case when tungsten surfaces become heavily oxidised, as they (quite conveniently) do towards the end of the cleaning procedure.

Given that the initial clean surface core level shift for W{110} is ≈ -300 meV (i.e. to lower binding energy) it is clear that an induced chemical shift of +1 eV will transport the surface atom contributions to the spectrum through the bulk peak and leave them in the region of $\approx$ 700 meV to the high binding energy side of the bulk peak as shown in Figure 4.13. This effectively leaves the bulk peak standing 'free' of any surface contributions on an almost flat background, allowing us the luxury of being able to fit a single atom-type contribution without the complication of any deconvolution, and hence to accurately determine the lineshape parameters. The lineshape which best fits this feature has a Doniach-Sunjic [11] form with a lorentzian width of 50 meV and an asymmetry parameter of 0.05, in good agreement with theory

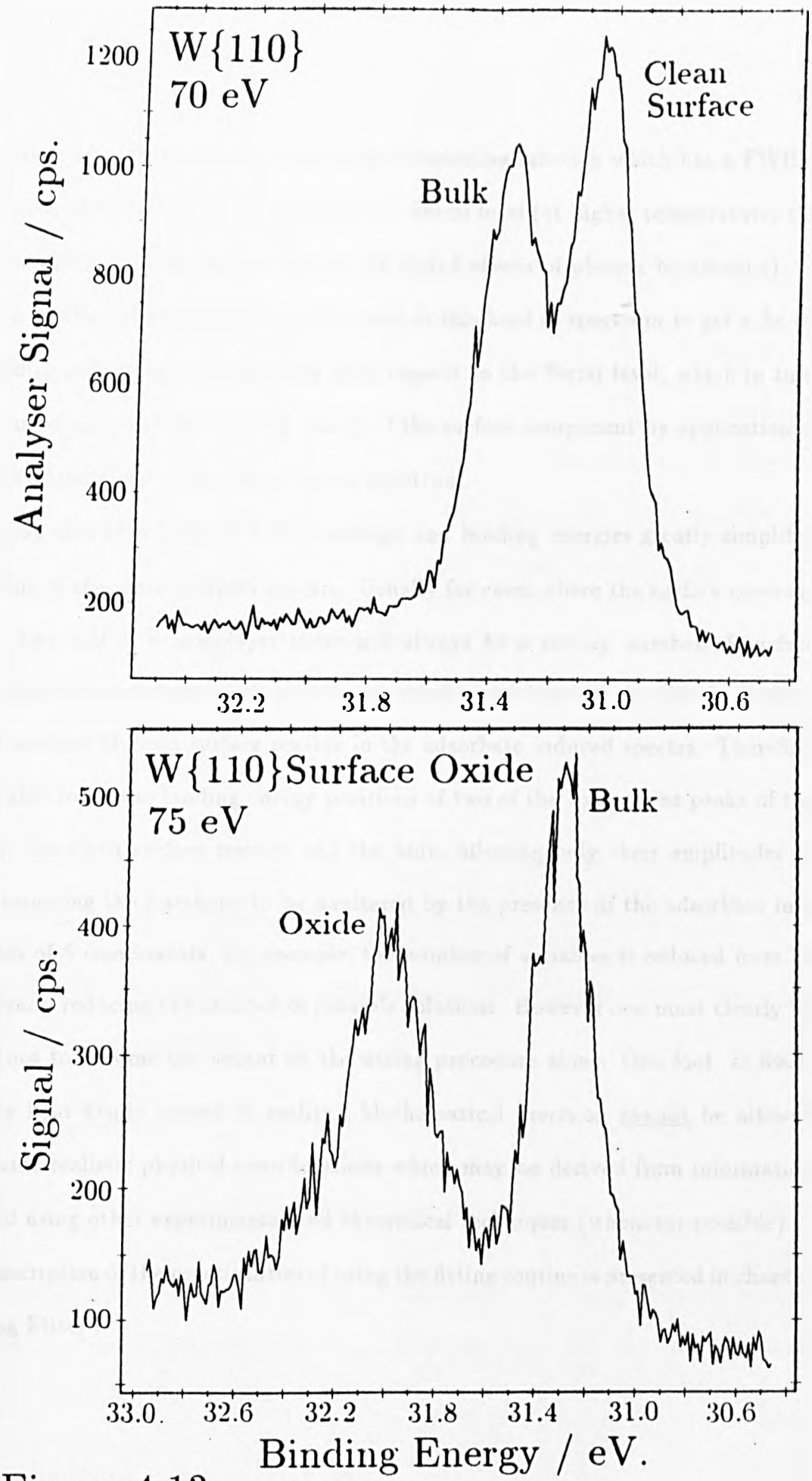

Figure 4.13

W $4f_{7/2}$ spectrum taken from a heavily oxidised W{110} spectrum showing an isolated bulk peak.

[12], convolved with a gaussian instrument broadening function which has a FWHM of 190 meV at 80 Kelvin as measured at the Fermi level (at higher temperatures the gaussian width becomes greater due to the added effects of phonon broadening). In addition to this information we are also able in this kind of spectrum to get a fix on the binding energy of the bulk peak with respect to the Fermi level, which in turn allows us to pin-point the binding energy of the surface component by application of the bulk parameters to the clean surface spectrum.

Having this knowledge of both lineshape and binding energies greatly simplifies the fitting of the more complex spectra. Usually for cases where the surface coverage is less than half of a monolayer there will always be a certain number of surface atoms which are not associated with the adsorbate, and hence there will always be a certain amount of clean surface residue in the adsorbate induced spectra. Therefore we are able to fix the binding energy positions of two of the component peaks of the spectra, the clean surface residue and the bulk, allowing only their amplitudes to vary. Assuming the lineshape to be unaltered by the presence of the adsorbate in a spectrum of 5 components, for example, the number of variables is reduced from 25 to 8, *greatly* reducing the number of possible solutions. However one must clearly be careful not to become too reliant on the fitting procedure alone. One foot, at least, must be kept firmly rooted in reality. Mathematical precision cannot be allowed to override realistic physical considerations which may be derived from information obtained using other experimental and theoretical techniques (whenever possible).

A description of the practicalities of using the fitting routine is presented in chapter 6, 'Using Fitter'.

Bibliography

[1] For examples see D. Spanjaard, C. Guillot, M.C. Desjonqueres, G. Treglia, J. Lecante Surf. Sci. Reports 5(1/2) (1985). W.F. Egelhoff Jr. Surf. Sci. Reports 6(6-8) (1986).

[2] Tran Min Duc, C. Guillot, Y. Lassailly, J. Lecante, Y. Jugnet, J.C. Vedrine Phys. Rev. Lett. 43(11) (1979) 789.

[3] A. Rosengren Phys. Rev. B25 (1981) 7393.

[4] R.J. Smith, C. Hennessey, M.W. Kim, C.N. Whang, M. Worthington, and Xu Mingde Phys. Rev. Letts. 58(7) (1987) 702.

[5] J.P. Bourdin, G. Treglia, M.C. Desjonqueres, J.P. Ganachaud, D. Spanjaard Solid State Comm. 47(4) (1983) 279.

[6] D.A. King Physica Scripta T4 (1983) 34.

[7] I.N. Stranski Naturwissenschaften 28 (1942) 425.

[8] J. Jupille, K.G. Purcell, G.P. Derby, J. Wendelken, D.A. King Structure of Surfaces II, Proc. ICSOS II (1987) Springer-Verlag, Ed. J.F. van der Veen and M.A. Van Hove.

[9] C.R. Brundle Surf. Sci. 48 (1975) 99.

[10] K.G. Purcell, J. Jupille, D.A. King Proc. Solvay Int. Conf. Austin, Texas, Springer-Verlag in press.

[11] S. Doniach and M. Sunjic J. Phys. C3 (1970) 285.

[12] D. Sebilleau, G. Treglia, M.C. Desjonqueres, C. Guillot, D. Chauveau, D. Spanjaard J. Phys. C June 30(1987).

4.2 Oxygen Adsorption On Tungsten {110} : Formation of the p(2×1) Structure.

Introduction.

The O/W{110} adsorption system has been the subject of many LEED studies in the past [1], and has proven to be quite an interesting one which, by the nature of the various phases observed, might be usefully studied with surface core level spectroscopy (SCLS). Indeed it has once before been the subject of such a study carried out by Treglia et al [2], and we shall refer to their results later in the discussion.

The adsorption can be divided into two regimes; θ<0.5 monolayer(ML), and θ>0.5 ML. For the lower coverage regime it is generally agreed that there are two coexistent phases for adsorption at T=300 K.

1. disordered 'sea' of isolated oxygen adatoms; and
2. islands of (2x1) structure

There has been some discussion as to the adsorption site of the isolated oxygen atoms which make up the disordered phase. On a W{110} surface there are several viable options: three-fold hollow, long bridge, short bridge, or the on-top site. Equally, the registry of the ordered islands with the surface (Figure 4.21) has received some attention [4, 5, 6]. These islands grow with exposure until at θ=0.5 ML the (2x1) LEED pattern half order beams show a maximum in intensity corresponding to completion of an ordered overlayer. This (2x1) structure consists of alternate rows of adsorbed oxygen atoms, and at increased exposures such that the coverage exceeds 0.5 ML the empty rows become occupied to build up an ordered p(2x2) structure [7, 8], the completion of which corresponds to a coverage of around 0.75 ML. When the coverage

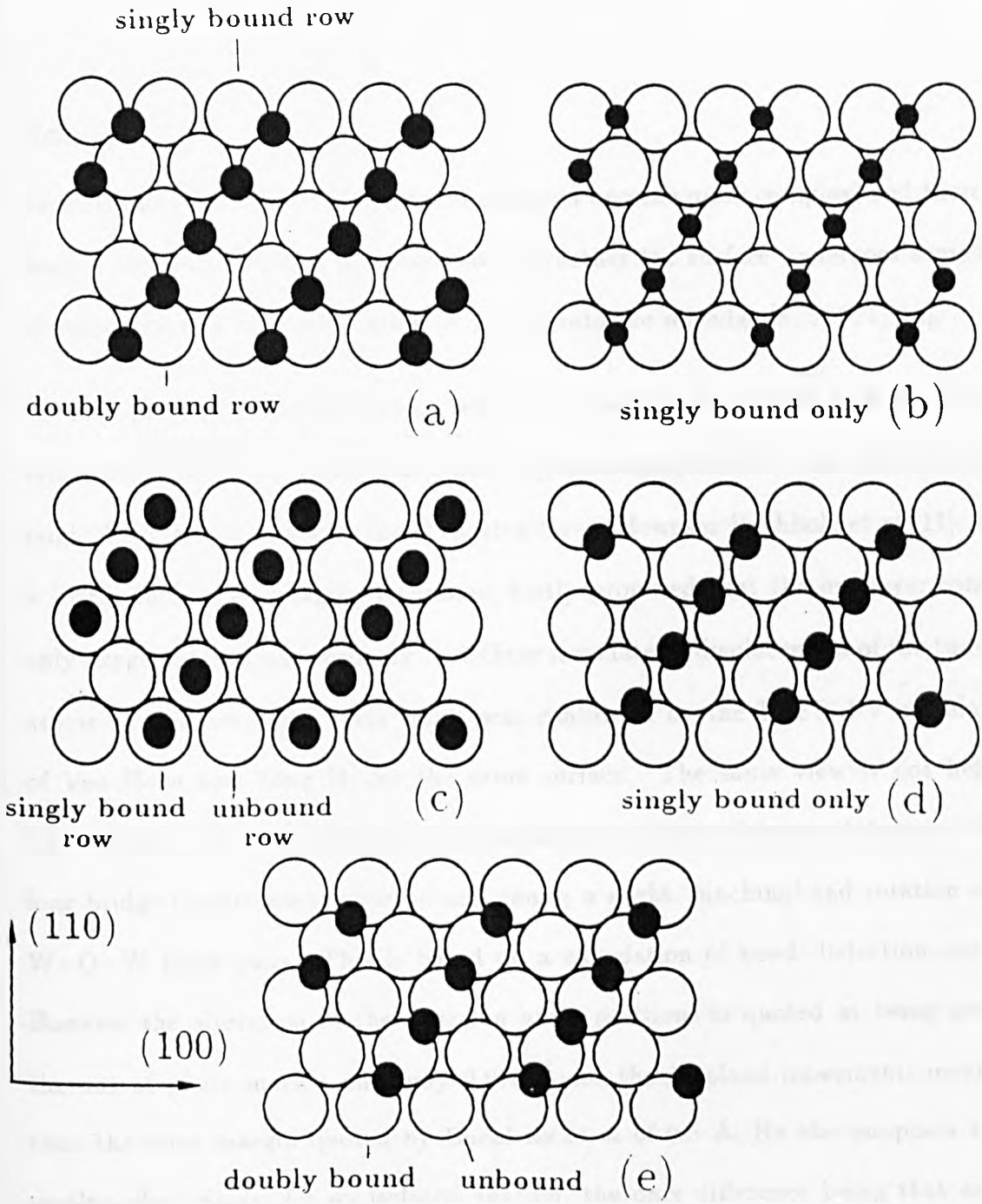

Figure 4.21

Possible binding configurations for an atomic adsorbate forming a (2x1) overlayer structure on a W{110} surface. Open circles are surface tungsten atoms. filled circles are overlayer atoms. (a) Three-fold hollow. (b) long (or distorted) bridge. (c) on-top. (d) short bridge across rows. (e) short bridge along rows.

exceeds this limit the LEED patterns observed become more complex, and there has been a certain amount of discussion as to whether the surface undergoes some kind of reconstruction or incorporation of oxygen into the selvedge [8, 5, 9, 7, 12].

The question of reconstruction was first raised in connection with the 0.5 ML structure at 300 K by Germer and May [8], who suggested that the (2x1) structure might be due to a mixed oxygen-tungsten layer. However Buchholz et al [11], using a LEED intensity averaging technique, firstly proposed that the overlayer contains only oxygen atoms, and secondly that there is no lateral displacement of the tungsten atoms at this coverage. This result was confirmed by the LEED I-V calculations of Van Hove and Tong [4] for the same surface. The same view is not held by Theodorou [5] who claims that at half monolayer coverage oxygen adatoms sit in the long-bridge (centre sites) position and causes a slight 'pinching' and rotation of the W−O−W bond pairs. This is based on a calculation of bond distortion energies. However the alteration in the tungsten atom positions is quoted as being zero for the out of plane motion and only 0.076 Å for the in plane movement, much less than the error margin quoted by Buchholz et al of 0.5 Å. He also proposes that a similar effect occurs for an isolated adatom, the only difference being that each of the tungsten atoms affected is displaced along a single direction. There is no rotation of the W-O-W bond-pairs. Engel et al [12] have carried out a detailed experimental study of this system for the low coverage regime in which they have applied LEED, adsorption/desorption kinetics determination, and work function observations. They suggest that the ordered adlayer is not reconstructed below 1700 K but, in apparent agreement with Theodorou, propose that for θ<0.1 ML the surface is reconstructed at 300 K, although they do not state the nature of this reconstruction.

Also from their data they conclude that for a coverage of 0.1 ML, 26 % of the

adsorbed oxygen is in islands which begin to merge after 0.25 ML is reached, which seems to be borne out by further work of Lagally [13, 14, 15] into the ordering kinetics of the system, suggesting that at θ=0.25 almost 50% of the adsorbed oxygen resides in islands.

The existence of a θ=0.5 ML (2x1) overlayer is well established, and in general it is agreed that the initial stages of adsorption involve island formation. However, the adsorption sites that have been proposed for the adatoms within these islands have largely been intuitive. Initial LEED I-V work of Buchholz et al [11] narrowed the possibilities down to either a short-bridge or an on-top site (Fig. 4.21). This study concentrated on primary beam energies (E_p) above 150 eV which to some extent limited the sensitivity to the overlayer, but their work was extended by Van Hove whose method of analysis spanned the range $20<E_p<200$ eV. By comparison of their calculated I-V data with the experimental curves of Lagally, Van Hove and Tong placed the oxygen adatoms in the three-fold adsorption sites equidistant from all three tungsten atoms. Theodorou disputes this result claiming that the energy difference between the 3-fold site and the long-bridge (centre) site, which he uses, is quite small. In fact the data of Van Hove do show reasonable agreement with those for Buchholz et al [11] for both the long-bridge and 3-fold sites. Engel et al refer to on-top sites for their discussion of the (2x1) phase.

More recently DiNardo et al [6] used HREELS to study the low coverage regime. By comparison of their data to that taken from the H/W{110} and O/W{100} adsorption systems they conclude that the adsorbate layer undergoes a coverage-dependent bonding rearrangement. At low coverages there is only a single loss peak occuring at 67 meV, which they attribute to the symmetrical stretch of a bridge-site but this apparently shifts to 72 meV at higher exposures which they assign to the stretching

mode of an oxygen atom in the 3-fold site. Also at these higher coverages they observe an extra feature at 47 meV indicative of a 'wagging' mode for an oxygen adatom in a threefold site. They also do not rule out the possibility of surface disordering induced by adsorption, which they draw from the results of Rutherford backscattering experiments.

In addition to the coexistence of two distinct phases during adsorption at 300 K the nature of the adsorbed layer changes as the surface temperature is increased. In fact it undergoes an order-disorder phase transition as the temperature is raised; the transition temperature at θ=0.5 is around 700 K [16, 17, 12]. Buchholz et al find that the transition involves only one type of binding site (at this time they were applying the on-top site) and involves random occupation of the empty rows of the (2x1) structure, as indicated by the behaviour of the LEED beam intensities with temperature. The observed increase in angular width of these beams points to the loss of long-range order. In an extension of this work Wang et al [10] constructed a phase diagram showing the transition temperature to be heavily dependent on coverage; above θ=0.35 ML the transition occurs at around 700 K, below θ=0.30 ML disorder occurs at around 450 K. They describe the low coverage regime as being a p(1x1) sea containing p(2x1) island 'precipitates'.

The same effects were observed by Engel et al, ie the variation of beam intensity and angular width, and using these data Ertl and Schillinger [18] were able to apply a monte-carlo simulation technique to determine values for the indirect adatom-adatom interaction energies. They find there to be nearest neighbour repulsion and next-nearest-neighbour attraction along the $(\bar{1}11)$ direction, and nearest neighbour attraction along the $(1\bar{1}1)$ azimuth.

This investigation includes only the low coverage regime $0<\theta<0.5$. A detailed

LEED, TDS, and work function study for the high coverage phases has been reported by Bauer and Engel. The only aspect of this that is of interest to us here is the formation of a p(2x2) structure between $0.5<\theta<0.75$ ML, for adsorption at a surface temperature of 300 K.

The oxygen on W{110} system has also attracted some interest prior to this in the field of core level spectroscopies. Barrie et al [19] observed the effects of adsorbing a monolayer (20 L) of oxygen on the binding energies of the W $4f_{7/2(5/2)}$ core levels using Al K_α radiation. Similar studies of the effects of tungsten oxide formation on these levels have since been carried out by Himpsel et al, and Morar et al [20, 21] using the much lower photon energy of 110 eV. Most of this work has been confined to polycrystalline samples in an attempt to link the magnitude of the observed shift directly to oxidation state of the substrate. The most recent detailed surface core level shift study similar to our own of the formation of the (2x1) phase was made by Treglia et al [2] who originally chose gaussian lines with which to fit their data, but which they have since re-analysed using the same Doniach-Sunjic lineshape parameters that we have applied here. In their latter treatment of the data there emerges an extra feature which corresponds to a peak they originally proposed to be coincident with the bulk peak. Within the tight-binding approximation they have calculated the expected shifts in the W and Ta 4 $f_{7/2}$ core levels for the case of an isolated oxygen atom in a threefold site and for tungsten atoms within (2x1) islands. In the case of an isolated adatom they propose that there should be two extra surface shifted peaks in addition to the reduced clean surface contribution, due to two different types of W-O bonding interaction (they apply Van Hove's model of three equal W-O bond lengths). There is qualitative agreement between theory and experiment. For the complete (2x1) phase they observe two new peaks of almost equal intensity (the clean

surface peak is zero at this point).

Results and Discussion.

The spectra shown here were collected as a function of exposure (Langmuirs) and the surface coverages were estimated from the curve shown in Figure 4.22, which was constructed from sticking coefficient measurements and exposure curves published elsewhere [9-11].

In the following the terms singly-bound and doubly-bound refer to tungsten atoms which are bonded to one and two oxygen atoms respectively. To a certain extent for adsorption at $T_{surface}$=300 K our results bear a similarity to those of Treglia et al. However there are some discrepancies in the magnitude of the shifts concerned. The main features are listed in Table 4.21 along with a preliminary assignment of each component. They are in qualitative agreement with those of the French group and are shown in Figure 4.23. Graphical representations of the intensity behaviour of each of the component peaks are shown in Figure 4.24. They are :

1. During the course of adsorption the intensity of the clean surface peak is seen to decrease.
2. In the early stages of the adsorption there is a significant degree of intensity between the clean surface and bulk peak positions, which is reduced in the latter stages.
3. During the main part of the adsorption there is new intensity in the region to the high binding energy side of the bulk peak.
4. Near the completion of the half monolayer structure we observe the appearence of a peak positioned around +600 meV with respect to the bulk position (this feature is not as intense in the French data at this stage of

Peak	Shift w.r.t. Bulk/meV	Assignment
B	000	Bulk.
S	−298	Clean (unbound) surface.
O_I	−200	Surface bound to isolated adatom.
O_S	+200	Surface singly bound to island adatom.
O_D	−370	Surface doubly bound to island adatoms.
O_T	−610	Surface triply bound to island adatoms.

Table 4. 21

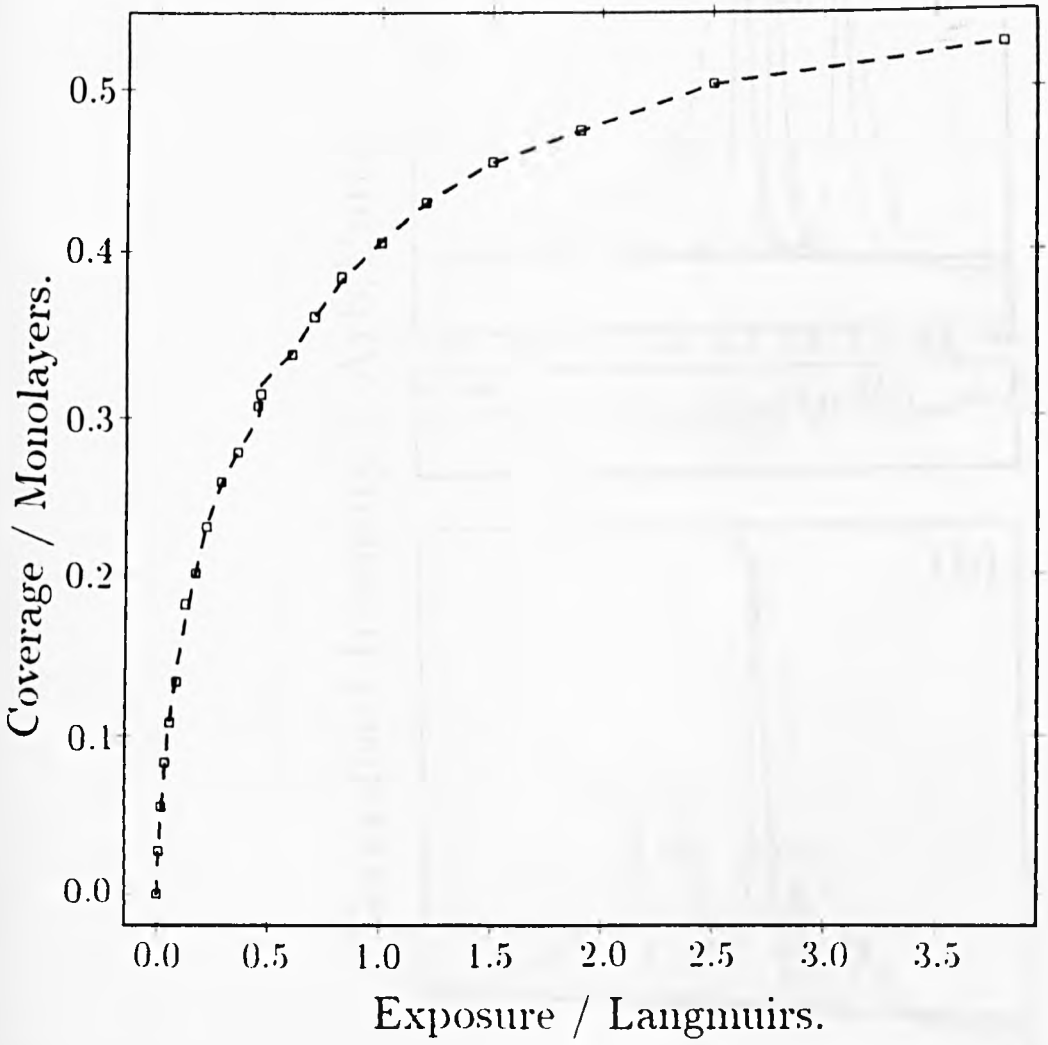

Figure 4.22

Coverage versus exposure curve for oxygen on W{110} at room temperature.

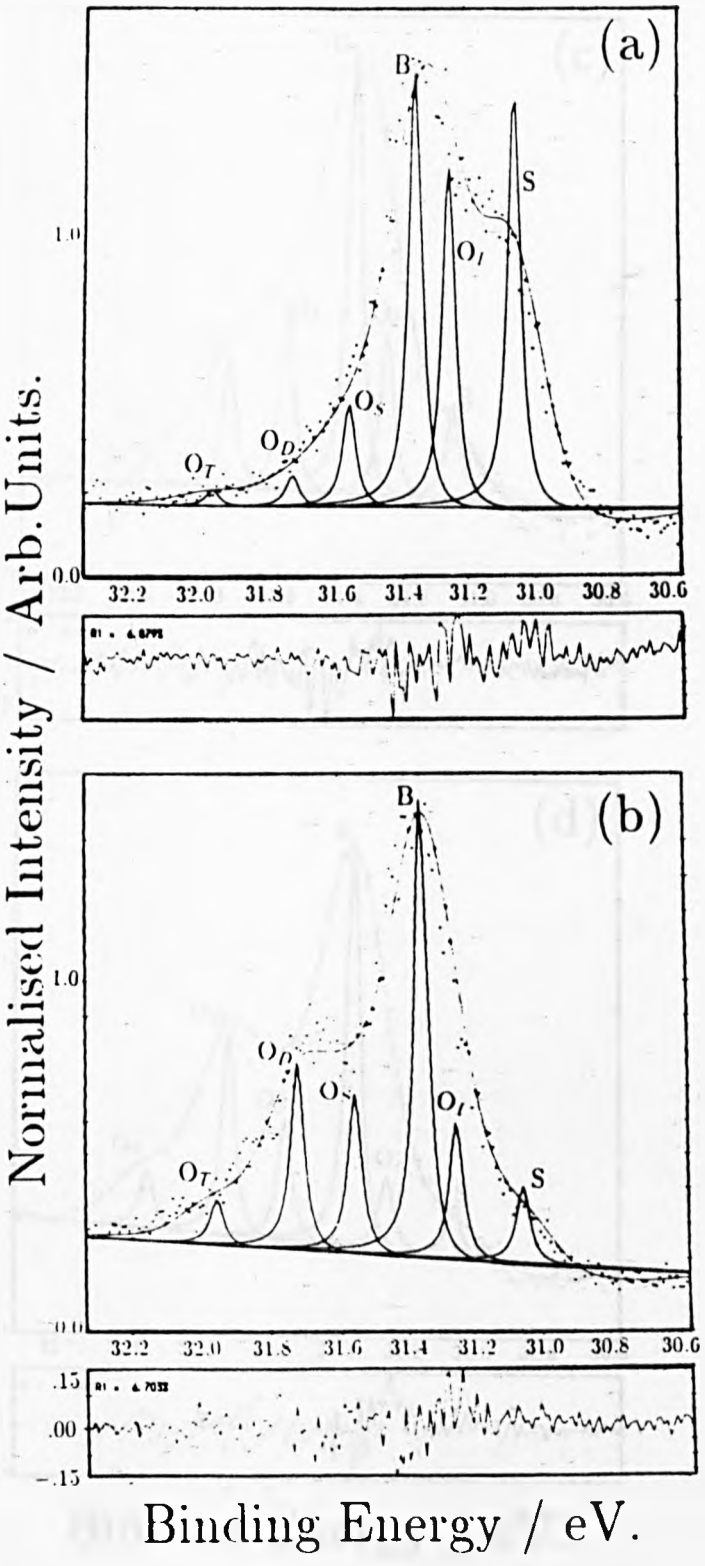

Figure 4.23

Fitted core level spectra from oxygen overlayers on W{110} at room temperature for several exposures. (a) 0.05 L. (b) 0.75 L (c) 1.25 L (d) 2.0 L. See text for explanation of individual components.

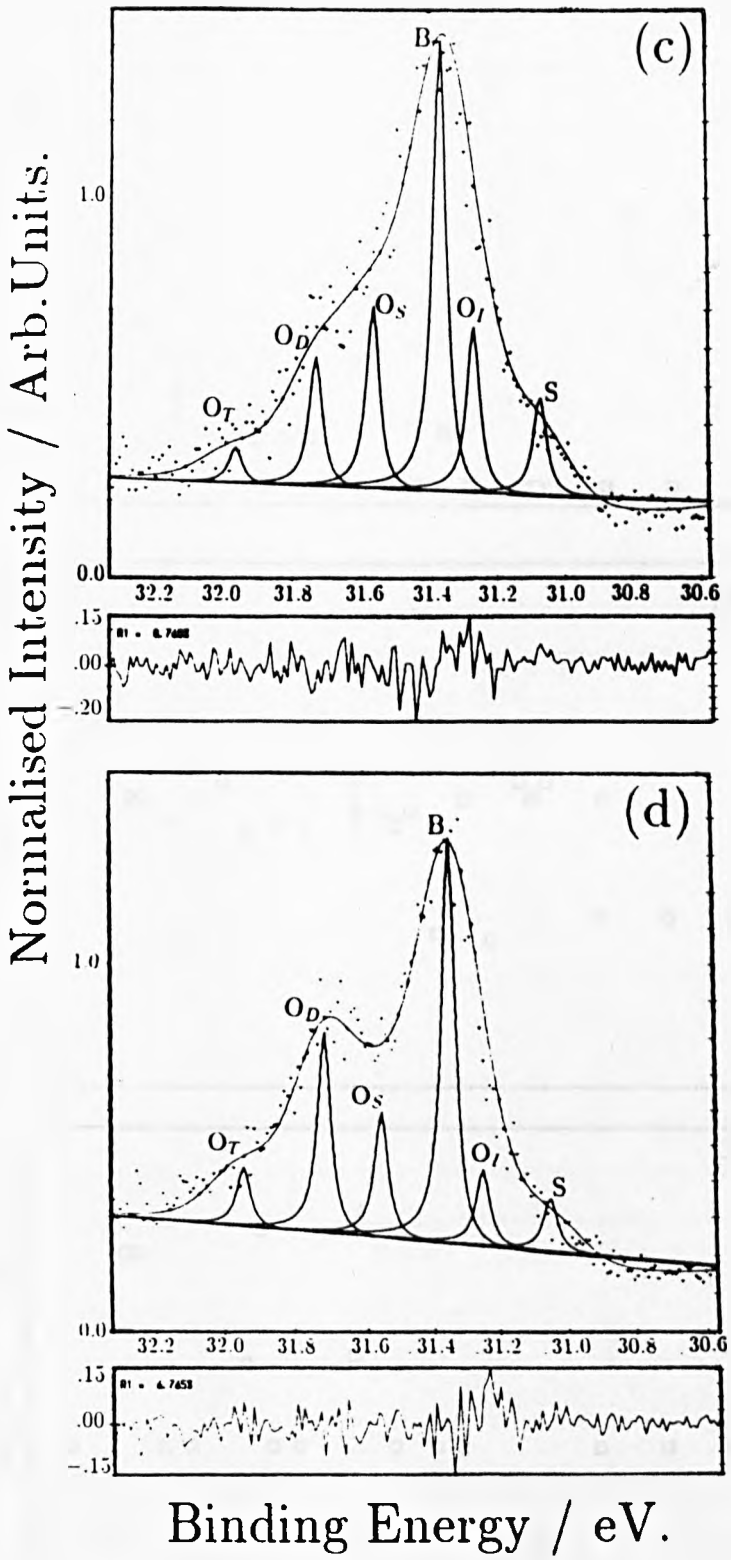

Figure 4.23(continued)

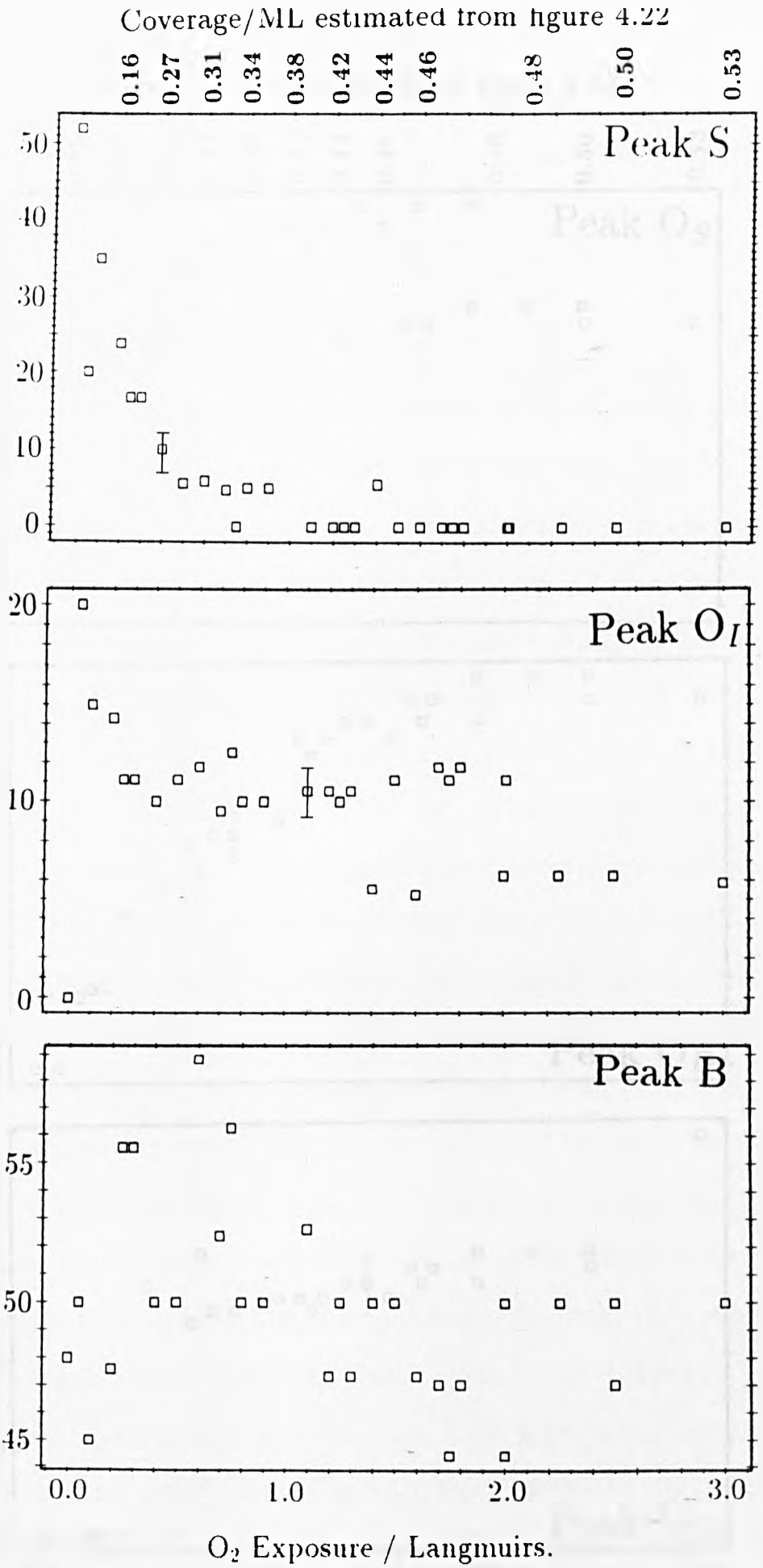

Figure 4.24

Intensity behaviour of each of the six components that make up the W 4f-$_2$ core level spectra taken from oxygen overlayers on W{110} as a function of exposure.

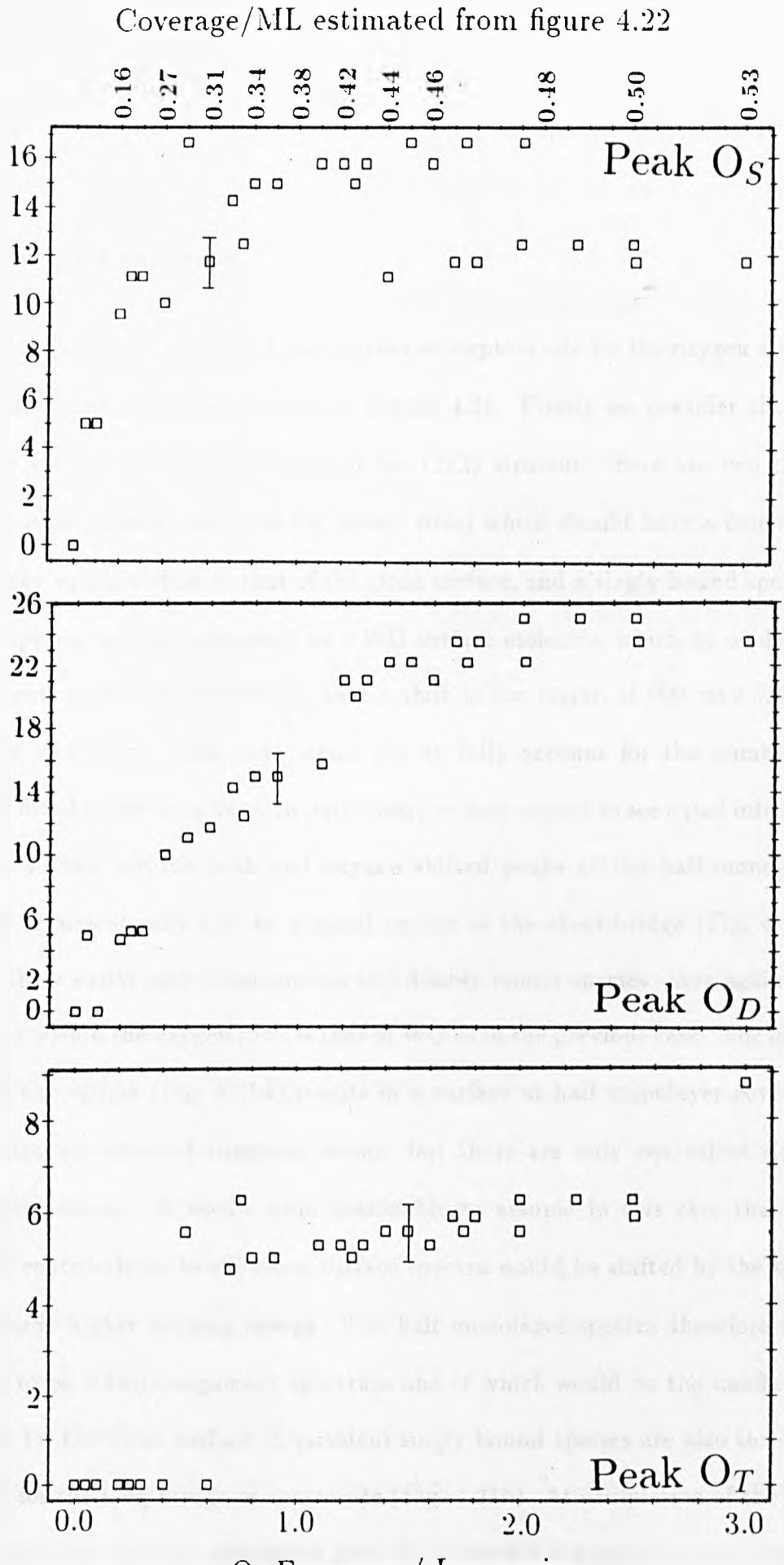

Figure 4.24(continued)

the overlayer formation).

Adsorption Site Conclusion.

The above results may be used to define a given adsorption site for the oxygen atoms. Let us consider the possibilities shown in Figure 4.21. Firstly we consider the on-top site (fig 4.21c). At the completion of the (2x2) structure there are two types of tungsten atom present; unbound (or 'clean' sites) which should have a core level binding energy equal or close to that of the clean surface, and a singly bound species. This latter species may be considered as a WO surface molecule, which by oxidation state arguments might be expected to have a shift in the region of 900 meV [20,21] (+ 600 meV wrt bulk). This case seems not to fully account for the number of components fitted to the data here. In particular, we may expect to see equal intensity of the clean surface residue peak and oxygen shifted peaks at the half monolayer point. This argument may also be applied to one of the short-bridge (Fig. 4.21e) sites where there exists only clean surface and doubly-bound species: here again the stoichiometry within the oxygen rows is that of WO as in the previous case. The other short-bridge site option (Fig. 4.21d) results in a surface at half monolayer coverage which contains no unbound tungsten atoms; but there are only equivalent singly bound species present. It would seem reasonable to assume in this case that the total surface contributions to the clean surface spectra would be shifted by the same amount towards higher binding energy. The half monolayer spectra therefore may be expected to be a two component spectrum one of which would be the unaffected bulk peak as for the clean surface. Equivalent singly bound species are also the only sites present for the long-bridge or centre site (Fig. 4.21b). At completion of the half monolayer structure the only adsorption site which offers a reduction to zero in the

intensity of the clean surface peak and more than one extra feature (as fitted here) due to oxygen binding is the threefold hollow site (Fig. 4.21a), which provides singly and doubly bound species.

Let us expand further on the intensity behaviour of these peaks individually.

Peak S

The clean surface peak (S) undergoes a smooth exponential-like decay as the exposure increases, in accordance with the coverage/exposure curve shown in Figure 4.22. In fact by the time the exposure has reached 1 Langmuir the surface peak is almost extinguished, and this corresponds to a coverage of around θ=0.4 ML.

Peak O_I

The peak labelled O_I occurs at a binding energy of +200 meV with respect to the clean surface component, which is in agreement with the position given by the French group for the shift induced by an isolated oxygen adatom. However they have calculated two binding energy contributions derived from this state. Over the greater part of the exposure range investigated here, the intensity of this peak exhibits no discernible trend. It should be pointed out, however, that quite early on in the adsorption process i.e. at θ=0.05 ML this peak is relatively large and decays quite rapidly up to 0.25 L, corresponding approximately to a coverage of 0.20 ML, at which point almost 50% of the adsorbed oxygen is in islands [12-14]. After this point the decay is more gradual, tending towards zero at an exposure in excess of 3.0 Langmuirs which is equivalent to 0.5 MLand the completion of the (2x1) structure.

This behaviour is consistent with the proposal put forward by Treglia et al, on the basis of their calculations, that the shift arising from tungsten atoms bound to

a single isolated adatom are different to those which are singly bound but lie within islands. We therefore assign this peak to tungsten atoms which are singly bound to isolated adatoms, in agreement with the French group. The former are split into two components, and the latter exist as a single feature. In their interpretation they propose that the isolated adatom state produces a contribution which is coincident with the bulk peak, but which should have double the intensity of the free component. We observe no decrease in bulk peak intensity with increasing exposure as the isolated adatoms begin to form islands. In their original analysis, based on Gaussian peak forms, this change was compensated for by a coincident peak due to the island formation. However they do not refer to any bulk peak variations for the early part of the exposure range in their re-analysis in which they resolve both island components.

Peaks O_S and O_D

Peaks O_S and O_D were originally represented as a single peak in the data presented by the French group, but in a more recent re-analysis adopting Doniach-Sunjic lineshapes they resolve two peaks as we do here. The intensity curves (Fig. 4.24) both show a general increase with increasing exposure at the beginning of adsorption. The peak labelled O_S rises to a maximum in the region $0<\theta<0.4$ ML, and then turns over and then continues to decrease up to the half monolayer point. In contrast O_D increases smoothly up to a maximum at θ=0.45 ML, near the completion of the (2x1) structure, and then levels out. It is possible to ratify these two features with the growth of the ordered (2x1) overlayer. The behaviour of O_S tends to suggest that there is some conversion occuring i.e. occupation of this state being reduced as the intensity somewhere else in the spectrum is increasing. This peak has recently been assigned by Spanjaard to the presence of tungsten atoms within islands which are

singly bound, and if we assume this to be correct then we can explain the reduction in peak O_S in the following way. At 0.45 ML the (2x1) structure is well established and it seems likely that further adsorption will occur at the empty-rows as shown in Figure 4.25(a). This corresponds to the early stages of the (2x2) structure reported by Engel and Bauer [7]. During adsorption at a threefold site within these empty rows there are two conversions occuring. Firstly an adjacent singly bound tungsten atom will be converted into a doubly bound type, and secondly the adjacent doubly bound state will become triply bound. In fact adsorption of this kind should produce no loss of intensity in the doubly bound state, which may continue to increase slowly beyond this point to the completion of the ordered overlayer, as is observed here for the peak labelled O_D. This assignment could be experimentally backed up by a study of the higher coverage regime. The (2x2) structure is formed in the region $0.5<\theta<0.75$ ML and if this assignment is correct the intensity of O_S should tend to zero as the coverage approaches 0.75 ML since there are no singly bound species in the (2x2) structure. Indeed above 0.75 ML the row filling increases producing eventually a (1x1) overlayer which consists of a single triply bound tungsten species, so above this coverage there should also be a steady decrease in the doubly bound peak O_D.

Peak O_T

O_T intensity is difficult to map due to its position at the edge of the high binding energy side of the spectra where the signal-to-noise ratio is perhaps at its worst. However there appears to be no activity in this region below θ=0.25 ML. At greater coverages things become slightly confused, but certainly this peak displays a general increase in intensity which may extend to higher coverages not shown here. We assign this peak to the formation of a triply-bound state occuring at phase boundaries

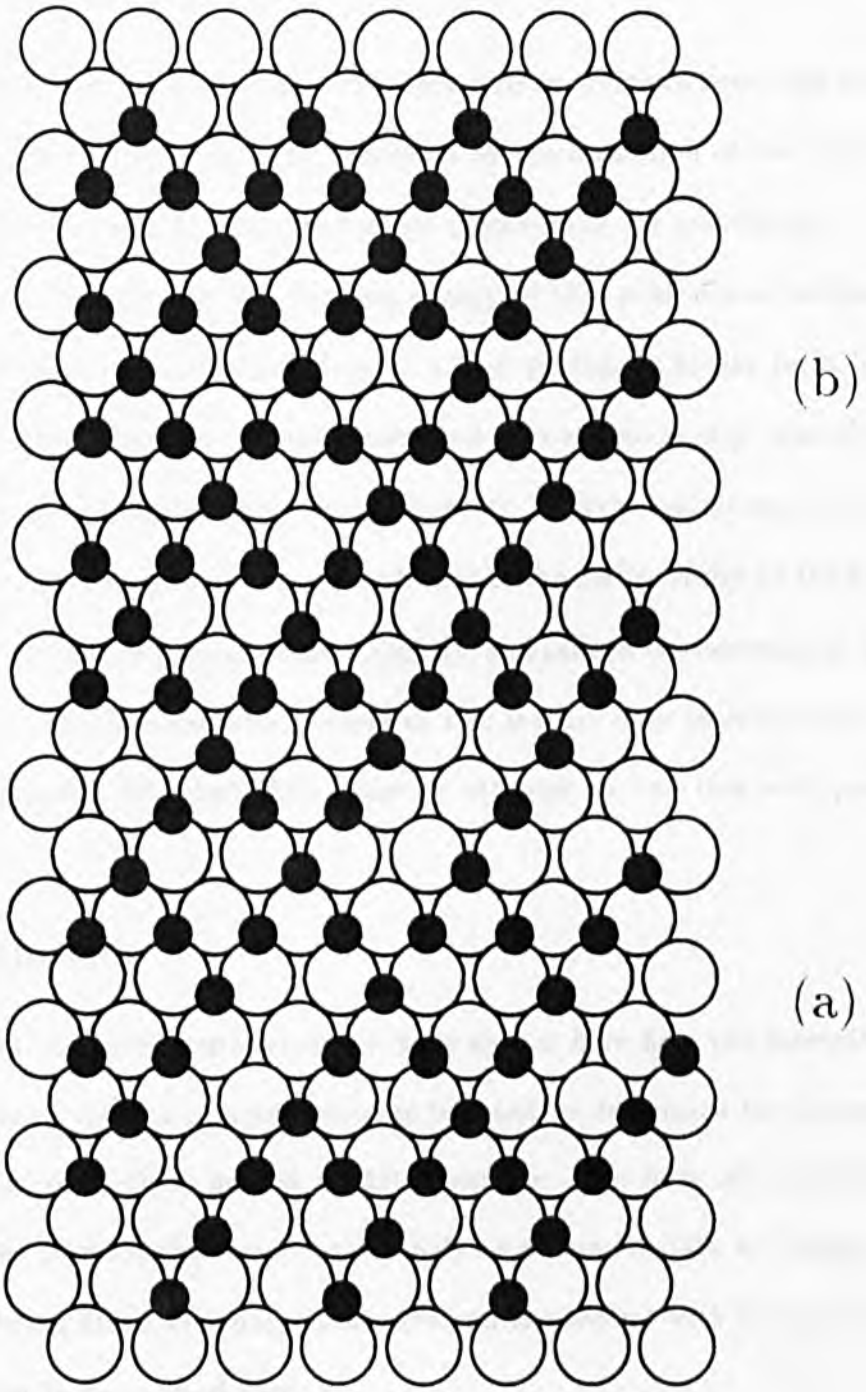

Figure 4.25

Atomic oxygen adsorption overlayer structure
on a W{110} surface (a) Early stages of (2x2) formation showing occupation of the empty rows of the (2x1). (b) (2x2) overlayer formed at θ=0.75 ML.

caused by island merging, and at higher exposures corresponding to coverages of more than 0.5 ML we expect this peak to be enhanced by the formation of the (2x2) and subsequent (1x1) structures as mentioned above (proceeding via row filling).

It is interesting to note that the binding energy of this peak occurs within the region corresponding to an oxidation state of +2 as quoted by Morar for a lightly oxidised surface. One monolayer would correspond to a stoichiometry equivalent to WO, with each surface tungsten atom being bound to 3 Oxygen adatoms situated in threefold hollows. This assignment agrees with that of the earlier study by the French group, although the energy position differs slightly, and indeed the coverage at which the peak appears. The previous study refers to this feature only in connection with their highest exposures, although they make no attempt to link this with possible coverages.

4.2.1 Conclusion.

Within the limits of experimental error we have shown here how the intensity behaviour of core level spectra components may be used to determine the adsorption site of an adatom on a close packed tungsten surface. We have also highlighted some descrpencies between the two separate analyses of similar data by Treglia et al [2, 3]. The first being fitted with pure Gaussians and the second with Doniach-Sunjic parameters similar to those used here.

Bibliography

[1] J.C. Tracey, and J.M. Blakely Surf. Sci. 15 (1969) 257.

[2] G. Treglia, M.C. Desjonqueres, D. Spanjaard, Y. Lassailly C. Guillot, Y. Jugnet, Tran Minh Duc, and J. Lecante. J. Phys. C14 (1981) 3463.

[3] D. Spanjaard, C. Guillot, M-C Desjonqueres, G. Treglia, J. Lecante Surface Science Reports 5 (1985) 1.

[4] M.A. Van Hove, S.Y. Tong Phys. Rev. Lett. 35(16) (1975) 1092.

[5] G. Theodorou Surf. Sci. 81 (1979) 379.

[6] N.J DiNardo, G.B. Blanchet, E.W. Plummer Surf. Sci. 140 (1984) L229.

[7] E. Bauer and T. Engel Surf. Sci. 71 (1978) 695.

[8] L.H. Germer, and J.M. May Surf. Sci. 52 (1975) 237.

[9] J.C. Buchholz, G.C. Wang, M.G. Lagally Surf. Sci. 49 (1975) 508.

[10] G.C. Wang, T.M. Lu, M.G. Lagally J. Chem. Phys. 69(1) 1978 479.

[11] M.G. Lagally, J.C. Buchholz, G.C. Wang J. Vac. Sci. Technol. 12(1) (1975) 213.

[12] T. Engel, H. Niehus, E. Bauer Surf. Sci. 52 (1975) 237.

[13] T.M. Lu, G.C. Wang, M.G. Lagally Surf. Sci. 108 (1981) 494.

[14] G.C. Wang and M.G. Lagally Surf. Sci. 81 (1979) 69.

[15] M.C. Tringides, P.K. Wu, M.G. Lagally Phys. Rev. Lett. 59(3) (1987) 315.

[16] J.C. Buchholz and M.G. Lagally Phys. Rev. Lett. 35 (1975) 442.

[17] W.Y. Ching, D.L. Huber, M.G. Lagally, G.C. Wang Surf. Sci. 77

[18] G. Ertl and D. Schillinger J. Chem. Phys. 66(6) (1977) 2569. (1978) 550.

[19] A. Barrie and A.M. Bradshaw Physics Letters 55A(5) (1975) 306.

[20] F.J. Himpsel, J.F. Morar, F.R. McFeely and R.A. Pollak Phys. Rev. B30(12) (1984) 7236.

[21] J.F. Morar, F.J. Himpsel, G. Hughes, J.L. Jordan and F.R. McFeely J. Vac. Sci. and Technol. A3(3) (1985) 1477.

4.3 Adsorption of Hydrogen on W{110} at a Surface Temperature T_S=80 K.

Introduction.

The H/W{110} adsorption system has generated a great deal of interest in the past having had many surface analytical techniques applied to it, the reason being the 'basic' structural nature of the hydrogen adatom which it was hoped would give a relatively uncomplicated picture of fundamental chemisorption processes. There are perhaps two main points of controversy which have arisen from these studies.

1. At full coverage are the adatoms bound in a single type of adsorption site or are there two distinct binding situations.
2. If two sites do exist, are they filled sequentially or simultaneously?

Hydrogen has a low initial sticking probability on the {110} plane of tungsten at room temperature ($\approx$ 0.07) [1, 2, 3]. Field emission studies [4] have shown that while at a surface temperature of 300 K chemisorption on the {110} plane proceeds quite readily, at progressively lower temperatures (144 K, 80 K, 66 K) the rate of adsorption on this plane decreases. In fact at T_S=38 K there is only molecular adsoption on this plane. It is therefore proposed that population of this plane is an indirect process relying on the diffusion of atomic hydrogen from rougher regions of the surface. For a single crystal of {110} orientation this would refer to defect areas such as steps presumably of {100} character, and population of the {110} plane becomes possible only after saturation of the rough regions has occurred. At 80 K the diffusion coefficient is coverage dependent varying from $3\text{x}10^{-13}$ cm^2/sec at θ=0.1 to $7\text{x}10^{-12}$ cm^2/sec at θ=0.6 ML dropping to around $2\text{x}10^{-12}$ cm^2/sec at θ=0.9 ML

[28]. Diffusion becomes more viable when the hydrogen concentration of these rough regions is high, due to adatom-adatom repulsive interactions [5]. There is a drop in the desorption energy from 35 to 20 kcal/mol at θ=0.6 ML. Such macroscopic samples will have a relatively small area of 'rough' regions and so it is expected that there will not be any appreciable delay in those regions becoming saturated and hence acting as sources for total surface population. This model seems to explain the angular dependence of the sticking probability found for the {110} surface, S_0 decreases sharply as the incident molecular beam reaches glancing incidence. At an incidence angle of ϕ=60° the ratio S_ϕ/S_0 is only 0.5 for W{110} [6, 7] an effect which is not seen on the {100} surface where chemisorption occurs directly at any pair of fourfold surface sites. There is in fact a slight increase in the S_ϕ/S_0 ratio for {100} with increasing incidence angle in accordance with classical condensation theory via momentum transfer. Plummer and Bell [9] maintained that there is only a single adsoprtion site, in agreement with the conclusions of Tamm and Schmidt discussed below.

Thermal desorption spectra [10, 1] show two peaks at T=430 K, and T=540 K which are filled sequentially. This result has been interpretted as two adsorbate states, but may also be due to lateral interactions between adsorbate atoms as the coverage exceeds 0.5 monolayers.

Initial LEED investigations carried out at room temperature [11] failed to provide new structural insights into the system due to the relatively weak scattering properties of hydrogen. But some later work by Gonchar [12, 13, 14] for low temperature adsorption (30 K) has shown the existence of a (2x1) pattern for θ=0.5 ML which becomes a (2x2) for θ>0.75 ML. The (2x1) structure disorders at around 170 K, and the (2x2) structure disorders in the region of 220 K. Saturation coverage yields a

(1x1) pattern. Similar behaviour has been observed for oxygen adsorption by several investigators and discussed in one of the earlier sections. The extra beams have low intensity but are none the less sharp, as more recently confirmed by Chung et al [15]. Matysik [16], when applying RHEED to the problem, observed only a (2x1) up to saturation coverage with apparently no reduction in intensity as the coverage exceeded θ=0.5 ML. Chung et al have raised the question of a surface reconstruction. They have monitored variations in the I-V profiles of the $(0,\bar{1})$, $(\bar{1},1)$, (0,1) and $(1,\bar{1})$ LEED beams which are all identical for normal incidence at the clean surface. As the hydrogen exposure is increased above 0.5 ML there is loss of symmetry in the form of a reduction in the number of mirror planes present, from 2 to 1. They also observe a change in the LEED pattern from (2x1) to (2x2) as coverage exceeds 0.5 ML. However, since a similar overlayer transformation occurs during oxygen adsorption without any detectable variation in the I-V characteristics of the integral order beams, they reject this as a possible cause for the observed effect. Instead, they attribute it to a lateral shift of the topmost layer of tungsten atoms such that they occupy the threefold hollow sites of the underlayer. Such an occurence would cause an increase in the effective coordination of the surface layer as those atoms moved from the bulk-like sites into the three-fold hollows of the underlayer. Under ideal conditions this would be observed in core level spectra, but would be within the limits of experimental resolution here. In their model adsorption is assumed to be initially in the long-bridge or 'hourglass', site but once the half monolayer point has been passed the entire adlayer is bound into the three-fold hollow sites.The driving force behind the lateral shift is a reduction in hydrogen-surface binding energy caused by the distortion of the potential well.

Several photoemission studies have been carried out on this system [17, 19, 20, 21]. Angle resolved spectra show two adsorption induced features at around 2.6 and 4 eV below the Fermi level which are associated with the low and high coverage states respectively. The two are sequentially occupied although occupation of the latter state begins before the former is saturated. Above 0.5 ML the intensity of the feature at 2.6 eV is seen to decrease. It has been pointed out that this intensity behaviour may be due to changes in the angular distribution of the emission and this has to some extent been corroborated by the angle integrating studies of Plummer et al [21] who recorded no attenuation in the 2.2 eV feature that they observe. A plot of peak height against work function change (their coverage monitor) reveals that the two states are filled simultaneously but at different rates. The 2.2 eV feature is favoured below half monolayer, and a feature at 3.9 eV for the high coverage regime. Their own interpretation of this data runs along similar lines to that of Tamm and Schmidt's interpretation of the TDS data, namely that of a single adsorption site i.e. the long-bridge. Within this model, as stated before, the reduced desorption energy is the result of repulsive lateral interactions within the adsorbate layer as long as the local density is greater than one adatom to two surface atoms. This accounts for the LEED structures observed by Gonchar and Chung et al but not for the RHEED observations of Matysik for the complete coverage regime. There would seem to be another problem with this assignment. The 2.2 eV peak is associated with an orbital from a molecular complex having only one hydrogen atom bound to the tungsten and the 3.9 eV feature with a double hydrogen molecular complex. If this is the case and a single adsorption site is supported then at some time during the latter part of the adsorption scheme (for example during conversion from (2x1) geometry to that of (2x2)) some sites of singular hydrogen complex must surely begin to be converted

to sites of double hydrogen complex, thus resulting in a reduction in intensity of the 2.2 eV feature for high coverages.

An interesting alternative to the single versus multiple site option has been proposed by Blanchet et al [20] who speak in terms of a coverage induced order-disorder phase transition. An important point highlighted in this investigation is that there are no new hydrogen induced features in the photoemission spectra. In fact adsorption only causes changes in photoemission intensities from surface states which are present in the clean surface spectra. The sequential occupation effects observed by previous investigators can be reproduced by altering the orientation of the incident electric vector. They state for θ>0.5 ML the hydrogen occupies a different bonding configuration than for θ<0.5 ML which to a certain extent would seem to tie in with the LEED I-V observations of Chung et al.

Blanchet et al have complimented their photoemission data with an HREELS study in which they observe two main loss features which are independent of coverage for room temperature adsorption, an observation which has been duplicated several times by other groups [22]. These features occur at 96 and 160 meV. There is a third component of the spectrum occuring at 80 meV and this appears as a shoulder on the 96 meV peak. The difference between this data and that which went before is the observance that none of these states is dipole active. (Dipole selection rule: loss features having strong maxima in the specular direction are produced by vibrational modes with dipole moments normal to the surface. Impact scattering: caused by short ranged potentials generated by vibrational modes not peaked in the specular direction.) Their interpretation of the data is that of single site occupancy of either the long bridge or the threefold hollow (they refer to this as the distorted bridge) sites and they do not seem to be constricted by the data collected using other techniques.

They ignore the EID [23] data available on the grounds that it is contradictory, and pay no heed to the RHEED observations of Matysik. They do express a suspicion that LEED stuctures should not be observed due to the weak scattering nature of hydrogen and that possibly those that have been observed are due to changes in the substrate structure. The result of this is the assumption that at low coverages the overlayer has a c(2x2) structure based on symmetry arguments. At θ=0.5 ML there is a symmetry reduction and this is accounted for by an order-disorder transition. In contrast to this Jayasooriya et al [24] propose a two site adsorption model similar to that of Holmes and King [17]. This proposal is based on comparison of the HREELS data compiled for hydrogen adsorption at a surface and vibrational information available for model cluster compounds. However this interpretation relies heavily on the work of Backx et al, as does that of Holmes and King, which was collected for a single scattering geometry and assumed dipole active behaviour. Backx et al propose the two site model using on-top and long-bridge as the possibilities whereas Jayasooriya et al put forward the short-bridge and threefold hollow as the two viable options. The 160 meV band is assigned to the bridge site here and the 96 meV band to the hollow or deformed-bridge site.

Davies and Erskine [25] have also probed this system using EELS but their study differs somewhat from those already discussed in that they follow the azimuthal dependance of the 160 meV loss feature intensity. The coverage probed was saturation but it is not clear what the adsorption temperature is; we assume that the surface is at room temperature since there is no reference to cooling the sample. The polar plot of intensity versus azimuthal angle for specular collection contains four major lobes (one in each quadrant) and two minor ones along the $(1\bar{1}0)$ axis. By comparison with results for adsorption of chlorine (which provides an isotropic dispersion with az-

imuthal angle) they concluded that dipole scattering contributes less than 30 % to the intensity of this peak. The minima observed near the $(1\bar{1}0)$ axis are consistent with the existence of an asymmetric stretching mode for the short-bridge species. Those minima in the perpendicular direction are consistent with the asymmetric stretching mode of a long-bridge species. Blanchet et al assigned this feature to the three-fold hollow site based on observations made at only two azimuthal angles corresponding to the (001) and $(1\bar{1}0)$ directions. Both groups agree that they cannot clearly distinguish between occupation of the long-bridge site and the three-fold hollow site on the basis of selection rules only. What seems evident from the work of Davies and Erskine is that two sites are occupied at saturation coverage.

From surface reflectance measurements it is possible to derive the surface dielectric function, and also therefore any changes due to adsorption. Blanchet et al [26, 27] have recorded SRS spectra for this system and the dielectric function compared with that calculated for different hydrogen configurations. They conclude that for room temperature adsorption at saturation coverage the hydrogen adatoms reside in the long bridge sites. However, they have only calculated the changes for two possible ad-sites, the long bridge and the on-top using a single site adsorption model. The single site model is again favoured in Di Foggio and Gomer's surface diffusion work [28] in which they refer to the EELS work of Backx et al and re-assign the loss feature at 95 meV to a vibration perpendicular to the long axis of the 'hour glass' of a long-bridge bonded adatom species. The diffusion path is defined by the narrow necks separating each of the 'hour-glass' features, a point which was returned to later by Blanchet et al in relation to the order-disorder transition at half monolayer coverage.

Results and Discussion.

The coverage versus exposure curve shown in figure 4.31 is reproduced from the work of Barford and Rye [3]. Figure 4.32 shows a series of spectra collected from a W{110} surface at 80 K for several hydrogen exposures. The assignment of the component peaks and their respective shifts relative to the fixed clean surface peak are given in Table4.31. Figure 4.33 shows graphically the behaviour of each of these components as a function of exposure between zero and 15 Langmuirs. The clean surface peak, as previously noted, undergoes an exponential-like decrease in intensity during the early stages of adsorption, becoming zero in the region of 4 L.

In agreement with an earlier investigation [29, 30] we see an initial filling of the H_I state which has been assigned to isolated adatoms. This feature is rapidly saturated and begins to decrease after an exposure of 1 L reaching zero at 8 L. Hydrogen adsorption on this tungsten face occurs in a similar way to that of nitrogen discussed later i.e. not on the {110} regions but on the {100} defects and step sites. Occupation of the surface is achieved by migration of the adatoms away from these defect regions [4]. Under such conditions the maximum number of isolated hydrogen adatoms that could surround such a region will be attained quite early on in the adsorption sequence. During the later stages of adsorption this intensity is provided by isolated atoms away from these islands which have perhaps migrated from edge positions. As the ordered (2x1) overlayer populates the entire surface so these single adatoms become incorporated into the final structure, thus the signal attenuates to zero.

The other two features exhibit almost exactly the same behaviour reaching a maximum at an exposure of around 8 L, one of these being the bulk peak. Their intensity versus coverage profiles being similar would seem to equate them both with the same process, namely the formation of the ordered (2x1) overlayer. Unlike any of

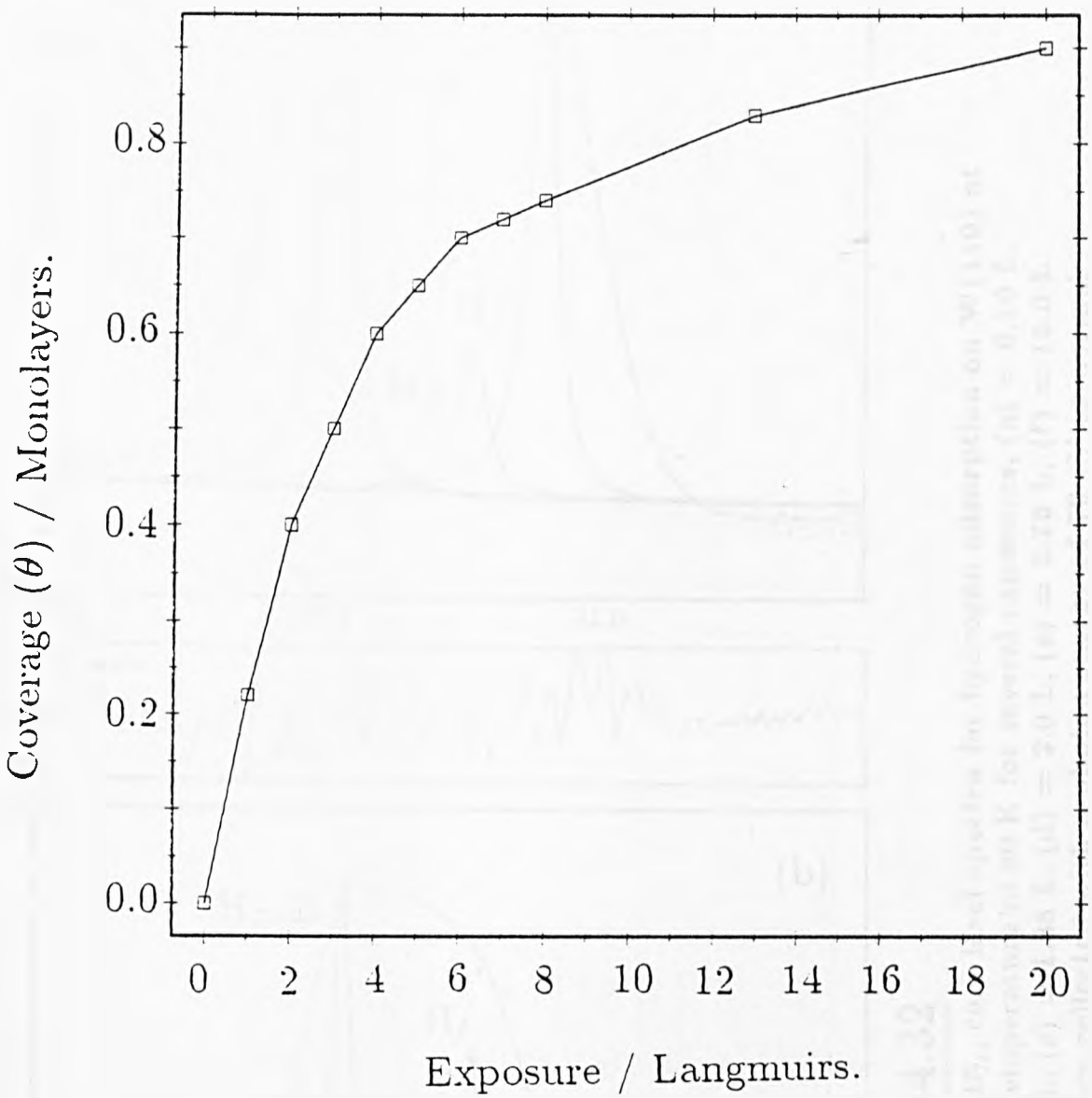

Figure 4.31

Coverage versus exposure curve for hydrogen on W{110} at a surface temperature of 300 K, reproduced from Barford and Rye [3]

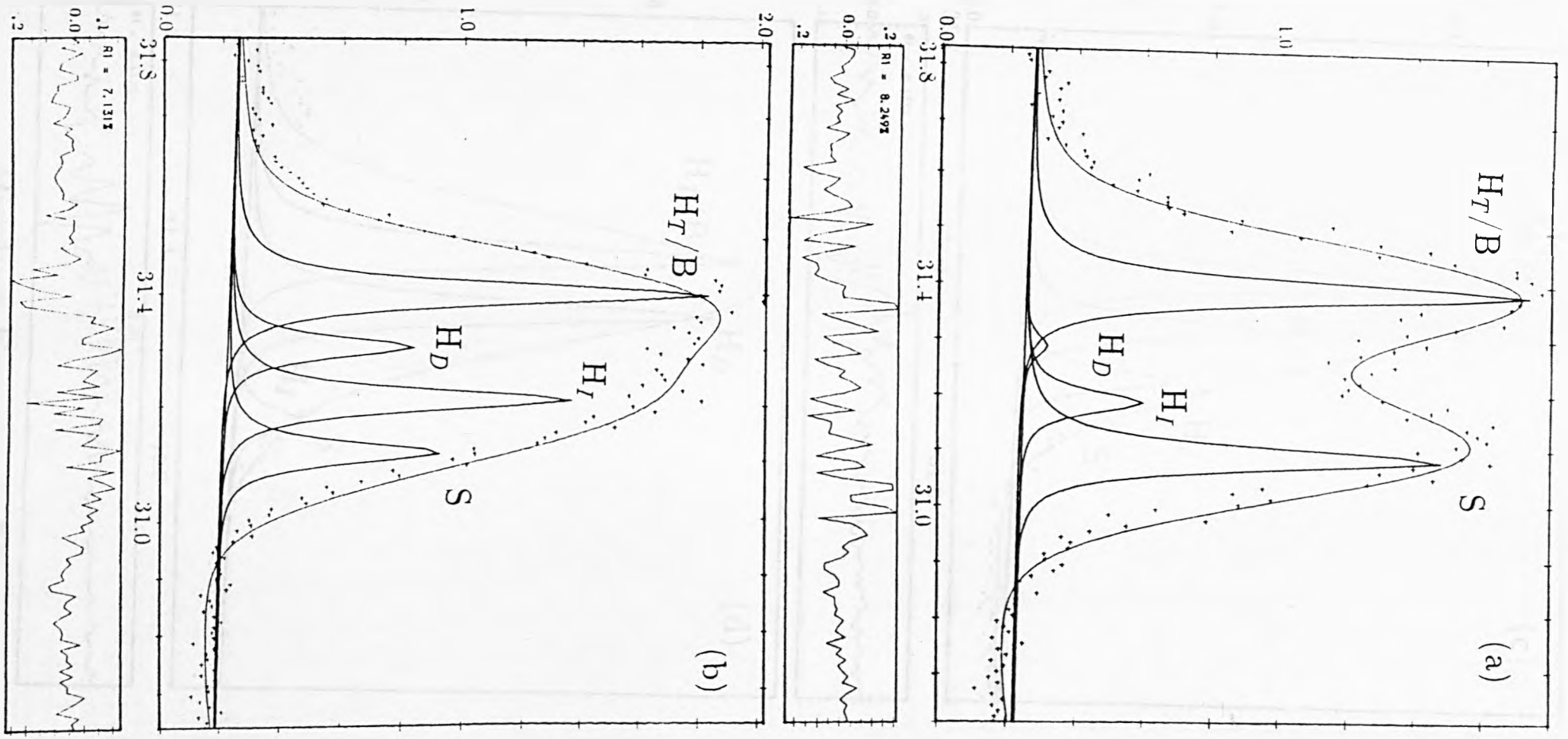

Figure 4.32

Fitted W $4f_{7/2}$ core level spectra for hydrogen adsorption on W{110} at a surface temperature of 80 K for several exposures, (a) = 0.10 L, (b) = 0.6 L, (c) = 1.88 L, (d) = 2.0 L, (e) = 2.75 L, (f) = 15.0 L. Spectra were collected with a photon energy of 70 eV at normal emission.

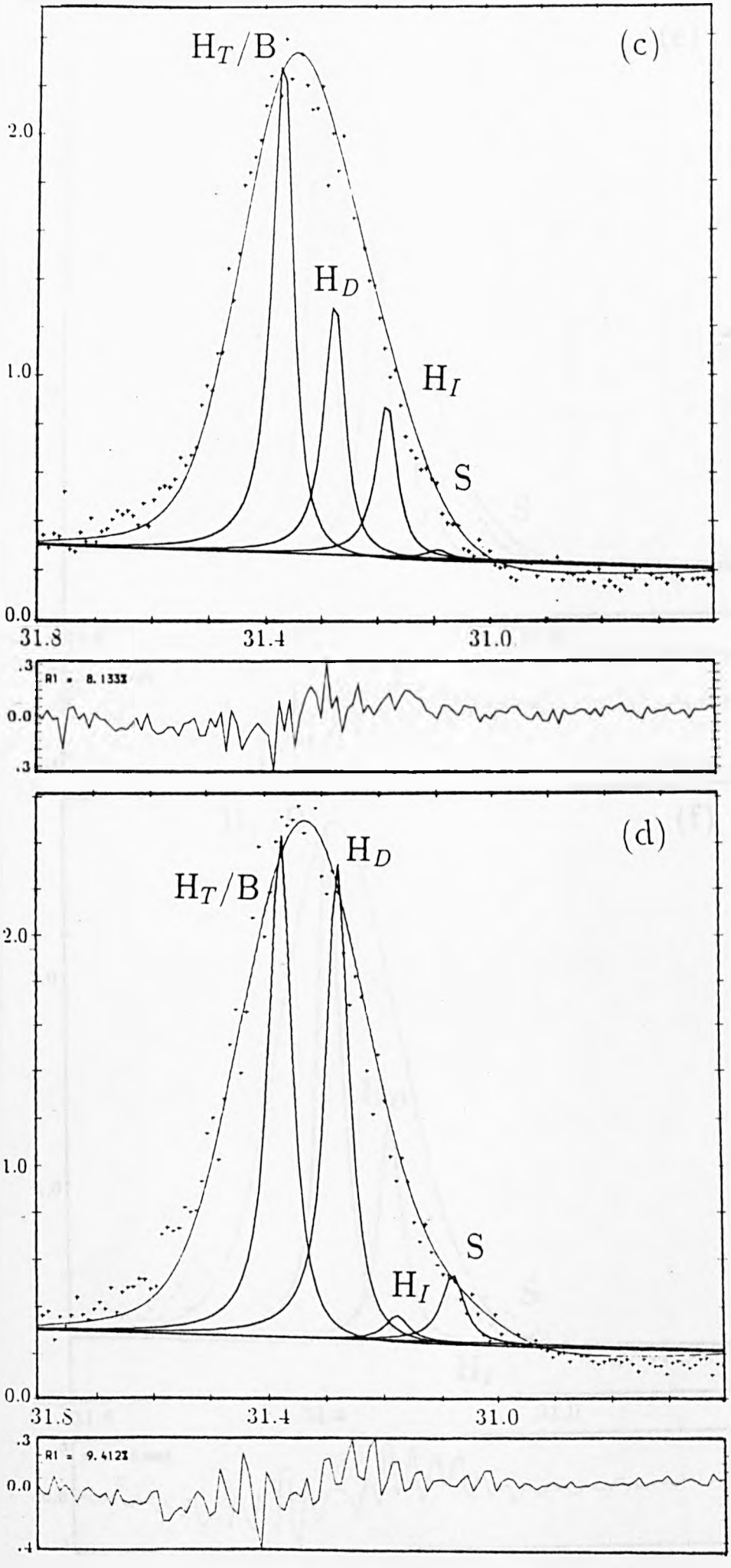

Figure 4.32(continued)

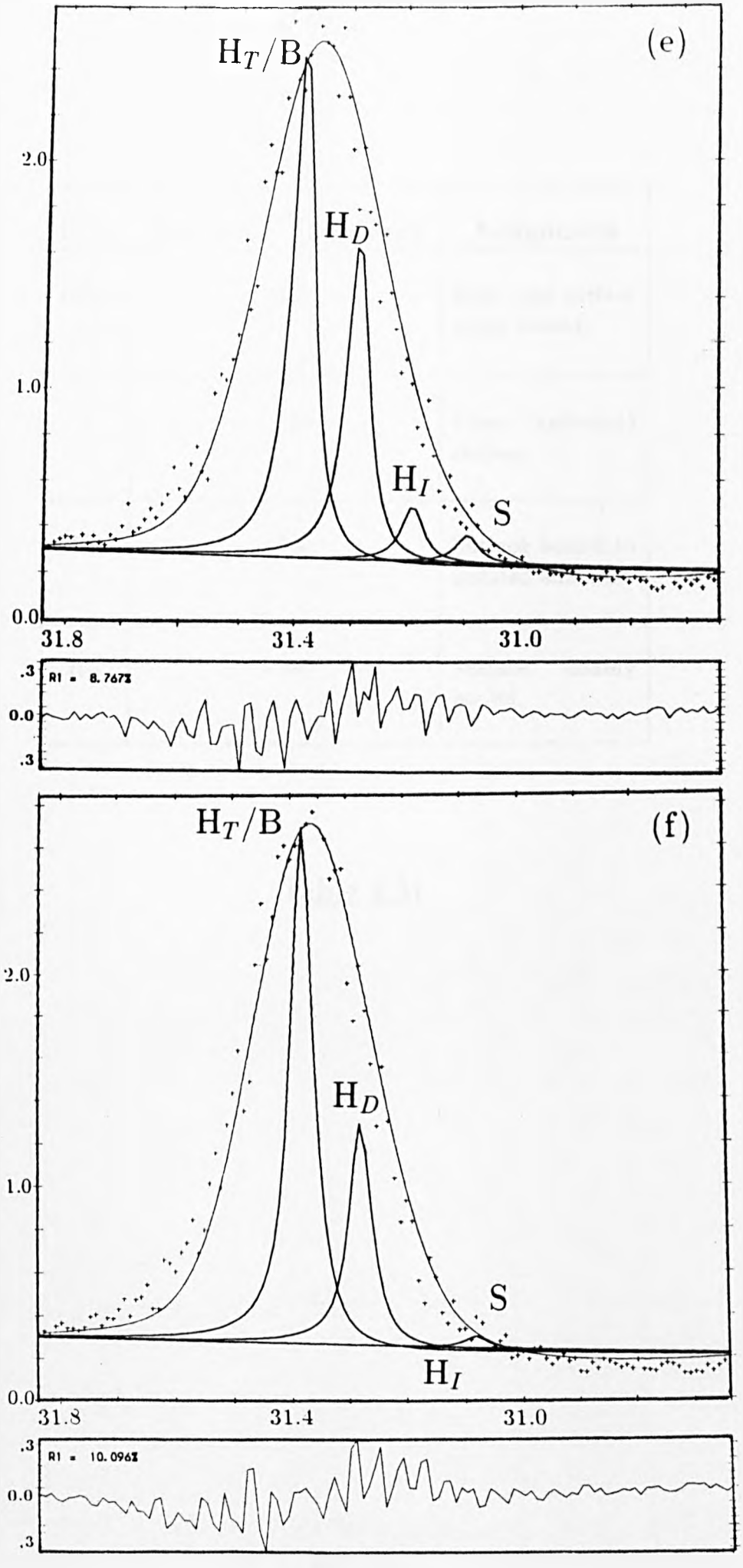

Normalised Intensity / Arb. Units.

Binding Energy / eV.

Figure 4.32(continued)

Peak	Shift w.r.t. Bulk/meV	Assignment
B/H_T	000	Bulk, and surface triply bound.
S	-298	Clean (unbound) surface.
H_I	-200	Surface bound to isolated adatom.
H_D	-100	Surface doubly bound.

Table 4.31

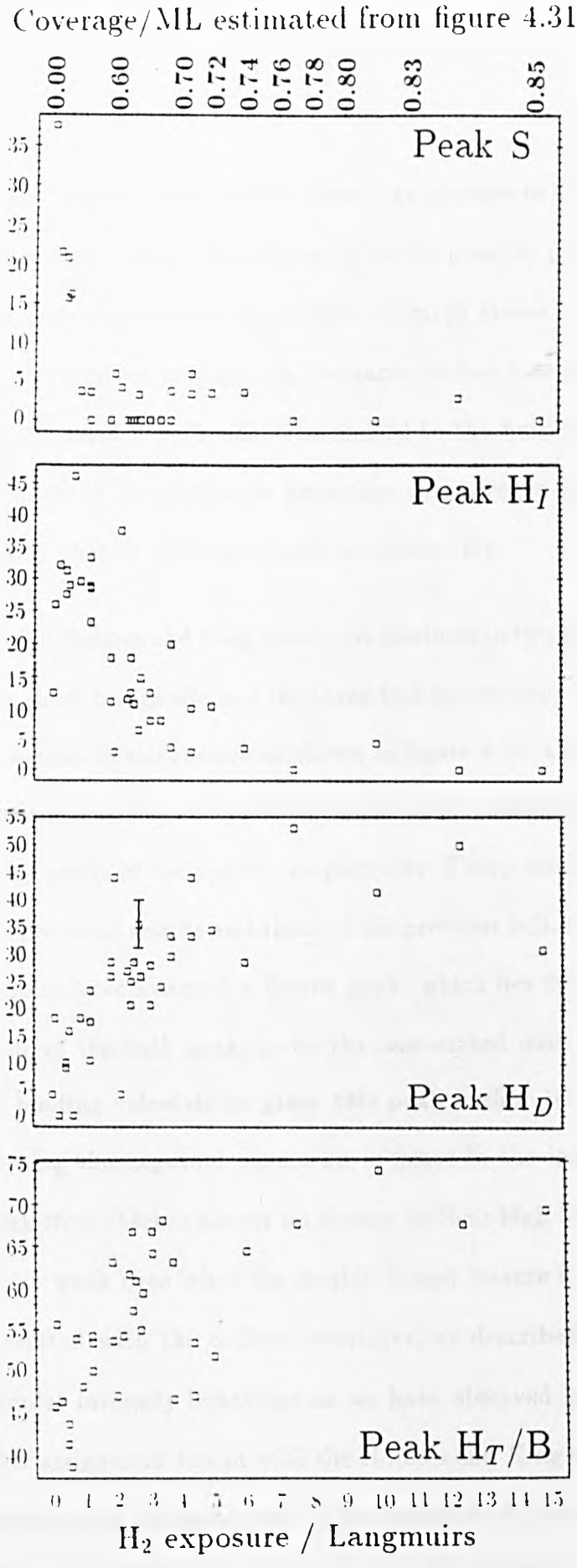

Figure 4.33

Intensity behaviour of the component peaks of the hydrogen induced tungsten surface core level spectra collected from W{110}.

the other systems discussed here we observe that there is an increase in the 'bulk' peak intensity. On this close-packed surface there seems to be no possible physical reason for an increase in clean surface coordination to other tungsten atoms i.e. no surface distortion as has been observed for nitrogen on the same surface (see next section), to such an extent that the surface peak might be shifted to the bulk position. The increase must be the result of an additional peak due to hydrogen chemisorption which is unresolvable from that of the bulk, which we denote H_T.

The structural model of Holmes and King places the adatoms in two different types of site at saturation, the short-bridge site and the three-fold hollow site. This provides two different tungsten species in the surface as shown in figure 4.34, those which are bound to two hydrogen atoms and those which are bound to three adatoms. These we assign to the H_D and H_T peaks of the spectra respectively. There would seem to be here a discrepency between these results and those of the previous SCLS investigation [29, 30]. The French group have assigned a fourth peak, which lies 200 meV to the high binding energy side of the bulk peak, to be that associated with triply bound tungsten. Their tight binding calculations place this peak within 100 meV of the bulk peak.While increasing the exposure causes an increase in the intensity of the H_D (doubly bound) peak they observe almost no change in their high binding energy peak, and it remains very weak even when the doubly bound feature is a maximum. If both peaks are associated with the ordered overlayer, as described above, then both should exhibit similar intensity behaviour as we have observed here. It is not clear therefore how their assignment ties in with the Holmes and King model as they suggest, whereas we believe that our treatment of the data does fit this structure. Is it now possible to eliminate the other proposals based on the behaviour observed?

Single site adsorption is the other popular option, placing the adatoms in the

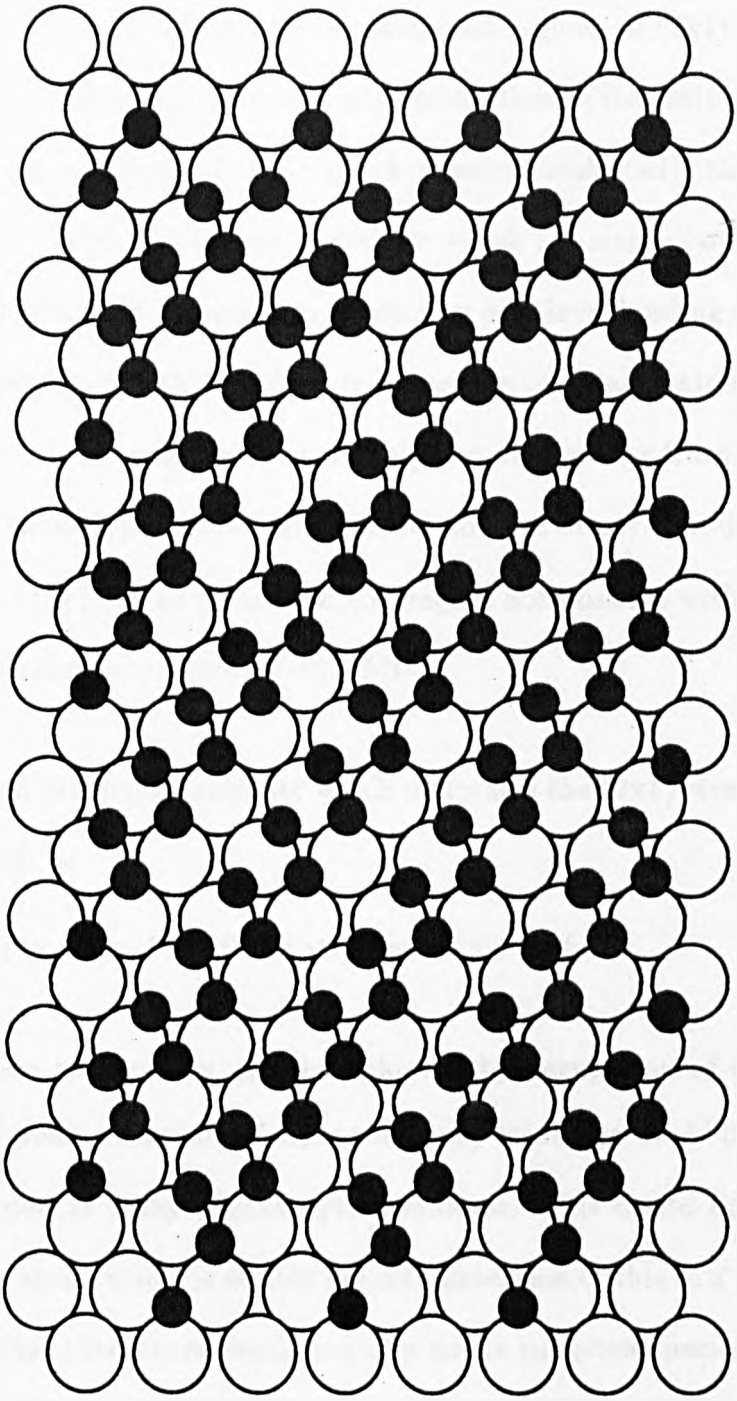

Figure 4.34

Hard sphere representeation of the Holmes and King model for the (2x1) overlayer stucture formed on W{110}. showing two distinct adsorption sites i.e. the threefold hollow and the short bridge aligned with the adsorbate rows. Open circles are the tungsten surface atoms.

long-bridge sites. Up to θ=0.5 ML there must exist regions of (2x1) structure and isolated adatoms. During this phase of adsorption there exist only two species of surface tungsten (in addition to those which remain unaffected), those which are singly bound to the isolated adatoms and those which are singly bound but within islands. This could result in a maximum of two new core level binding energies in the sub half monolayer region with that feature being due to isolated atoms having zero intensity at θ=0.5 ML. If we ignore the small high binding energy feature observed by the French group then this is a possibility in the absence of our own data. However, the continuation of (2x1) up to saturation coverage is not possible within this model. One of two things must occur above θ=0.5 ML.

1. A second distinguishable site which maintains the (2x1) structure must be occupied; or
2. the empty rows of the (2x1) structure must be filled.

The second of these two options may be achieved by occupation of alternate sites within the empty rows eventually forming a (2x2) structure at θ=0.75 ML, such behaviour is common to many chemisorption systems. This would produce a third species of tungsten atom, which is doubly bound. Extension of this to a full monolayer would result in a (1x1) structure consisting of a single tungsten species which would be doubly bound. Since in this model our spectral assignment would be: H_I, isolated singly bound; H_D, island singly bound (by analogy with the oxygen spectra discussed previously); and H_T, bulk plus doubly bound; the result at saturation should consist of a single peak at the bulk binding energy and this is clearly not the case.

At saturation the specific adsorption site within the unit cell would alter the initial assignment of peaks. For example, a three-fold hollow site would produce H_D,

island doubly bound; and H_T Bulk plus island triply bound. The important point to notice is that the number of adsorption induced components present up to 0.5 ML would be 3, and above 0.75 ML would be two and eventually at saturation coverage only one. Given the present deconvolution and assignment the final appearance of the spectrum would be a single peak at the bulk binding energy since we have not resolved the higher hydrogen coordinated tungsten species from the bulk peak.

Another alternative would be to fill the alternate empty rows randomly (figure 4.35), which is equivalent to the coverage dependent order-disorder transition discussed by Blanchet et al.. This would still account for the existence of a (2x1) LEED and RHEED pattern up to θ=0.75 ML, although the background intensity would be increased but would not allow for the (2x2) pattern described by Gonchar et al [12, 13]. What would be the effects of such a structure on the core level spectra? The tungsten species present differ, depending on adsorption site. Blanchet et al [20] discuss adsorption in the context of the long-bridge site in which there exist singly bound and doubly bound surface tungsten atoms only. For a full monolayer producing again a (1x1) structure, there can be only doubly bound tungsten atoms present and the spectra produced would be expected to follow the same trends described above. In this case if the adsorption site within the unit cell was the three-fold hollow site then above θ=0.5 ML there is the possibility of three adsorption induced species; singly, doubly, and triply bound to hydrogen. As the coverage approaches one monolayer there would be first a decrease in the singly bound population followed by the demise of the doubly bound species and again producing a single peak spectrum for triply bound species which is coincident with the bulk binding energy as above.

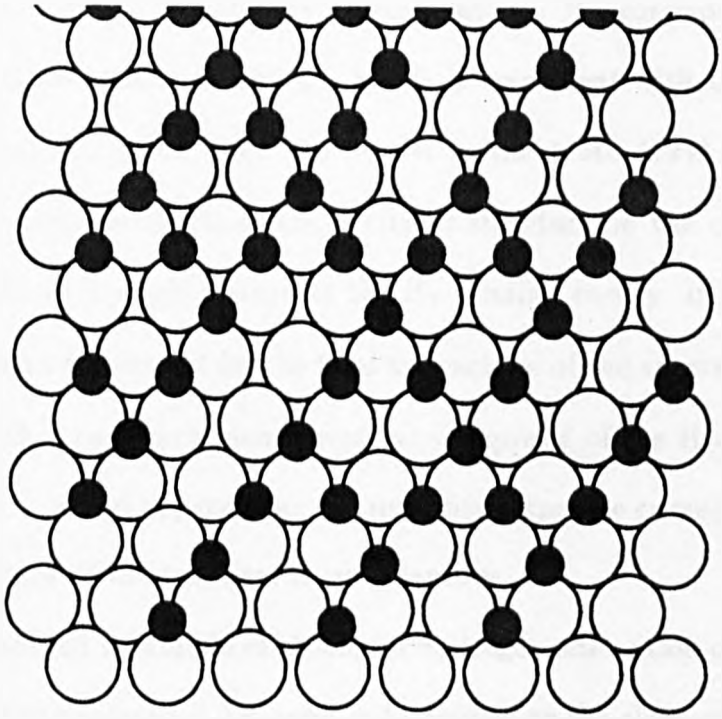

Figure 4.35

Hard sphere representation of hydrogen adsorption on W{110} utilising the single site adsorption model (threefold hollow) and demonstrating random occupation of the space rows of the initial (2x1) overlayer.

Conclusion.

Three hydrogen induced features have been identified in this work. H_I for surface tungsten atoms bound to isolated hydrogen adatoms, H_D corresponding to surface atoms bound to two adatoms, and H_T which is coincident with the bulk for three adatoms. By extending the single site model to the 1 ML (1x1) structure we can extrapolate the possible effects of the overlayer structure on the core level spectra. The result would be a single feature at the H_T binding energy. It is the double site model which seems to account for the final appearance of the spectra at full coverage providing us with a two component spectrum comprised of the H_D and H_T features alone. However, it would appear from the intensity/exposure curves of peaks H_D and H_T that occupation of the two sites is simultaneous.

The shift observed by Jupille et al [36] for hydrogen adsorption on W{100} in the θ>0.5 ML is in the region of + 110 meV with respect to the clean surface peak. This they assign to surface atoms which maintain bulk-like positions but are coordinated to one or more hydrogen adatoms. This correlates with the shift recorded here for singly bound surface atoms (H_I).

Bibliography

[1] P.W. Tamm and L.D. Schmidt J. Chem. Phys. 54(11) (1971) 4775.

[2] Schmidt Physical basis for Heterogeneous Catalysis (1975) 451.

[3] B.D. Barford and R.R. Rye J. Chem. Phys. 60 (1974) 1046. stick

[4] R.S. Polizzotti and G. Ehrlich J. Chem. Phys. 71(1) 1979 259.

[5] A Horlacher Smith, R.A. Barker and P.J. Estrup Surface Science 136 (1984) 327.

[6] Ch. Steinbruchel and L.D. Schmidt Phys. Rev. Letts. 31 (1974) 594.

[7] Ch. Steinbruchel and L.D. Schmidt Phys. Rev. B10 (1974) 4209.

[8] M. Sato J. Phys. C: 16 (1983) 5701.fem

[9] E.W. Plummer and A.E. Bell JVST 9 (1974) 1046.

[10] P.W. Tamm and L.D. Schmidt J. Chem. Phys. 55(9) (1971) 4253.

[11] Stern Applied Physics Letters 5 (1964) 218. leed

[12] V.V Gonchar, O.V. Kanash, A.G. Naumovets, A.G. Fedorous JETP Lett. 28 (1978) 330.

[13] V.V. Gonchar, Uy M. Kagan, O.U. Kanash, A.G. Naumovets, A.G. Fedorous JETP 57 (1983) 142.

[14] L.D. Roelofs and P.J. Estrup Surface Sci. 125 (1983) 51.

[15] J.W. Chung, S.C. Ying, P.J. Estrup Phys. Rev. Lett. 56(7) (1986) 749.

[16] K.J. Matysik Surface Science 29 (1972) 324.

[17] M.W. Holmes and D.A. King Surface Science 110 (1981) 120.

[18] M.W. Holmes, D.A. King, J.E. Inglesfield Phys. Rev. Lett. 42 (1976) 394.

[19] B. Feuerbacher and B. Fitton Phys. Rev. B8 (1973) 4890.

[20] G.B. Blanchet, N.J. Dinardo, E.W. Plummer Surface Science 118 (198?) 496.

[21] E.W. Plummer et al Progress in Surface Science Vol. 7.

[22] C. Backx, B. Feurbacher, B. Fitton, and R.F. Willis Physics Letts. 60A (1977) 145.

[23] D.A. King and D. Menzel Surface Science 40(1973) 399.

[24] U.A. Jayasooriya, M.A. Chesters, M.W. Howard, S.F.A. Kettle, D.B. Powell, and N. Sheppard Surface Science 93 (1980) 526.

[25] B.M. Davies and J.L. Erskine J.Electron Spec. and Related Phenomena 29 (1983) 323.

[26] G.B. Blanchet, P.J. Estrup, P.J. Stiles Phys. Rev. Lett. 44 (1980) 171.

[27] G.B. Blanchet, P.J. Estrup and P.J. Stiles Phys. Rev. B23 (1981) 3655.

[28] R. DiFoggio and R. Gomer Phys. Rev. B25(6) (1982) 3490.

[29] C. Guillot, G. Treglia, J. Lecante, D. Spanjaard, M-C desjonqueres, D. Chauveau, Y. Jugnet, and Tran Minh Duc J. Phys. C 16 (1983) 1555.

[30] C. Thault-Cytermann, M-C Desjonqueres and D Spanjaard J. Phys. C: Solid State Phys. 16 (1983) 5689.

[31] P. Nordlander, S. Holloway, J.K. Norskov Surface Sci. 136 (1984) 59.

[32] Hopkins and K.R. Pender Surface Science 5 (1966) 316.

[33] Hopkins and S. Usami Surface Science 23 (1970) 423.

[34] Armstrong et al Canadian J. Phys. 44 (1966) 1753.

[35] R.A. Collins et al J. Applied Physics 40 (1969) 539.

[36] J. Jupille, K.G. Purcell, G.P. Derby, J. Wendelken and D.A. King Proceedings of Int. Conf. on Structure of Solid Surfaces Ed. M.A. van Hove and J.F. van der Veen. pub. Springer (1987) 463.

4.4 A Case Of Underlayer Adsorption: β-N on W{110}

Introduction.

The adsorption rate of nitrogen on tungsten exhibits a large crystallographic anisotropy [1, 2], with an initial sticking probability that varies from 0.73 on the {310} surface to 5 x 10^{-3} on W{110} at 300 K. Formation of the atomic β-state occurs via dissociation of the molecule at adjacent pairs of fourfold (100) sites [3], which on the close-packed {110} surface are only to be found at defects, such as steps. The exothermicity of the chemisorption process produces 'hot' adatoms which are then free to migrate and populate the entire surface. At 300 K this process is inefficient but may be enhanced by repeated heating to 600 K and re-adsorption. The heating assists migration away from the region adjacent to the defect sites allowing further dissociative adsorption to occur on cooling. This 'cyling' is carried out in an ambient pressure of 2 x 10^{-6} mbars of N_2 until a saturation coverage of θ=0.25 ML, as indicated by a (2x2) LEED pattern [4], is reached. We found the best quality LEED pattern to be achieved after a total exposure time of 3-5 mins, involving 6-7 heating/cooling cycles.

In their ion scattering and Auger depth profiling study of the N/W(110) system, Somerton and King [4] suggested that nitrogen held in the β-state does not in fact form a conventional overlayer structure but instead exists as an underlayer species, and we have sought to substantiate this using SCLS.

Results and Discussion.

Spectra taken from the (2x2)-N structure show a rather unnatural looking flat-topped distribution of photoelectron binding energies, as shown in Figure 4.41, the analysis

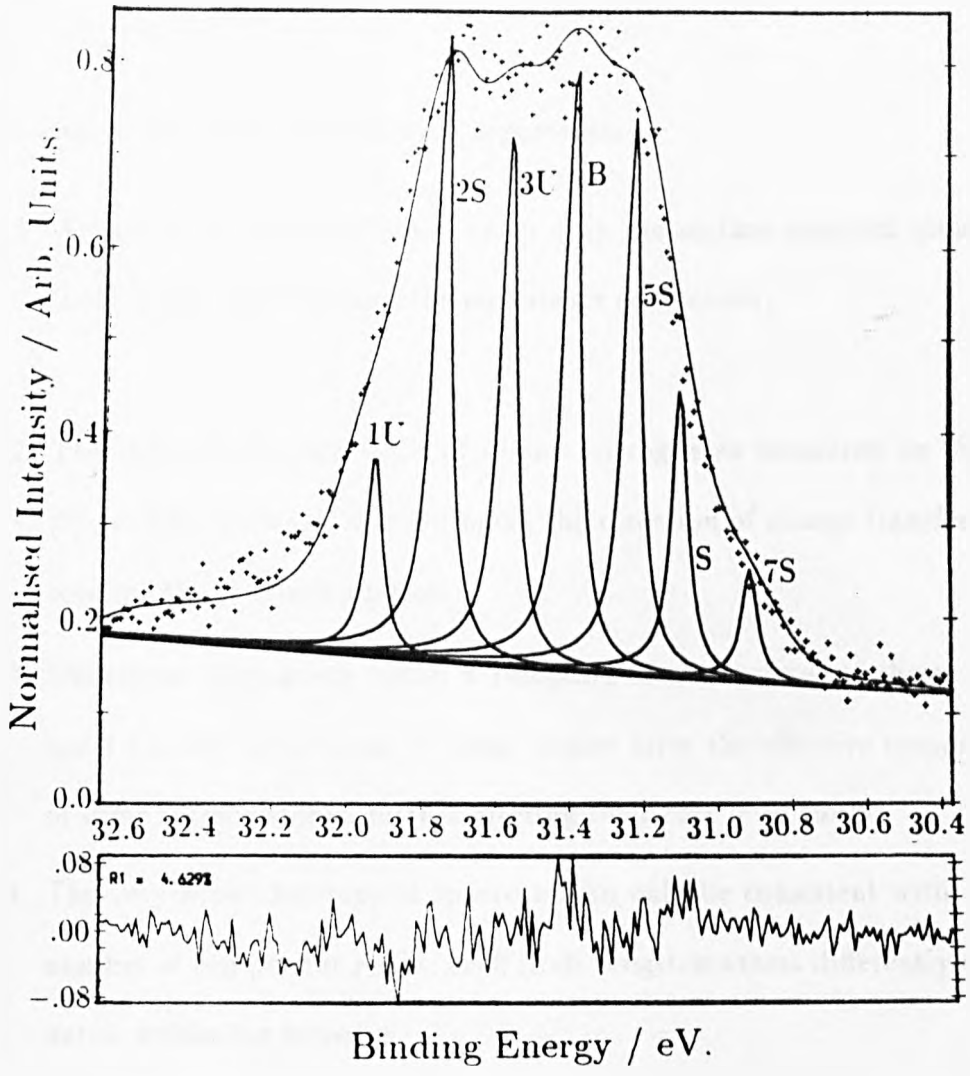

Figure 4.41

Fitted core level spectrum collected from the nitrogen underlayer structure. The surface displayed a (2x2) LEED pattern for the same structure. Note the curious flat-topped nature of the spectrum.

of which was based around the following arguments:

1. An overlayer structure would affect only the surface tungsten atoms; the 'bulk' peak, which carries the underlayer component,

2. The induced chemical shift of atomic nitrogen as measured on W{100} [5], is of the order of 400-500 meV, the direction of charge transfer being towards the nitrogen adatom.

3. Underlayer adsorption causes a rumpling of the surface, as shown in figure 4.42, and hence must to some degree alter the effective coordination of some surface atoms, further altering their core level shifts.

4. The very broad flat-topped spectrum can only be consistent with a large number of component peaks, each from tungsten atoms differently coordinated within the selvedge.

The results of applying the fitting procedure are summarised in Table 4.41. Firstly, before any normalisation of the spectra, a comparison of intensity in the bulk region from the (2x2)-N structure with that on the clean (1x1) surface reveals a significant decrease on nitrogen adsorption, see Figure 4.43. This bulk intensity is restored on desorption. We conclude therefore that adsorption is having some significant effect on the energy position of the underlayer component of the spectrum. The model proposed by Somerton and King [4] suggests that the N-adatoms occupy the 3-fold hollows of the underlayer (Fig. 4.42) binding directly to three of the underlayer tungsten atoms and only one in the surface. This model leaves the effective coordination number N_{eff}, as given by equation 1 [6]:

$$N_{eff} = \sum_{i=1}^{i=3} N_i / r_i \qquad (4.1)$$

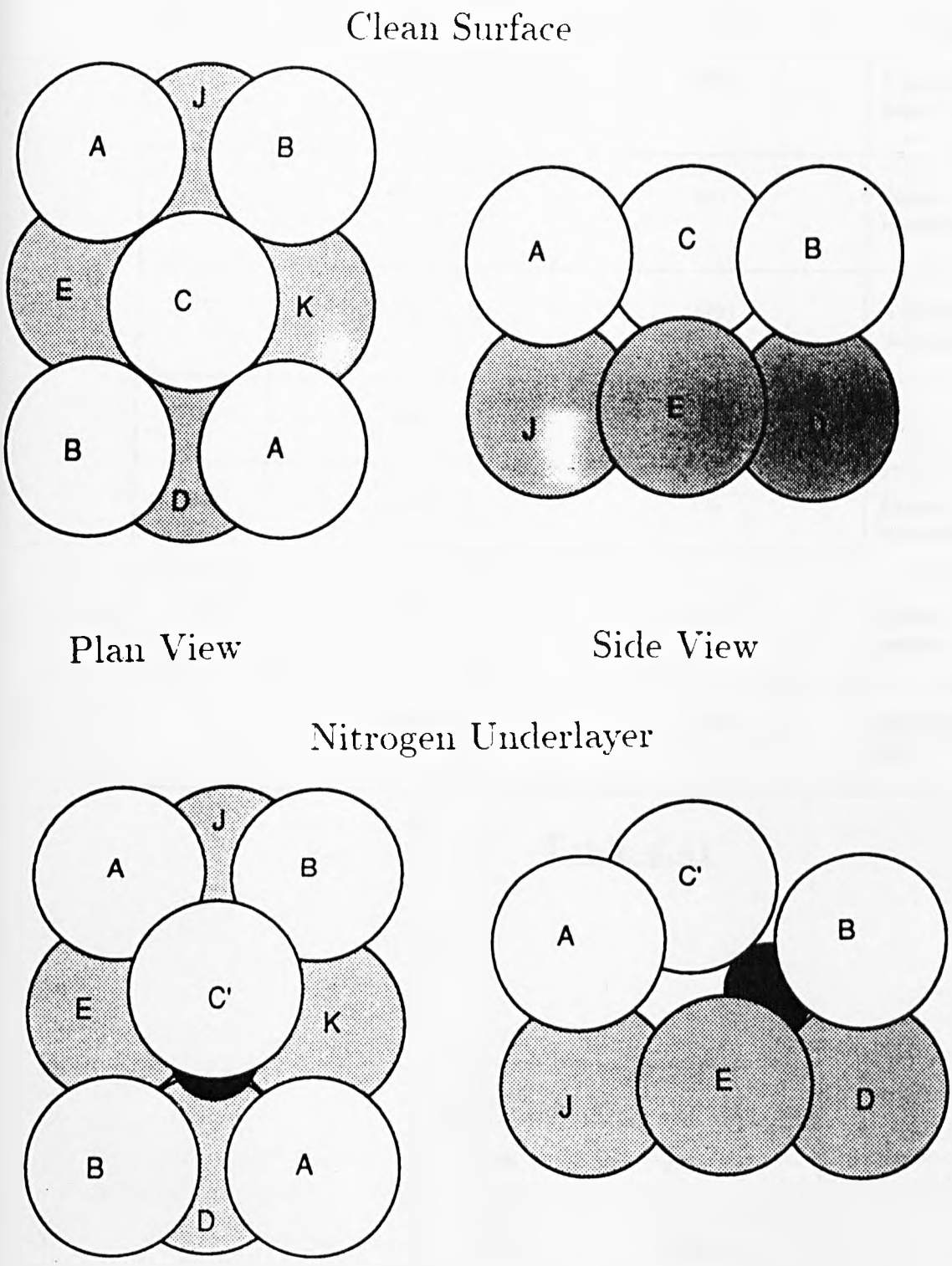

Figure 4.42

Hard sphere representation of the effects of underlayer adsorption of nitrogen on W{110} showing 'rumpling' of the surface.

Peak No.	Shift w.r.t. Bulk/meV	Shift w.r.t. Surface/meV	Assignment
1U	531	(829)	Underlayer directly bound to nitrogen.
2S	(353)	651	Surface directly bound to nitrogen.
3U	172	(470)	Underlayer 'near-bound'.
4	000		Bulk
5S	(−167)	131	Surface 'near-bound'.
6	−298	000	Clean surface residue.
7S	(−484)	−186	Tops-of-steps type sites

Table 4.41

Atom Type	W-N Distance/pm
A/B	279±10
J	305±10

Table 4.42

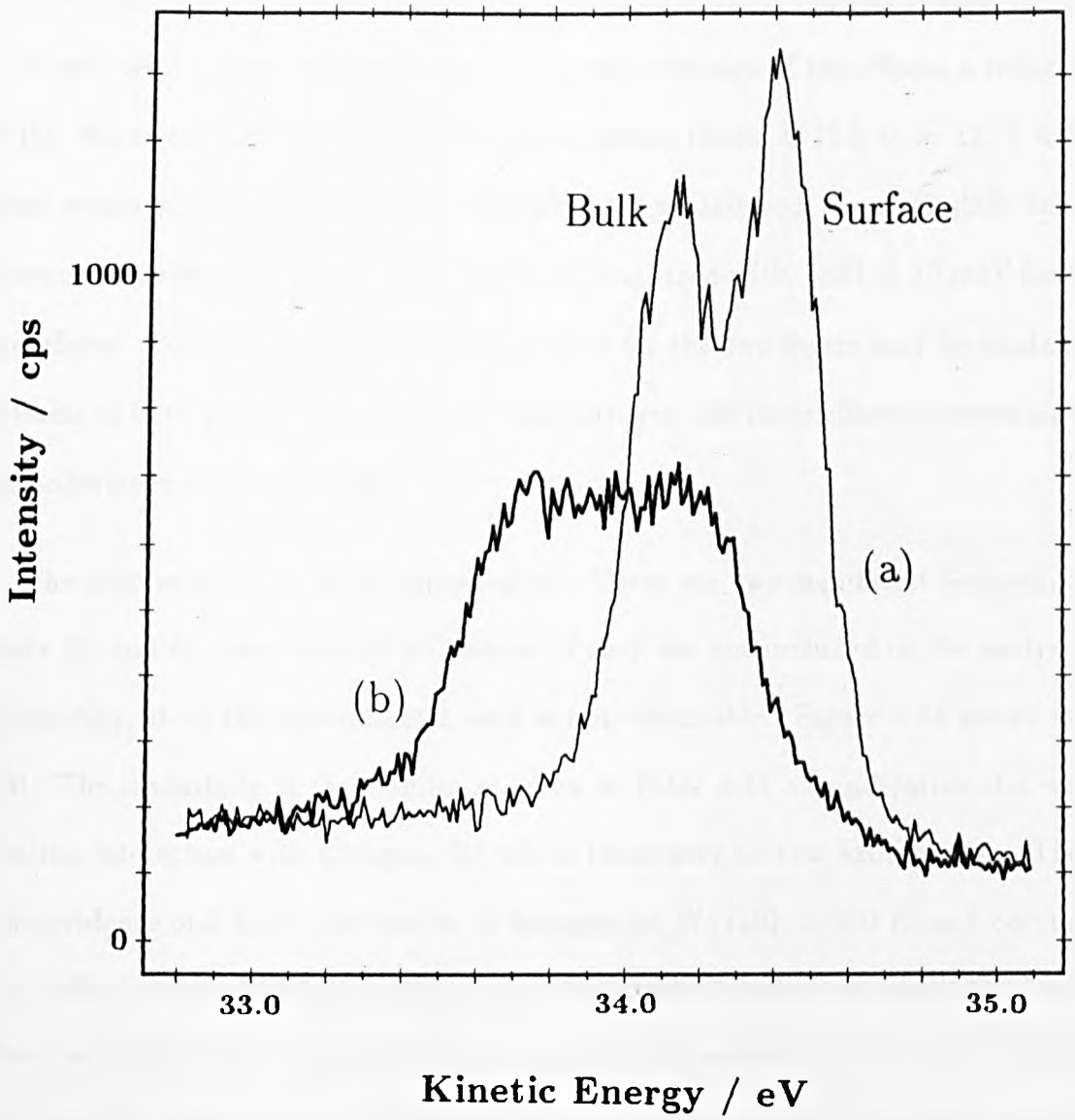

Figure 4.43

Raw data, curve (a) is the W $4f_{7/2}$ core level spectrum collected from a clean W{110} surface. Curve (b) shows the spectrum taken from the (2x2) nitrogen underlayer structure. Both spectra were collected under the same phototemission conditions.

of the 'rolled' surface atom considerably reduced, and thus it's apparent shift of +651 ± 10 meV with respect to the clean surface peak is the sum of two effects, a reduction of the effective coordination to the tungsten lattice (from ≈ 13.8 to ≈ 12.7) which alone would produce a shift of ≈ −50meV, and an induced chemical shift due to nitrogen adsorption of about +700 ± 10 meV compared with +531 ± 10 meV for the underlayer. The difference in the induced shift for the two layers may be explained in terms of both a lower coordination to the nitrogen and more effective screening for the underlayer tungsten atoms.

The picture must be more complicated. There are two significant features, i.e. peaks 3U and 5S, unaccounted for and yet if they are not included in the analysis a satisfactory fit to the experimental data is not obtainable. Figure 4.44 shows such a fit. The magnitude of these shifts as given in Table 4.41 are indicative of a weak bonding interaction with nitrogen, for which there may be two explanations. There is no evidence of a molecular species of nitrogen on W{110} at 300 K, and certainly it is difficult to envisage a situation on a close packed surface in which this would affect both surface and underlayer, so we reject this possibility. If we now consider the geometric arrangement of tungsten atoms in relation to the N-adatom we find the 'bond' distances given in Table 2 (based on a hard sphere model). We propose that the peak shifted by +172 ± 10 meV with respect to the bulk position is the result of a weak interaction of J-type atoms, see Fig. 4.42, with the adsorbed nitrogen whilst that shifted by +131 ± 10 meV from the clean surface peak we associate with atoms of type A and B in the surface. Here we find the surface to be less coordinated with the nitrogen than the single underlayer atom hence a smaller shift.

During the fitting procedure the energies of both the 'bulk' and surface peaks were fixed at their clean surface positions, and the others allowed to vary to obtain

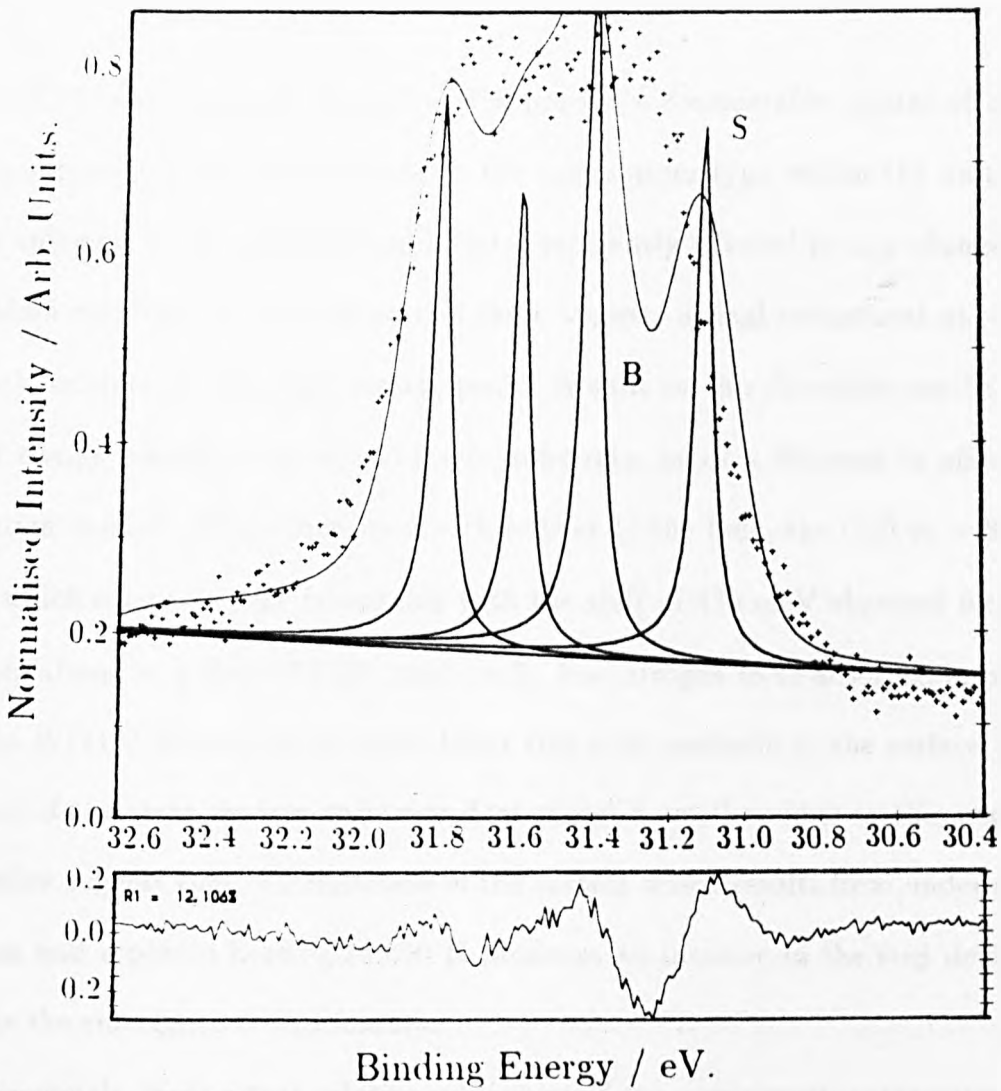

Figure 4.44

Attempts to fit the data with only the four components we had originally expected proved unsatisfactory. Raw W $4f_{7/2}$ core level spectra

the best fit. There remained throughout the process a considerable residue of clean surface component which we attribute to the single atom type within the unit cell which is unbound to the adatoms and is not significantly affected by any changes in coordination number. In addition to this there appears a final component at -186 ± 10 meV relative to the clean surface peak. A shift in this direction can be the result of charge transfer from adsorbate to substrate, or of a decrease in effective coordination number. When measured with respect to the bulk, the shift is -484 ± 10 meV which compares very favourably with the shift of 430 meV observed for the top-of-step atoms on a clean W{320} surface [7]. For nitrogen to be adsorbed into the β-state on W{110} there must be some defect step sites available on the surface, and inspection of the clean surface spectrum does reveal a small residue in this region. We therefore suggest that the distortion of the surface which results from underlayer adsorption and repeated heating to 650 K produces an increase in the step density, and hence the emergence of this feature.

The seemingly inconsistent relative intensities of the component peaks arise directly from the photoelectron diffraction characteristics of the newly 'rumpled' surface; with angle resolved photoemission there is no direct quantitative relationship to the number of atoms occupying each binding state. Experiments are currently underway to verify this.

Conclusion.

While the detailed deconvolution and assignment of peaks presented here may be tentative, the peculiar flat-topped shape of the spectrum is very clear evidence for the existence of many closely spaced components that more than one layer of tungsten atoms is involved in bonding to N-adatoms. Underlayer adsorption is strongly supported by the data obtained for β-CO adsorption, which unlike this system shows

no reduction in the intensity of the bulk peak which for this surface also incudes the underlayer contribution.

The presence of so many component peaks under this flat-topped spectrum begs the question, how reliable is the assignment? In any adsorption system there will always be the possibility of overlapping states i.e. some surface atoms in different initial state environments exhibiting similar core level binding energies due to different degrees of substrate-adsorbate interaction. A prime example of this is the adsorption of nitrogen on W{320}, here we have {110} terraces separated by {100} steps. Imagine adsorption on the terraces via dissociation at the steps resulting in a (2x2) structure similar to that described above. Using data from previous studies of N/W{100}, N/W{110} and clean W{320} it is possible to estimate the effects of such a system on the core level spectra. Table 4.43 shows the projected shifts for such a system. There are at least 14 different possible chemical environments within this structure. If they were well separated, and the experimental resolution was favourable there would be no problem in identifying the processes occuring at the surface. However, it is clear that under the present experimenatal conditions we would only be able to resolve 8 components at most, assuming equivalent lineshape parameters. Several of these eight component peaks would be the result of more than one type of atom i.e. atoms in different chemical environments. To complicate matters further the effect of annealing the surface to form the (2x2) structure, on any give peak, may be to leave the intensity of that peak unaltered as one contributory species is substituted by the other. Thus the changes that occur within the structure remain hidden. It is in this kind of situation that surface core level shift spectroscopy meets its limitations.

Assignment	Shift w.r.t. Bulk/meV
N/W{110} low coordination peak	-484
Top of step	-430
Terrace	-300
N/W{110} surface near bound	-167
Top of step + 1 adatom	-130
$U_{\{100\}}$	-125
Bulk	000
Base of step + 1N	000
Top of step + 2N	+170
N/W{110} underlayer near bound	+172
$U_{\{100\}}$ + 1N	+175
N/W{110} Surface bound	+353
Base of step + 2N	+379
N/W{110} underlayer bound	+531

Table 4.4 3

Bibliography

[1] S.P. Singh-Boparai,M.Bowker,D.A.king Surface Science 53(1975) 55.

[2] M.Bowker,D.A.King Journal of Chem. Soc. Faraday Trans.I(1975) 2100.

[3] M.G.Wells,D.A.King Proc.Roy.Soc.(London) A339(1974) 245.

[4] C.Somerton,D.A.King Surface Science 89(1979) 391.

[5] J.Jupille,K.G.Purcell,D.A.King Solid State Comm. 58(1986) 529.

[6] K.G. Purcell, J. Jupille, D.A. King Proc. Solvay Int. Conf., Austin, Texas (1987) published Springer in press.

[7] K.G. Purcell, J. Jupille, and D.A. King Surface Science 208(3) (1989) 245.

[8] Treglia, M.C.Desjonqueres, D.Spanjaard, YLasailly C.Guillot, Y.Jugnet, Tran Min Duc, Lecante J.Phys C:Solid State 14(1981) 3463

[9] ourdin, G.Treglia, M.C.Desjonqueres, D.Spanjaard Solid State Comm.47(4) 279.

[10] E. Madey and J.T. Yates Nuovo Cimento Suppl. 5(1967) 486.

[11] amm and Scmidt Surface Science 26 (1971) 286.

[12] Ehrlich and F.G. Hudda J. Chem. Phys. 35 (1961) 1421.

[13] Besocke and H. Wagner Surface Science 1979/1980?

Chapter 5

Conclusion.

In conclusion to the work presented here it might be useful to highlight the main features. It has been demonstrated on many previous occassions and in this text that the magnitude of observed surface core level shifts is dependent on the degree of bonding between surface atoms and adsorbates. The main aim of this programme has been to establish the extent to which SCLS can be applied to structural studies. It has become clear during this work that this techinique, similarly to most other techniques, cannot be applied in isolation. SCLS is very much a complimentary technique. However this does not detract from its usefulness as a structural tool. Quite often even the most quantitative techniques such as LEED I-V analysis can only reduce the number of possible binding sites to two or three. When SCLS is used in this context where the degree of binding may differ for several sites it can provide some quite unambiguous information. Having said this it remains at this moment in time a rather qualitative method for studying surface structures, although some early XPS work has demonstrated that the magnitude of shift is clearly linked to the oxidation state of the surface atoms, and surface atom coordination has been directly related to the magnitude of the shift observed.

The future of core level shifts must surely follow the line of quantifying the observed effects. Many adsorbate/substrate systems have been the subject of work-

function studies, in fact the technique has now reached a high level of sophistication. It is possible from this kind of information to determine the degree of charge transfer between the adatom and surface. One way forward might be to set up a series of adsorbate structures of increasing/decreasing charge transfer and measure the effects on the surface core level binding energies. This may provide a direct relationship between the two, bringing the study of SCLS well into the class of quantitative measurements available to us today.

Chapter 6

Using The Fitter

Here are a few words about the fitting program as used on the AS7000 at Daresbury, and with which all of this data was analysed. The AS7000 is currently being scrapped and replaced by the CONVEX and so fitter is in the process of being transferred. How much the input data and operation of fitter will be altered is not yet clear and so this section should serve only as a rough guide to future users. Hopefully we will be able to effect a succesful transfer without much disruption to the input file format.

FITTER is made up of 38 subroutines, most of which are concerned with data manipulation and plotting procedures. The main calculations are carried out by various NAG (Numerical Algorithms Group) routines which are called from within several of these subroutines. Detailed documentation of these routines can be found in the NAG manuals stored in the Data Acquisition Room at Daresbury. There are four main source routines which in turn call several other routines during operation, these are listed here with their descriptions as given in the NAG library manual;

- CO6FKF: calculates the circular convolution of two real vectors of period N.
- EO4JAF: a quasi-Newtonian algorithm for finding a minimum of a function $F(X_1,X_2,...,X_n)$, subject to fixed upper and lower bounds on the independent

variables X_1.....X_n, using function values only. This routine calls on EO4JBF, which is a comprehensive quasi-Newtonian algorithm for finding a minimum.

- EO1BAF: Determines the cubic-spline interpolant of a given data set.
- EO2BBF: Evaluates a cubic spline from its B-spline representation.

The overall purpose of FITTER is to fit a given experimental dataset by a least squares minimisation method, within the limits specified by the user.

The user is required to provide an initial data-file to serve as a starting point from which the fitting algorithm may proceed. An example of such a file is shown as List 1. There is no set order or sequence to the input but each item must be separated by a comma. At present the data is in IBM NAMELIST format and must begin with &DECON and end with &END, both ampersands need to be in the second column. These restrictions may be altered on transfer to the CONVEX. Perhaps the simplest way to explain what each of the parameters does (although they are mostly self explanatory) is to list each of them individually in the order in which they appear in List 1.

1. NPEAKS: Specifies the number of peaks to be used to fit the input spectrum. The value of NPEAKS may lie in the range $1 < n < 10$, although it is unlikely that the experimental resolution will allow 10 distinguishable peaks under a single core level spectrum.
2. E(n): The value E(n) is an initial estimate made by the user, of the energy position of peak n. Each peak energy may be allowed to vary within the range defined by the values EU(n), the upper limit, and EL(n), the lower limit.

3. EREL(n): Erel determines whether the peak n is allowed to move independently of all other peaks or as part of a group of two or more peaks. When the value of EREL is set to zero then the peak moves independently, E(n) must therefore be an absolute value. If EREL is set to a value 'x' then the energy of peak n is varied relative the peak 'x', and so in this case E(n) is the starting estimate relative to peak E(x). EU(n) and EL(n) then define the upper and lower bounds relative to the position of peak 'x'. 'X' may lie in the range $1 < X < 10$, with $X < n$.

4. NSPEC: Specifies the number of spectra to be dealt with by the routine using this particular parameter file. The maximum is ten.

5. A(n,S): This defines the amplitude of each peak and it works in the same way as E(n). A(n,S) is the initial estimate of the amplitude for peak n in spectrum S, with AL(n,S) and AU(n,S) providing the upper and lower limits.

6. AREL(n,S): This works in exactly the same manner as EREL, when set to zero the amplitude is varied independently of the other peak amplitudes.

7. FORM(n): Each peak in the fitted spectrum has it own FORM which is defined in the parameter file, see FPARM FORM specifies the form number. This allows the user to define different lineshape parameters for each peak if necessary.

8. BGND(S): Similarly the background for each spectrum has a form number associated with i. S is the spectrum number within the set under operation, $1 < S < 10$. The parameters describing the form appear later in the estimate file, see BPARM.

9. INST(S): Defines the form number of the instrument response function for

each spectrum. Similar to BGND, see IPARM.

10. NFORM(S): Specifies the number of peak forms that are to appear in spectrum S.
11. FLS(S): Defines the peak lineshape to be used in spectrum S (see List 2).
12. FPARM(p,f): This describes the peak forms numerically. In this case for example the parameters necessary to describe the Doniach-Sunjic lineshape are lorentzian width and assymetry parameter. The values 'p' and 'f' are parameter number and form number respectively. Again the user may specify a range within which these parameters may vary, the upper and lower limits being defined by FPARMU, and FPARML respectively.
13. NBACK: This is the total number of background forms to be used to fit the all the spectra submitted.
14. BLS(S): Defines the lineshape to be used for the background of spectrum S (see List 2).
15. BPARM(p,f): Operates in the same way as FPARM. The paramaters required vary with the lineshape used, here for example the gradient and Y-axis intercept are given for the linear background used.
16. NINST: Specifies the total number of instrument response function forms to be used to fit the set of spectra submitted.
17. ILS(S): Defines the instrument response function lineshape for spectrum S of the set submitted (see List 2).
18. IPARM(p,f): Describes the form parameters for the instrument response function, see FPARM.

Obviously if the number of variables can be reduced then the routine will run faster

and more effectively, so wherever possible the parameters should be fixed or their effective ranges reduced. For example, the data presented in this thesis have been fitted under similar conditions. The spectrometer used was the same in all cases and its instrument broadening function was determined experimentally from the width of the Fermi level at 80 K, this was therefore kept constant throughout the procedure. As explained in the results introduction the energies of the bulk and clean surface peaks were kept fixed at experimentally determined values. The lineshape which has been shown both theoretically and experimentally to be well fitted by a Doniach-Sunjic form has its parameters (width and asymmetry) fixed. This leaves only the background lineshape parameters free to vary, since we apply a linear background it is fairly simple to estimate a reasonably small range for these. The only true variables are the amplitudes and the energy positions of 'new' or 'mobile' peaks i.e. those that appear as the result of adsorption or temperature experiments for example. Application of previous experimental results (when available) to a given problem allows the user in some cases to keep the energy range to a reasonable minimum.

In addition to each of these there is a second namelist labelled the OPTION parameter set. PEEP and NORM are logical variables i.e they may have one of two values true(T) or false(F). If PEEP is set to true then at each iteration the the parameter steps are printed out. When NORM is set to true then the input spectrum is normalised such that the area under the curve is set to unity. Can be useful in removing scaling problems due to beam variations. RTYPE chooses the type of R-Factor (see List 3) used when comparing the trial spectrum to the real data.

List 1.

- &DECON
- NPEAKS=4,
- E(1)=031.400,EU(1)=031.400,EL(1)=031.350,EREL(1)=0,
- E(2)=-0.125,EU(2)=-0.125,EL(2)=-0.125,EREL(2)=1,
- E(3)=-0.298,EU(3)=-0.298,EL(3)=-0.298,EREL(3)=1,
- E(4)=-0.430,EU(4)=-0.430,EL(4)=-0.430,EREL(4)=1,
- NSPEC=1,
- A(1,1)=.002,AL(1,1)=.000,AU(1,1)=0.500,AREL(1)=0,
- A(2,1)=.000,AL(2,1)=.000,AU(2,1)=0.060,AREL(2)=0,
- A(3,1)=.007,AL(3,1)=.010,AU(3,1)=0.500,AREL(3)=0,
- A(4,1)=.000,AL(4,1)=.000,AU(4,1)=0.050,AREL(4)=0,
- FORM(1)=1,
- FORM(2)=1,
- FORM(3)=1,
- FORM(4)=1,
- BGND(1)=1,
- INST(1)=1,
- NFORM=1,

- FLS(1)=1,
- FPARM(1,1)=.050,FPARML(1,1)=.050,FPARMU(1,1)=.050,
- FPARM(2,1)=0.050,FPARML(2,1)=0.050,FPARMU(2,1)=0.050,
- NBACK=1,
- BLS(1)=5,
- BPARM(1,1)=0.000,BPARML(1,1)=-1.000,BPARMU(1,1)=5.000,
- BPARM(2,1)=00.000,BPARML(2,1)=-02.000,BPARMU(2,1)=05.000,
- NINST=1,
- ILS=2,
- IPARM(1,1)=.200,IPARML(1,1)=.200,IPARMU(1,1)=.200,
- &END
- &OPTION
- PEEP=F,NORM=T,RTYPE=2,
- &END

List 2.

Lineshape options available for ILS(S), BLS(S), FLS(S) within the main namelist parameter file.

- 1 = Doniach-Sunjic
- 2 = Gaussian

- 3 = Lorentzian
- 4 = Quadratic
- 5 = Linear

6.1 List 3.

R-Factors available for use in the OPTIONS namelist.

- RTYPE=1, Sum of the absolute differences.
- RTYPE=2, Sum of the squares of the differences.
- RTYPE=3, Fraction of X-range with slopes of different signs.
- RTYPE=4, Sum of absolute differences of the derivatives.
- RTYPE=5, Sum of the squares of the differences of the derivatives.
- RTYPE=6, Zanazzi-Jona, not implemented at last update (11 Nov 1986).
- RTYPE=7, Pendry R-Factor, not implemented at last update.